

Quantum Models for Effects of Extended Defects on Ion - Channeling

A thesis submitted for the award of the Degree of
Doctor of Philosophy

L. N. S. PRAKASH GOTETI



SCHOOL OF PHYSICS
UNIVERSITY OF HYDERABAD
HYDERABAD - 500 046
INDIA

JULY - 1999

To

* * * *my father*

CERTIFICATE

This is to certify that the work embodied in this thesis entitled **Quantum models for effects of extended defects on Ion-channeling** being submitted by L. N. S. Prakash Goteti is a record of work carried out under my supervision. This work has not been submitted to this or any other University or Institution for the award of a degree or diploma.

Place: Hyderabad

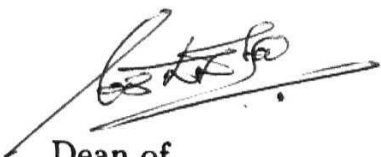
Date: 08 - 07 - 1999



Prof. A. P. Pathak

(thesis supervisor)

Prof. ANAND P. PATHAK
SCHOOL OF PHYSICS,
UNIVERSITY OF HYDERABAD
CENTRE FOR SPACE SCIENCE
HYDERABAD 500 046
INDIA



Dean of
SCHOOL OF PHYSICS,
UNIVERSITY OF HYDERABAD

DECLARATION

I hereby declare that the work embodied in this thesis entitled **Quantum models for effects of extended defects on Ion-channeling** carried out by me, under the supervision of **Prof. A. P. Pathak**, School of Physics, University of Hyderabad, has not been submitted for any other degree or diploma either in part or in full to this or any other University or Institution

Place: Hyderabad

Date: 08 - 07 - 1999


(L. N. S. Prakash Goteti)

ACKNOWLEDGEMENTS

It is never possible to achieve any thing with a lot of effort **and** attention, with out the help of numerous people. I could not have finished my thesis but for the enormous help and encouragement shown towards me and my work, by numerous people, who are very important to me and will be cherished for ever in my heart.

In the first place, it goes beyond my words for me to express my gratitude and indebtedness to my supervisor, **Prof. A. P. Pathak**, for giving me an opportunity to work with him, for his inspiring guidance throughout the period of my research work. In essence it is because of his wise, prudent and judicious guidance, constant and fostering encouragement and close supervision of my work that I am able to complete the entire thesis work most successfully in a reasonable span of time.

I thank the Dean, School of Physics for providing necessary facilities.

I am very much grateful to **University Grants Commission, New Delhi** for providing financial support through UGC **JRF** and SRF schemes.

Thanks to the office staff of the School of Physics who were very helpful at all times.

I would be failing in my duty if I do not thank my teachers and professors who were instrumental in making Mathematics and Physics not only the subjects that I love, but also to make it possible for me to understand the intricacies of them.

Here I would like to thank my very first Mathematics teacher Sri. Rama Sankaram, for inculcating the aptitude in me to learn and appreciate its beauty as a language to communicate Physics.

Next, I wish to express my warmest gratitude and sincere **thanks** to **my** teachers and professors especially, **Prof. G. S. Agarwal, Prof. A. K. Kapoor, Prof. S. Chaturvedi, Prof. V. Srinivasan, Prof. S. R. Shenoy, Prof. S. N. Kaul, Dr. Ashok Chatterjee, Dr. P. K. Panigrahi** who taught me in **M. Sc.** and **M. Phil.** courses and created the basic urge in me for research. Indeed, I was attracted to the research work and have taken it up *as* my profession mainly because of the keen interest, inquisitiveness, and innovative spirits enkindled in myself by their brilliant class lectures. In this context, I fervently hope and trust sincerely that their training will be my true guiding spirit in my persistent efforts and endeavours in my future career.

It gives me great pleasure to express my sincere thanks and gratefulness to Dr. V. Harikumar for his invaluable suggestions and discussions that I had at various stages of research; at the same time I would be failing in my duty if I do not thank my senior Azher M, Siddiqui, who helped me a lot during the course of my work *inspite* of his busy research work.

Once again I thank Azher, the research scholars Satya, Rajan, Kennedy and Sundar Rajan of Material Science Division, IGCAR (**Indira Gandhi Centre for Atomic Research**), Kalpakkam for providing very useful literature for my research work.

I thank Mr. Srinivas for helping me in typing this thesis.

I am very much thankful to Dr. Ramakrishna for his truly support, timely help and encouragement in my difficulties.

I am very much thankful to my colleagues Guru, GV, **Ramana**, Soma, Lok, Srinath for their co-operation and encouragement. A special thanks to my juniors Nagesh, Solomon, Phanikumar, Phani Muralikrishna, Sunil, Raishma, twins (Raghav and **Lakshman**) and Padmasree, not only for providing a lively and cordial atmosphere **but** also for their generous help, **co-operation**, constant and tremendous confidence in my ability.

It is almost impossible for me to thank my friend Koteswera Rao enough whose help, encouragement and support went a constant source of sustenance to me.

Heartfelt thanks to all the members of Sri. G. S. Narayana and family for making me feel at home in their home and welcoming me at all times and treating me as one of their family members.

I am very much indebted to my *one-in-a-million* uncle Sri. Nagabhushanam, aunt Susila who were always there in my need, encouraging me; and their words of advice went a constant strength to me through out my career. Their great endeavours, care and affection made me what I am.

I am grateful to Smt. Savithri Devi, my grandmother who took all the pains for my bright career.

I am thankful to my uncle, Rtd. WG. Cmdr. N. R. Achanta for his support to my family in all odds. I would also like to thank my cousin, Phanindra, for helping me in difficult situations.

I am very much thankful to my wonderful brother, Karthik whose help, practical words always boosted me in frustrating pressure situations.

I am thankful to my sisters Padmaja and Lavanya for their constant encouragement and support.

I do not find adequate words to express my gratitude and indebtedness to my parents, especially my mother who supported my decisions throughout my academic career and extended help despite difficulties at home. I am very grateful to my father for his true love, trust, sacrifice and kindness; I express my gratefulness by dedicating this work as a mark of respect and high esteem to my beloved father.

Synopsis

1 Introduction

1.1 Channeling

When charged particles are incident on crystals along one of the major crystallographic directions, their range increases anomalously and they penetrate larger distances in these crystals than when they are incident along random directions. This effect (so called channeling) is well established[1-3] and Lindhard's classical theory of channeling provides a complete description of this channeling phenomena for relatively heavy ions. This manifests that atomic rows/planes guide and steer the charged particles along the channels between rows and planes by means of correlated series of small angle soft collisions.

Channeling techniques find their applications in many frontier areas of physics. Crystal defect studies, semiconductor superlattices studies [4], backscattering analysis, ion beam analysis and ion implantation are very few among them. Both Rutherford backscattering and channeling are simultaneously used extensively for studying and understanding various phenomena in ion solid interactions. This channeling technique can be and has been used to locate foreign atoms in a crystal. The energy dependence of dechanneling gives information of the nature of the defects and magnitude of the dechanneling cross-section is used to find the amount of damage. A thorough knowledge of effects of defects on channeling and corresponding dechanneling phenomena is the basis for a better understanding of any phenomena in physics in general and in the field of channeling and its applications in particular [2,5].

Observation of radiation from channeled ions, especially light particles like electrons and positrons has opened possibilities of new applications in the fields of laser physics and medicine as a source of hard X-rays and γ -rays for nuclear pumping, hence for possible construction of a γ -laser.

1.2 Concepts used in the thesis :

When a charged particle moves along certain major crystallographic directions under channeling conditions, it does not feel the interaction due to individual atoms sitting at various lattice sites but experiences a collective effect of all the atoms along that particular axial or planar direction. The particle velocity component parallel to the axial or planar direction is such that the time of flight to cross one lattice spacing is less than the collision time with any individual target atom [2]. This implies that before the particle can experience the field of one atom, it is already in the field of the next atom along that string or plane and it will see only collective effect instead of individual atom field. For positive particles, the transverse motion perpendicular to the axis or plane is confined to the region around a potential minimum between the strings or planes of atoms. Since channeled particle travels large distances before its transverse momentum is significantly altered, it is a good approximation to regard the force exerted on the channeled particle as arising from a conservative potential. So for planar channeling the transverse potential is the planar average of the electrostatic potential within the lattice. In the thesis, for analytical calculations we use the planar potential used by Pathak[6] and this potential has been used extensively for channeling studies, particularly in complicated problems involving the effects of defects (like stacking faults and dislocations). This planar potential is basically a power law potential derived from Lindhard's standard potential.

1.3 Importance of Quantum-Mechanical Effects:

In electron and positron channeling the angular dips show a finely oscillating structure and the work on transmission electron microscopy (TEM) with crystalline materials, extended to channeling phenomena resulted clear indications of quantum and diffractive effects dominating the patterns [7]. The quantum mechanical treatments [8] indicated that it is the product of the mass of the particle and the strength of the interaction between the particle

and the crystal which determines applicability of classical or quantum picture. The classical features start becoming dominant as this product increases; when the particle energy is very high, the discreteness will slowly disappear and one can treat it classically. Thus protons and all other heavier ions behave classically whereas light particles like electrons, positrons, neutrons and mesons would be expected to show quantum-mechanical features. Even here, when the relativistic mass is large, the quantum mechanical effects are less dominant.

1.4 Dechanneling by extended defects :

Classically, a well-channeled particle is affected directly by the potential of the defect and hence its trajectory is modified. These effects are of obstruction type (eg. stacking faults, interstitial atoms, grain boundaries etc). If the defects give rise to distortion in a certain region of the crystal, disturbing the regularity of the material in that region, the effects are of distortion type, for example dislocations. These two kinds of defects give rise to obstruction dechanneling and distortion dechanneling respectively[9]. This reflects the importance of the ion beam interaction with the defects. The effects of these defects are described by the dechanneling probability $\chi(E, r(h, k, Z), \dots)$, depending upon the energy E in a channel (h, k, l) , situated at a distance r from the defect[10]. An estimate of χ and its dependence on various parameters like energy etc., gives important information about nature and concentration of defects.

Most of the work on dechanneling by defects is based on several simplifying assumptions and the classical calculations related to the effects of defects [9,11] on channeling are good enough for heavier particles like protons, α - particles and heavy ions[12]. Even though qualitatively the classical results on energy dependence etc. are reliable, the detailed dynamics of the particle during the passage through various regions of obstruction/distortion and the resulting dechanneling phenomena especially various symmetries involved in the problem are not clearly realized. Therefore more work, possibly using quantum mechanical

and/or field theoretical techniques is needed to treat the whole defect problem in a more accurate way. Moreover the interaction of lighter particles like positrons and electrons with solids should be described quantum mechanically[13].

We have quantum mechanical description for the case of extended defects like stacking faults and dislocations with specific reference to positron dechanneling. Quantum mechanically, the longitudinal and transverse components are separated out[13]. The transverse motion for positively charged particles (like positrons) is described by one dimensional Schrodinger equation with a harmonic oscillator potential and the solution gives rise to quantized transverse energies. Hence number of quantum states are formed and the transverse energy assumes a series of discrete values. The maximum number of bound states supported by transverse continuum potential (n_{max}), increases with the relativistic particle mass (γm) where the Lorentz factor, $\gamma = 1/\sqrt{1 - v_z^2/c^2}$ and m is the rest mass of the particle. This n_{max} is still small for positrons/electrons of a few Mev energy and n_{max} for positrons is smaller than that for the electrons because of the fact that transverse motion of positively and negatively charged particles is qualitatively different, in channeling situations. For the case of positrons the transverse potential may be approximated to harmonic oscillator in which the potential minima are located at middle axis of the axial/planar channel, whereas for electrons the potential minima are on the atomic strings or planes and hence corresponding transverse potential may be approximated to two or one dimensional hydrogen atom. In quantum mechanical approach, dechanneling effects (dechanneling/scattering of the particle due to the presence of defect) can be studied by evaluating the scattering amplitude which is expressed in terms of transition probability matrix element corresponding to respective wave functions in the transverse potential. In such a potential, the energies less than the height of the barrier namely below barrier states represent the initially channeled particles. On the other hand, the states with energies above the potential barrier are basically dechanneling states and they lead to dechanneling phenomena.

For relativistic channeled particles the longitudinal motion results in Lorentz contraction along the axes or planes and hence the strength of the continuum potential is enhanced by a factor γ in the rest frame of particle. The resulting Schrodinger equation describing the transverse motion is solved with relevant continuum potential due to strings or planes depending only on transverse coordinate.

The thesis consists of five chapters:

1. Introduction
2. Quantum description of dechanneling by stacking faults
3. Quantum description of dechanneling by dislocations
4. Time dependent formulations for dechanneling by dislocations
5. Concluding Remarks

The introductory chapter contains brief survey of channeling and the importance of quantum mechanical effects especially in channeling situations. In chapter 2, a quantum mechanical treatment of the effects of stacking faults on dechanneling is given. At the stacking fault boundary, these states make transitions for which probabilities have been calculated using sudden approximation. However, the continuum potentials in particular used in the discussion are in principle valid for infinite planes where in the case of stacking fault we had half planes i.e., those ending at the fault and those starting from the fault. So the transverse potential is slightly complicated just at the interface and one has to match the appropriate basis wave functions at the interface of the stacking fault boundary. An estimation regarding the effects of periodicity of transverse potential on dechanneling probabilities is made.

In chapter 3, a quantum mechanical treatment of the effects of dislocations on planar dechanneling is given. The effects of channel distortion due to dislocation are incorporated

through a relativistic centrifugal energy term. We evaluated the number of quantum states supported by this distorted channel and the transition probabilities among these states due to distortions in the planar channel; the resulting dechanneling probabilities for varying distortion are calculated using sudden approximation. The energy dependence of these dechanneling probabilities for initially well channeled particles has been estimated and we show that it varies linearly with energy for relativistic particles.

In chapter 4, a quantum mechanical formulation is developed by relaxing the sudden approximation used in the chapters 2 and 3, where bound - bound transitions are considered. In this chapter we consider the transitions from these bound states to scattering states due to lattice distortions in the planar channel, using time dependent perturbation theory. The resulting expressions for dechanneling probabilities and hence for dechanneling cross-section for initially well channeled particles has been estimated and qualitative features like dechanneling radius, energy dependence etc., are discussed.

Chapter 5 contains a summary of work, concluding remarks and comments on possible future directions of research work in this field .

A brief description of above mentioned chapters is given below, giving essential features in a concise form.

2 Chapter II: Dechanneling by stacking faults

A stacking fault is a line defect, where the channels surrounded by atomic planes on right side are shifted by an amount, say (a_s) w.r.t left side of the fault. For any channelon passing through the extended defect (obstruction/distortion), the longitudinal component of energy is not much effected but the transverse energy undergoes a change. Hence the respective channeling phenomena is governed by the transition probability evaluated in terms of matrix element of the wave functions corresponding to various portions of obstruction/distortion, where these effects are suitably incorporated.

Here in the case of stacking fault, the channeling phenomena is governed by the overlap integral of the wave functions corresponding to left channel and right channel $\langle \psi_i | \psi_f \rangle$, where

$$\psi_i = \psi_L = \varphi_n(x) = \left(\frac{\alpha}{\sqrt{\pi} 2^n n!} \right)^{1/2} \exp \left(\frac{-\alpha^2 x^2}{2} \right) H_n(\alpha x) \quad (1)$$

$$\psi_f = \psi_R = \varphi_m(x + a_s) = \left(\frac{\alpha}{\sqrt{\pi} 2^m m!} \right)^{1/2} \exp \left(\frac{-\alpha^2 (x + a_s)^2}{2} \right) H_m(\alpha x + \alpha a_s) \quad (2)$$

Under the sudden approximation, the overlap integral with harmonic oscillator wave functions $\psi_i = \varphi_n(\alpha x); \psi_f = \varphi_m(\alpha x + \alpha a_s)$ can be written as

$$\langle n | m \rangle = \frac{1}{\sqrt{\pi 2^{m+n} m! n!}} \exp \left\{ -\alpha^2 a_s^2 / 4 \right\} \int_{-\infty}^{\infty} \exp \left\{ -\left(t + \frac{b}{2} \right)^2 \right\} H_n(t) H_m(t + b) dt \quad (3)$$

where $b = \alpha a_s$; $\alpha x = t$ and the coupling constant $\alpha = \sqrt{\frac{m_{\perp} \omega}{\hbar}}$

To solve this integral and obtain a general expression one may start with usual generating function method. However it was found that it is complicated to compare the coefficients of parameter terms in the generating functions both sides and hence an ab-

stract notation was used so that the matrix element looks simple.

$$\text{Since } \psi_i(x) = |n\rangle \quad \text{and} \quad \psi_f(x) = |m\rangle ,$$

Here we write

$$\langle \psi_i(x) | \psi_f(x + a_s) \rangle = \langle n | \exp\left\{\frac{a_s \alpha}{\sqrt{2}}(a - a^\dagger)\right\} | m \rangle \quad \text{with } a^\dagger a | n \rangle = n | n \rangle \quad (4)$$

The general expression for $\langle n | m \rangle$ is obtained by evaluating above abstract form with successive iterative process for various values of 'n' and 'm' and by intuition after so much of analytical effort, I could finally succeed to get the general expression in the final form as

$$\langle n | m \rangle = \frac{\exp(-\alpha^2 a_s^2 / 4)}{\sqrt{2^{m+n} m! n!}} \left(\sum_{r=\max(0, m-n)}^m (-1)^{n-m+r} 2^{m-r} m_{cr} \frac{n!}{(n-m+r)!} (b)^{n-m+2r} \right) \quad (5)$$

Here 'n' and 'm' represent harmonic oscillator states corresponding to initial state (left part of the channel before the fault) and final state (after fault) respectively. This general expression is extremely useful in various fields. It reduces enormous machine time in computing various matrix elements, particularly when the transitions involving higher quantum numbers.

The transition/channeling probability in general, is then obtained through the expression $p_{m \rightarrow n} = |\langle n | m \rangle|^2 = p_{n \rightarrow m}$. The probability for particle to remain channeled after the fault is given by $p_n = \sum_{m=0}^3 |\langle n | m \rangle|^2$ and hence the dechanneling probability is obtained as $\chi_n = 1 - p_n$.

3 Chapter III: Dechanneling by dislocations

In this chapter we concentrate on a quantum mechanical model for the effects of dislocations on initially well channeled relativistic positrons in a planar channel. In the vicinity of the dislocation, the channels are distorted and obviously the treatment is complicated as compared to the previous stacking fault case. We consider the motion of the positrons described in the rest frame of the particle. In this frame as we discussed earlier, the particle “sees” continuum potential $\gamma V(x)$ because of the length contraction in the direction of propagation (z). When the particle enters into the distorted portion, the motion of the particle is modified due to the influence of the curvature and in this distorted part of the channel the modified continuum potential as “seen” by the particle becomes $\gamma V_{eff}(x)$ which is written as

$$\gamma V_{eff} = \gamma V(x) - \gamma^2 m v_z^2 \left\{ \frac{b}{\pi} \cdot \frac{r(\gamma Z)}{(r^2 + \gamma^2 Z^2)^2} \right\} x \quad (6)$$

The expression for dechanneling radius r_0 is obtained by equating the restoring force to the maximum value of the deflecting force due to curvature and due to these relativistic effects r_0 in usual non-relativistic classical expression, gets enhanced by a factor of $\sqrt{\gamma}$. We consider transitions among the energy levels in the transverse potential which are induced by the distortion created due to dislocations. As before, we use harmonic oscillator model for transverse potential and sudden approximation for transitions. Due to channel distortion the coupling constant α (appearing in the normal harmonic oscillator model potential) will change to α' in the distorted portion because the oscillation frequency of the particle gets modified in this distorted portion.

The harmonic approximation to the above effective planar potential gives an estimate of number of allowed states in this distorted channel and the analysis is appropriate for the channels that are situated far away from the dislocation. This in turn implies that we are considering crystals with low dislocation concentrations (typically 10^6 to 10^7 per cm^2).

Once the particle enters into the distorted portion, the potential minimum is shifted due to curvature. The channeling/dechanneling phenomena under this situation is governed by the overlap integrals of the appropriate wave functions in various regions.

The transition probability for the passage of initially well channeled particle through dislocation will be the product of the transition probabilities across various parts of the channel, where the effects of distortion are suitably incorporated. The general expression for the total channeling probability of the particle with a specific initial state $|i\rangle$ so that the particle feels itself again in the straight channel with final state $|f\rangle$ (after passing through the various portions of distortion) has been obtained and is given by

$$P_{i \rightarrow f} = \sum_{k^{(2)}=0}^{k_{max}^{(2)}} \left(P_{k^{(2)} \rightarrow f} \left[\sum_{j^{(1)}=0}^{j_{max}^{(1)}} P_{i \rightarrow j^{(1)}} \times P_{j^{(1)} \rightarrow k^{(2)}} \right] \right) = P_{f \rightarrow i} \quad (7)$$

Here $|i\rangle = \varphi_i(\alpha x)$ (before distortion); $|j^{(1)}\rangle = \varphi_j(\alpha'x + \alpha'a_r)$ (first portion of distortion); $|k^{(2)}\rangle = \varphi_k(\alpha'x - \alpha'a_r)$ (second portion of distortion) and $|f\rangle = \varphi_f(\alpha x)$ (after distortion). As discussed earlier, $\varphi(x)$ is harmonic oscillator wavefunction and a_r is shift in the potential minimum due to distortion. The total channeling probability for initially well channeled particle, to find itself again in the straight channel after passing through various portions of the distortions is given by

$$p_0 = \sum_{f=0}^{f_{max}=3} (p_{0 \rightarrow f}); \quad \chi_0 = 1 - p_0$$

We computed the dechanneling probabilities for initially well channeled particles ($|i\rangle = 0$) and those for first excited state ($|i\rangle = |1\rangle$). The calculations for initially well-channeled particles show that dechanneling probability varies linearly with particle energy.

4 Chapter IV: Time dependent formulations

Here we use time dependent perturbation theory to present a more realistic model by relaxing the sudden approximation. These calculations show that scattering states play a vital role in dechanneling. This is because of the occurrence of additional bound states in the planar channel with change in curvature. Event hough, the constant curvature model and the sudden approximation helped in better quantum mechanical understanding of the dechanneling mechanism, the consideration of non-uniformity of the curvature during the propagation of the particle, as done here is obviously more appropriate. In the present calculations the non-uniformity effects in curvature mentioned earlier are taken in terms of a time-dependent force term. This perturbative energy term is obtained by replacing $Z = v_z t$ in eqn (6) causing a transition from bound state to scattering state .The dechanneling phenomena under this situation is governed by the transition of the particle from a bound state (harmonic oscillator) to a scattering state (plane wave). Because of the assymmetric nature, first order perturbation theory will not give any shift in the energy. On the other hand above perturbation induces transition from a bound state to scattering state for lower radius of curvatures and this corresponds to dechanneling. The initial and final wave functions of the positron are given by

$$\begin{aligned}\psi_n(x, y, z) &= \frac{1}{L} \left(\frac{\alpha}{\sqrt{\pi} 2^n n!} \right)^{1/2} \exp(ik_z z) \exp(ik_y y) \exp(-\frac{1}{2} \alpha^2 x^2) H_n(\alpha x) \\ \psi_f(x, y, z) &= L^{-3/2} \exp(i\vec{k}_f \cdot \vec{r})\end{aligned}$$

The distortions of planar channel shifts particle motion in transverse direction (x) whereas in ‘ z ’ direction the propagation is nearly constant. The expression for dechanneling probability of a particle with initial bound state ψ_n (due to channel distortion) to a scattering state ψ_f is given by

$$\chi_n = \frac{1}{\hbar^2} \left| \int V_R^{fn} e^{i\omega_{fn} t} dt \right|^2; V_R^{fn} = \langle \psi_f | V_R(x, t) | \psi_n \rangle \quad (9)$$

Due to scattering, the particle goes to continuum of states. Hence total dechanneling probability to any one of final states is obtained by integration over density of final states and is obtained as

$$\bar{\chi}_n = (2n + 1) \bar{\chi}_0 \text{ with } \bar{\chi}_0 = \left(\frac{m\tilde{\omega}b}{2\sqrt{2}\hbar\alpha} \right)^2 \exp\left(-\frac{2\tilde{\omega}r}{\gamma v_z}\right) \quad (10)$$

The above expression for χ_0 is obtained with specific reference to initially well channeled particles. The dechanneling probability is maximum for those channels which are situated below the dechanneling radius (i.e., critical distance of the channel from the dislocation below which the particle completely gets dechanneled). This happens for $\tilde{\omega} = \text{---}$. Thus one can make a qualitative estimate for dechanneling radius for initially well channeled particles and it is obtained as

$$r_0 \approx \frac{b}{5.436} \sqrt{\frac{\gamma E}{2E_\perp}} \quad (11)$$

The dechanneling cross-section with reference to initially well channeled particles is obtained by the expression

$$\bar{\lambda} = \int \chi_0(r) dr = 2r_0 \quad (12)$$

Classically, the transverse energy $E_\perp \approx E\psi_p^2$, where ψ_p is planar critical angle [3]. So for the case of non-relativistic positive particles and other heavy ions $\gamma = 1$ and one may replace the E_\perp by equivalent classical expression. The above expression then becomes

$$\bar{\lambda} = \frac{b}{2.718} \sqrt{\frac{E}{4\pi Z_1 Z_2 e^2 N_p a_{T.F}}} = (0.44) \bar{\lambda}_{Quere} Z_2^{1/6} \sqrt{b} \quad (13)$$

where b is in A. The dechanneling widths λ_n are estimated for positrons along Al(111) for which $b = 2.86A$. Corresponding dechanneling width for *He* ions has also been estimated and compared with existing theory and experimental data[12] showing reasonable agreement

5 Chapter V Thesis Summary and conclusions

We present a quantum mechanical description in sudden approximation for transition / channeling probability during the passage of the particle through extended defects (like stacking faults and dislocations) where we discuss various aspects of the related effects(like for example dechanneling at the interfaces, effects of periodicity in the transverse direction etc). We developed time dependent formulations for the dislocation case where we obtain an expression for dechanneling width for the first time purely on the basis of quantum mechanical considerations. By incorporating appropriate limits in the present expression for dechanneling width, equivalent classical expression is obtained. This expression is very close to that obtained by Quere's classical analysis where continuum model in classical approximation is considered. The theory also predicts well-known classical results in suitable approximation, qualitatively. We found quantitative results for dechanneling widths are also in good agreement with experimental data[12]. The dechanneling cross-section varies linearly with E at relativistic energies as confirmed by the bent crystal channeling experiments done by R. A. Carrigan, Jr. [14]. He also mentioned that increasing the bending is in “some sense” like raising the atomic number of the crystal. From the eqn.(13) one can see that the dechanneling radius increases with Z_2 which means that the critical region increases with Z_2 which in turn implies that the channels are distorted heavily. We tried to integrate the normal dechanneling with bent crystal dechanneling and we show that targets with high atomic numbers are favourable for bent crystal channeling experiments.

REFERENCES

1. D. S Gemmel, *Rev. Mod. Phys.* **46**, 129(1974).
2. *Channeling, Theory, Observations and applications*(Ed.) D. V. Morgan (John Wiley & Sons, New York), (1973).
3. A. P. Pathak *Rad. effects* **61**, 1(1982).
4. L. C. Feldman, *Physica Scripta*, 28, 303(1983);
J. W. Mayer, *Rad. Effects* 12, 183(1972).
5. W. Vali, V. Vali, *Proc. IEEE* **51**, 182(1963); J. U. Andersen, W. M. Angustyniak, E. Uggerhøj *Phys. Rev. B* 3, 705(1971).
6. A.P.Pathak *Phys. Rev. B* 13, 4688 (1976); A. P. Pathak and S. Satpathy *Nucl. Inst. Meth. B* 33, 39(1988); A. P. Pathak and B. Rath *Rad. effects* 63, 227 (1982).
7. L.T. Charderton, *J. Appl. Cryst.* 3, 429(1970).
8. R. E. Dewames, W. F. Hall and G. W. Lehman *Phys. Rev.*, **148**, 181(1966).
9. J. Mory and Y. Quere, *Rad. effects* 13, 57(1972).
10. Y. Quere, *Phys. Rev. B* **117**, 1818 (1975).
11. Y. Quere, *Phys. Stat. sol* 30, 713(1968).
12. S. T. Picraux, E. Rimini, G. Foti and S. Campisano, *Phys. Rev.B* **18**, 2078(1978).
13. F. Grasso, M. Lo. Savio and E. Rimini, *Rad. Effects* 12, 149(1972);
M. A. Kumakhov and R. Wedell, *Phys. Stat. sol(b)* **84**, 581(1977).
14. Richard A. Carrigan Jr., editor, "*Relativistic channeling*"
NATO ASI series B **165** 339-368(1986)

List of Publications

1. Azher M. Siddiqui, V. Harikumar, L. N. S. Prakash Goteti and Anand P. Pathak *Modern Phys. Letters B* 10,745 (1996).
2. L. N. S. Prakash Goteti and Anand P. Pathak *J. Phys. Cond. matter* 9, 1709 (1997).
3. L. N. S. Prakash Goteti and Anand P Pathak *Phys. Rev. B* 58, 5243 (1998).
4. L. N. S. Prakash Goteti and Anand P Pathak *Phys. Rev.* 5 59,8516(1999).
5. Annu Sharma, Shyam Kumar, S. K. Sharma, N. Nath, V. Harikumar, A. P. Pathak, L. N. S. Prakash Goteti, S. K. Hui and D. K. Avasthi *J. Phys. G* 25, 135 (1999).
6. Anand P Pathak, L. N. S. Prakash Goteti and Azher M. Siddiqui AIP Conference series *{Denton Accelerator conference}* (in press).

Table of Contents

1	Introduction	1
1.1	Evolution of channeling concept:	1
1.2	Theory of Channeling - Continuum model:	4
1.2.1	Interatomic potentials:	9
1.3	Applications of Channeling:	11
1.3.1	Study of defects (radiation damage):	11
1.3.2	Surface Studies:	12
1.3.3	Ion implantation in technology:	12
1.3.4	Channeling Radiation:	12
1.3.5	Beam extraction by bent crystal channeling:	13
1.4	Dechanneling by defects:	14
1.5	Quantum-Mechanical Effects:	17
1.6	Outline of the Thesis:	19
2	Quantum description of dechanneling by stacking faults	27
2.1	Introduction to quantum dechanneling theory:	27
2.1.1	Electron and Positron Channeling:	30
2.1.2	Basis of the present model:	32
2.2	Theory and formulation:	35
2.2.1	Sudden Approximation:	37
2.2.2	Operator formalism:	37

2.2.3	Evaluation of number of states in the continuum potential well: .	39
2.2.4	Dechanneling effects at the stacking fault:	46
2.2.5	The effects of periodicity in the transverse space:	48
2.3	Results and Discussion:	49
References		60
3	Quantum description of dechanneling by Dislocations	62
3.1	Introduction:	62
3.2	Basis of the present model:	64
3.2.1	Relativistic expression for the curvature:	66
3.2.2	Effects of distortion on the force constant:	69
3.3	Theory and formulation:	71
3.3.1	Channeling probabilities across(I) interface:	73
3.3.2	Channeling probabilities across (II) interface:	75
3.3.3	Channeling probabilities across (III) interface:	76
3.4	Results and Discussion:	77
References		86
4	Time dependent Formulation for dechanneling by Dislocations	88
4.1	Introduction:	88
4.2	Basis of the time dependent approach:	89
4.3	Results and Discussion:	98
References		100
5	Summary and Conclusions	101

Chapter 1

Introduction

1.1 Evolution of channeling concept:

In the beginning of 20th century, the *X-ray diffraction experiments* revealed that scattered photons propagate through the *open crystal channels* with relative ease[1]. This consequently lead to conjecture about the transmission of charged particles through these *open channels* in crystals. Thus X-ray diffraction experiments brought the fact into light that the crystals have open space, apart from their regular arrangement of atoms and hence contain open channels. In order that charged particles should pass through these crystallographic channels, they need to meet two essential requirements [2]. (1) The particle should find sufficient open space between the atomic rows (as realized from the *Braggs* diffraction). (2). As the particle propagates along the channel, there should be a driving force to prevent the possible close collisions with the atoms and at the same time *steer* the particle towards the middle axis of the open channel. Keeping these conditions in mind, *Stark* proposed an experiment in 1912 with protons [3]. However this suggestion was overshadowed by the intense activity in *X-ray diffraction* in crystals at that time. Much later in early *sixties*, a series of experiments were performed and this eventually lead to the discovery of the *Channeling* phenomena. These experiments are basically either measurement of the ranges [4] or sputtering experiments [5,6]. The later one showed that the sputtering ratio for ions impinging into single crystal depends upon the orientation of the crystal [5].

The computer simulations by *Robinson* and *Oen* on 1-10 keV Cu atoms [7] in various targets indicated that the ions with initial velocities lying close to the principal axial directions penetrate to abnormally larger distances in the crystal.

The incident beam is effectively resolved into two components namely, channeled and random components. In general, the random component undergoes statistically independent atomic collisions during the process of its passage through a crystalline solid and suffers energy loss which is identical to that expected for an amorphous material. As shown in Fig. (1.1), the channeled component avoids all the close impact parameter phenomena and the particle gets steered along the axial or planar channels.

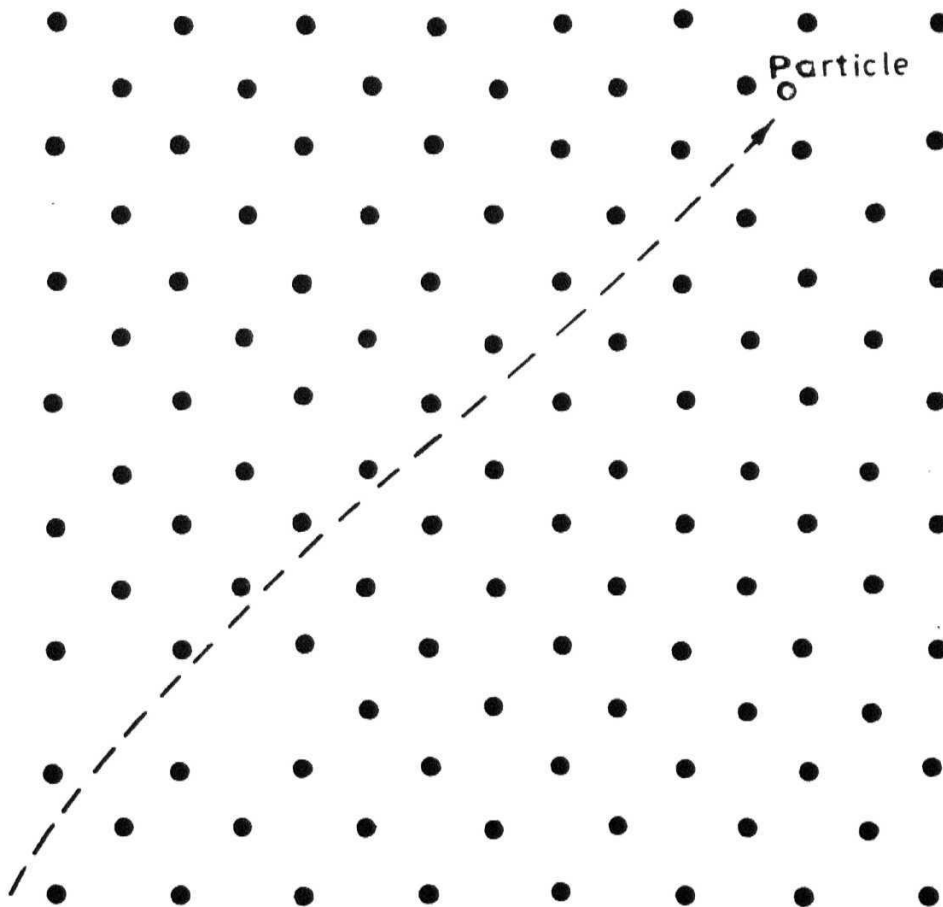


Fig. 1.1 : The channeling phenomena showing how the particle is steered along an open channel in the crystal.

The effects of these channeling and blocking are studied by defining a limiting distance of approach to the atomic rows/ planes of atoms. Especially for the channeling studies, where we are interested in the successful transmission of these charged particles through the open channel, this closest distance of the approach depends on the angle of incidence. In order to avoid possible large angle scattering, we define a small limiting angle of incidence, within which a particle must enter before it can pass through the rows/planes of atoms. Providing the angle to these crystallographic scattering centers is always less than this *limiting value*, the particle trajectory will be constrained to move in open space (regions of low electron density) and the large angle scattering will be avoided. On the other hand, those particles which do suffer large angle scattering, are deflected by these atomic rows and planes at an inclination which is always greater than this same *limiting angle*. So in a perfect crystal, therefore, the channeled and random components are mutually exclusive and this angle decides the fate of the particle beam and hence called as *Critical angle*. That means those particles which are injected into the crystal with an angle greater than this critical angle, suffer a total scattering. So critical angle and corresponding closest distance of approach discussed earlier are very essential parameters, in **channeling** situations.

This *Channeling* phenomena is further demonstrated by the experiments with monocrystalline targets [8a)]. This channeling technique has wide range of applications and significant amount of work on channeling and its applications has been done during last three decades as several review articles and books are already published. Lindhard's theory of channeling and continuum approximation are widely used to study the dynamics of the projectile particle during its propagation inside the crystal and these are discussed briefly in the following sections.

1.2 Theory of Channeling - Continuum model:

When the charged particles incident nearly parallel to major crystal axis/plane, the ion trajectories are governed by correlated *soft collisions* with atoms. These collisions are in such a way that hard collisions are avoided. As mentioned in earlier section, channeling is basically the influence of the crystal on the ion - trajectories penetrating into the crystal. Hence this term so called *Channeling* visualizes atomic rows and planes “*acts*” as guides that *steer* the charged particles along the crystallographic channels by means of correlated small angle soft collisions. This condition is to avoid the processes like RBS, innershell excitation etc., which eventually lead to the scattering of the beam from the actual path of propagation. During the propagation of the charged particle along a channel, the projectile interacts with the free electron gas and some of the outer shell electrons of the target atoms.

If an incident charged particle happens to bombard the crystal along one of the crystallographic directions, (say for example $\langle 110 \rangle$ axial channel [86]) in diamond as shown in Fig. (1.2)), it is likely to penetrate into the crystal to much larger distances than a particle with random direction. When a charged particle moves along these directions, under certain conditions it may not be able to feel the interaction due to individual atoms sitting at various lattice sites but rather experiences a collective effect of all the atoms sitting along that particular axial or planar direction; so that the moving particle will experience only *continuum* strings or planes. Incorporating these points, *Lindhard* [9] and *Erginsoy* [10] obtained mathematical relationship between the time of flight and the collision time. The particle velocity component parallel to the axial or planar direction is such that the time of flight to cross one lattice spacing is less than the collision time with any individual atom. This collision time depends on transverse velocity with which particle approaches that particular atom.

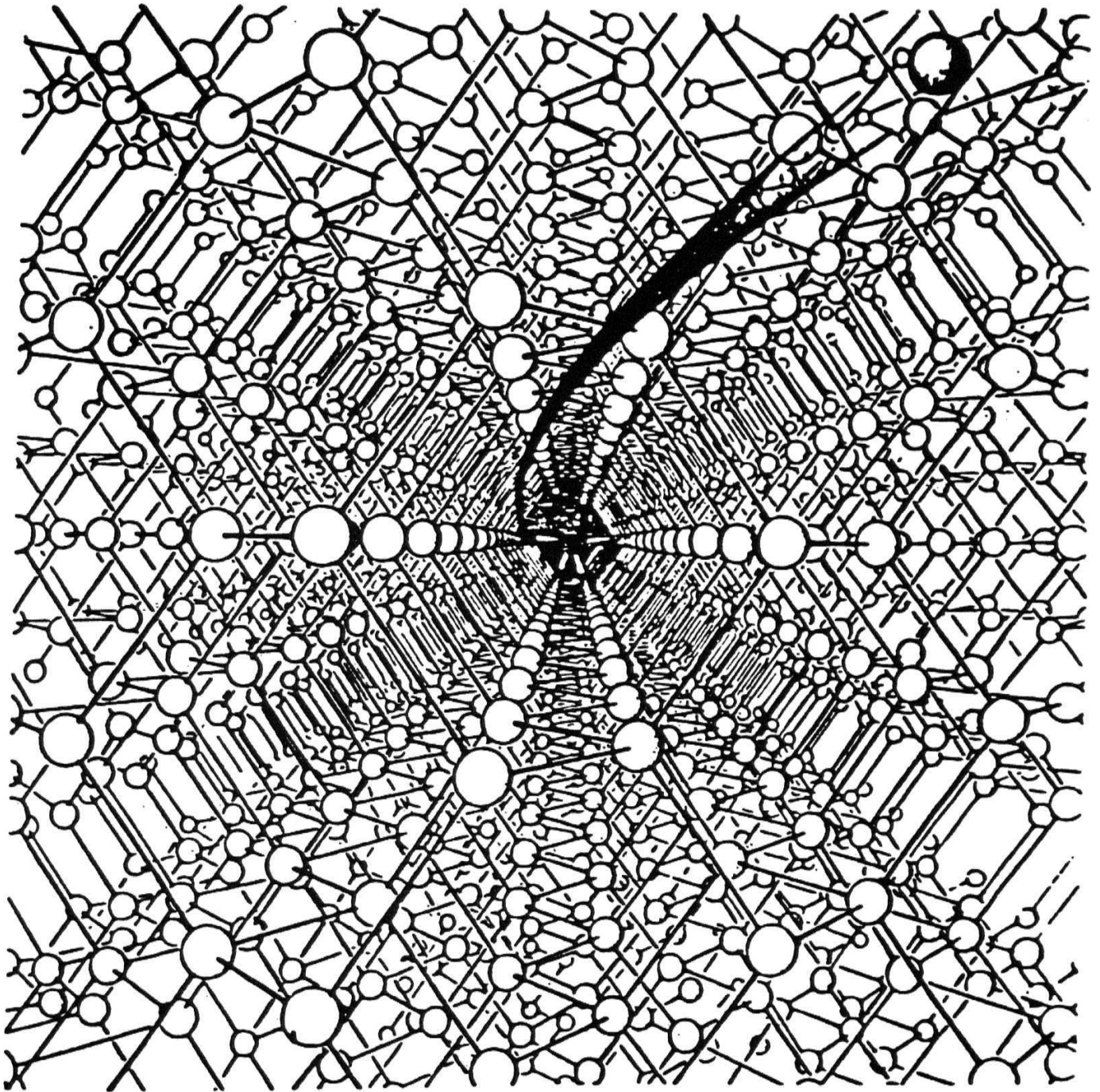


Fig. 1.2 : View down the $\langle 110 \rangle$ axial channel in a diamond structure showing the spiral path followed by a typical channeling particle.

That means by the time the particle can feel to be in the field of one atom, it is already in the field of next atom along the string or plane and it will see only continuum potential instead of individual atom field. This condition for *continuum approximation* can be written as

$$\frac{r_{\min}}{v \sin \psi} > \frac{d}{v \cos \psi} \quad (1.1)$$

As shown in Fig. (1.3), ' r_{\min} ' is distance of minimal approach to the string; ' d ' is interatomic spacing along the axis; ' ψ ' is angle that the incident particle moving with velocity v , makes with the channel.

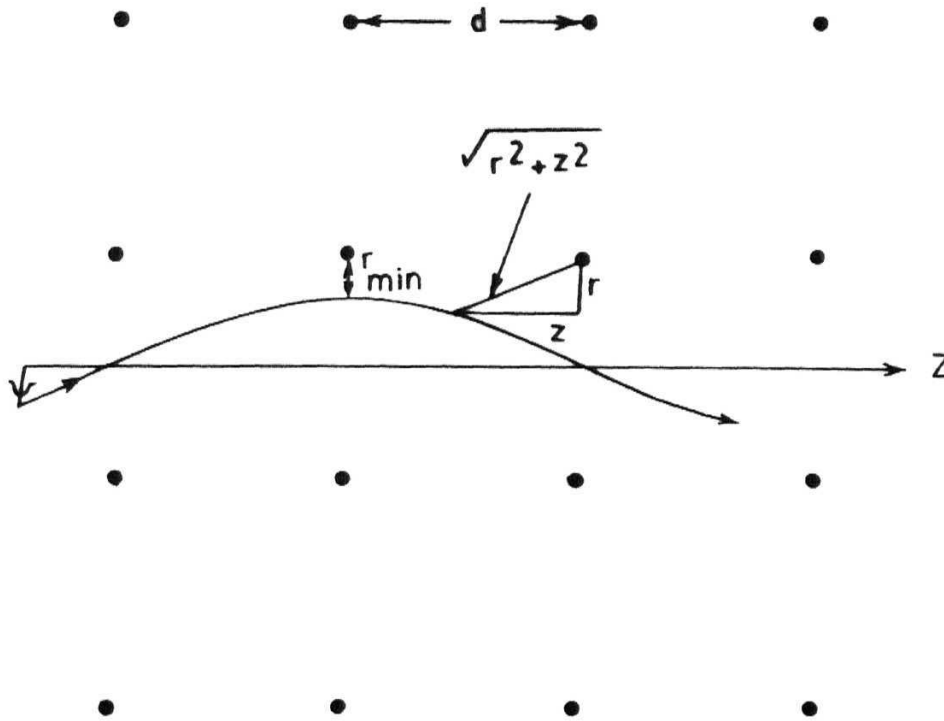


Fig. 1.3 : A channeled trajectory showing various quantities like incident angle minimum distance of approach and interatomic distance.

Here ' r_{\min} ' is obtained by equating the repulsive interaction due to continuum string, with the transverse kinetic energy as

$$U(r_{\min}) = E \sin^2 \psi . \quad (1.2)$$

The continuum potential $U(r)$ for axial case is given by

$$U(r) = \frac{1}{d} \int_{-\infty}^{\infty} dz V(\sqrt{(z^2 + r^2)}), \quad (1.3)$$

where r is the distance from the string and $V(R)$ is interatomic potential.

Comprehensive work has been done regarding the choice of interatomic potential. These potentials are derived by various methods and each of them has its own advantages and draw backs. Out of these potentials Lindhard's potential, statistical potential and power law potential proposed by Pathak are most frequently used potentials. Lindhard's standard potential is used for calculating various parameters like critical angle etc. This potential is given by

$$V_{Li}(R) = Z_1 Z_2 e^2 \left[\frac{1}{R} - \frac{1}{\sqrt{R^2 + C^2 a_{T.F}^2}} \right] \quad (1.4)$$

where C is Lindhard constant ($=\sqrt{3}$) and $a_{T.F}$ is Thomas-Fermi screening radius given

$$a_{T.F} = \frac{0.8853}{\sqrt{Z_1^{2/3} + Z_2^{2/3}}} a_o, \quad (1.5)$$

where a_o is Bohr radius; Z_1 and Z_2 are the atomic numbers of the incident ion and target atom respectively.

Substituting in (1.3) and evaluating the integral one gets

$$U(r) = \frac{Z_1 Z_2 e^2}{d} \ln \left[(C a_{T.F}/r)^2 + 1 \right] \quad (1.6)$$

In high energy limit, r values will be small because particle approaches closer to atom and rows so that $Ca_{T.F}/r \gg 1$ for most of the r values, hence

$$U(r) = \frac{2Z_1Z_2e^2}{d} \ln \frac{Ca_{T.F}}{r} . \quad (1.7)$$

From Eqns. (1.1)&(1.6) the range of validity of continuum approximation is given by

$$\psi < \sqrt{\frac{2Z_1Z_2e^2}{dE}} \quad \left(\text{for higher energies i.e., } E > \frac{2Z_1Z_2e^2d}{a_{T.F}^2} \right). \quad (1.8)$$

However for low energies i.e., $\left(E < \frac{2Z_1Z_2e^2d}{a_{T.F}^2} \right)$; r is generally large (including r_{\min}) and one should use full expression (1.6); so that the condition (1.1) leads to

$$\psi < \sqrt{\frac{Ca_{T.F}\psi_1}{d\sqrt{2}}} \quad (1.9)$$

A planar channeled positively charged particle travels large distances before its transverse momentum is significantly altered. Consequently it is a good approximation to regard the force exerted on the channeled particle as arising from a conservative, one dimensional potential which is the planar average of the electrostatic potential within the lattice. So for planar case the continuum potential is obtained by averaging over the particular plane and given by

$$V(y) = 2\pi N_p \int_0^\infty r V(\sqrt{r^2 + y^2}) dr \quad (1.10)$$

For *Lindhard* standard potential (Eqn. 1.4), the above potential takes the form

$$V(y) = 2\pi Z_1Z_2e^2N_p[\sqrt{y^2 + c^2a_{T.F}^2} - y] \quad (1.11)$$

where $N_p = Nd_p$ is planar density of atoms, N : bulk density of atoms in the crystal, d_p : Interplanar spacing, y : distance measured from the plane.

The critical angle for planar channeling is given by

$$\psi_p = \sqrt{\frac{2\pi N_p Z_1Z_2e^2a_{T.F}}{E}} \quad (1.12)$$

1.2.1 Interatomic potentials:

A thorough knowledge of the interatomic potential is essential for better understanding of various physical phenomena in the field of ion-solid interactions in general and channeling in particular. The choice of potential for use in the atomic scattering calculations has been discussed by *Lindhard et al.* [11]. For most of the scattering calculations, where overall effects are involved, the Thomas-Fermi statistical model is good enough in accuracy for most of the experimental situations. Anything beyond this statistical model of Thomas-Fermi, requires computer calculations.

Other forms of interatomic potentials [12] used include Moliere potential, Born-Mayer potential etc.

$$V_{M_o}(R) = \frac{Z_1 Z_2 e^2}{R} (0.35e^{-bR} + 0.55e^{-4bR} + 0.1e^{-20bR}) \quad (1.13)$$

where $b = 0.3/a_{T.F}$

Firsov proposed other form of screening given by [13]

$$a_F = \frac{0.8853}{(Z_1^{1/2} + Z_2^{1/2})^{2/3}} a_o \quad (1.14)$$

For $Z_1 \ll Z_2$, $a_F \cong a_{T.F}$.

Sometimes *Born-Mayer* [13] and *Bohr* [14] potentials have also been used.

$$V_{BM}(R) = A_{BM} \exp(-R/a_{BM}) , \quad (1.15)$$

a_{BM} is Born-Mayer screening radius.

Bohr potential is a simple potential of screened Coulomb type and given by

$$V_{BO}(R) = \frac{Z_1 Z_2 e^2}{R} \exp(-R/a_b) \quad (1.16)$$

$$a_b = a_o (Z_1^{2/3} + Z_2^{2/3})^{-1/2} \quad (1.17)$$

Here a_b has the drawback of excessive screening at large distances so that potential decreases too rapidly to fit actual ion-atom interactions. There is no single potential which can be used for all analytical calculations in the context of ion solid interactions in general and for effects of defects in particular. Alternative mathematical approximations of both planar [15] and axial [16] potentials have been made in order to get some analytical results in complicated problems involving the effects of defects like dislocations and stacking faults [17] etc., on channeling. Another form of potential proposed by the *Pathak* [18] is analytically simple, especially for the study of defects and dechanneling of the particles and hence it has been used extensively. So we use this potential through out the thesis which is given by

$$V_{PM}(R) = \frac{Z_1 Z_2 e^2}{R} \frac{C a_{T.F}^2}{(R + a_{T.F})^2} \quad (1.18)$$

Substituting $V_{PM}(R)$ in Eqn. (1.10), one gets

$$V_{PM}(y) = 2\pi Z_1 Z_2 e^2 N_p \int_0^\infty r \frac{1}{\sqrt{r^2 + y^2}} \frac{C a_{T.F}^2}{(\sqrt{r^2 + y^2} + a_{T.F})^2} dr \quad (1.19)$$

Evaluation of this integral is straight forward and one gets as

$$V_{PM}(y) = \frac{2\pi Z_1 Z_2 e^2 N_p C a_{T.F}^2}{y + a_{T.F}}. \quad (1.20)$$

As shown in Fig. (1.4), l is half width of planar channel ($l = d_p/2$); d_p being the interplanar distance, x is the distance measured from the axis of the channel in the transverse direction, $x_c \approx a_{T.F.}$ is distance of closest approach. The potential experienced by the particle in the channel is superposition of the potential due to both the planes (i.e., $V_{PM}(l \pm x)$) which is given by

$$V_{PM}(x) = 2\pi Z_1 Z_2 e^2 C a_{T.F}^2 N_p \left(\frac{1}{l + a_{T.F} - x} + \frac{1}{l + a_{T.F} + x} \right) \quad (1.21)$$

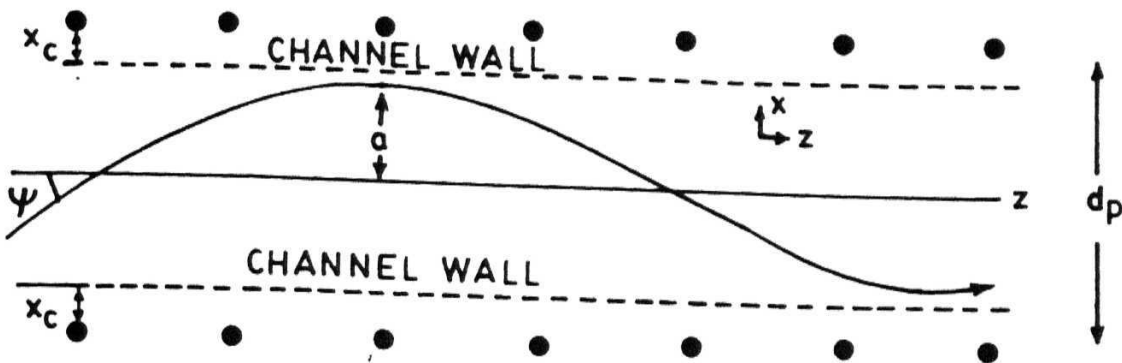


Fig. 1.4 : Propagation of the particle through the planar channel along z -direction. Here x is transverse co-ordinate.

1.3 Applications of Channeling:

The radiation damage studies on charged particle propagation have been essentially motivated by the technological importance of radiation damage in materials science. Charged particle propagation through damaged solids has been used mostly either as a *probe* for studying the defects themselves or for changing structural, mechanical or electrical properties of materials by implanting the required species into the host.

1.3.1 Study of defects (radiation damage):

Channeling technique is very useful in the study of both point and as well as extended defects in the solid. One can really pin point the exact position of the foreign impurity by performing channeling experiments [19] in various crystallographic directions. The channeling back-scattering technique has now been extended even to identifying the orientations formed by the foreign atoms or self interstitials with the irradiation-induced interstitial of the host lattice. One can study the nature and concentration of damage already present depending upon energy; dechanneling cross-section etc and these are discussed in the next section.

1.3.2 Surface Studies:

The application of ion beams to surface physics has been investigated by several authors [20, 21], both for pure and clean surfaces. Using channeling technique, one can deduce information on the structure of a few surface layers. At the same time one can measure the amount of strain present in these defective and damaged surfaces. This is very important especially in fabrication of semiconductor devices, where the knowledge and control of damage can be enormous value in technological applications.

1.3.3 Ion implantation in technology:

By ion-implantation it is possible to change various kinds of properties especially in semiconductor technology. The most important and useful application is to devices where, mainly three effects are used:

- (i) Impurity doping, where the doping amount as well as the depth distribution is required to be known for optimum use of the doped material.
- (ii) Compound formation at the surface and in the bulk of silicon crystals to get known thickness and concentration.
- (iii) Disorder introduction.

Ion implantation technique is also used in solar cell fabrication.

1.3.4 Channeling Radiation:

The idea that the oscillatory motion of channeled charged particles should lead to emission of radiation *has* been discussed from the very beginning, on the basis of electrodynamics. However since the oscillatory frequencies ω_o are low, the corresponding energies $\hbar\omega_o$ are of the order of a few eV only, the observation of the radiation seemed

difficult. The realization that relativistic effects will shift the photon energy into keV or even MeV region was a turning point, and the radiation was in fact observed for the case of positrons about 20 years ago [22]. This *channeling radiation* has been studied for the past 20 years and the subject has been reviewed by several authors [23]. Theory was formulated [24] in the relativistic quantum mechanical framework and the experimental confirmation is made for the case of positrons [22] and electrons [25]. Another interesting phenomena so called *quasi-channeling* is discussed by Henry Makowitz [26], with specific reference to positrons and electrons, where it has also been outlined regarding their feasibility to construct a short wave length laser. The radiation as a result of scattering of the channeled electrons by the point defects has been shown to be coherent [27] which again can be applied for generating tunable lasers.

Apart from their direct application, this observation of radiation from channeled ions has opened possibilities of new applications in the fields of laser physics and medicine as a source of hard X-rays and γ -rays for nuclear pumping, hence for possible construction of a γ -laser. These X-rays created as part of channeling, opens new prospectives in plasma physics research, laser technology and medicine. This lead to new phenomena namely *photon channeling* and related *X-ray optics* [28].

1.3.5 Beam extraction by bent crystal **channeling**:

The deflection of the charged particle beam using a curved crystal is distinctly different from deflection with a magnet. The amount of deflection is entirely determined by the physical curvature of the crystal planes, along which the particles are channeled. This effect namely steering of high energy (GeV) particles through *bent crystals* has tremendous practical applications [29]. A well channeled positive particle will follow the curved path along the bent channel, provided the curvature of the crystal is not too large to cause heavy dechanneling of the particle beam. However, dechanneling still

occurs due to ordinary **dechanneling** as well as because of the bending process. Bending of the crystal is basically equivalent to introducing a centrifugal energy potential and thereby lowering one side of the potential well and raising the other. So actual potential well in the channel is modified by this linear centrifugal energy barrier which depends upon the local curvature. As a result the channeled fraction of the beam followed the direction of the downstream end of the crystal. *Tsyganov* [30a)] estimated the critical radius of bending as $R_T = E/eE_c$, where E is total energy of the particle and E_c is the interatomic electric field intensity at a distance from the plane at which the particle is unstable due to interaction with individual atoms. This critical radius can be related to an equivalent magnetic field for a relativistic particle in a magnetic field as $R = p/0.03B$; p in (GeV/c), B is in kG and R in m. This crystal field is very strong and exceeds by many orders of magnitude as compared to external magnetic field produced in the laboratory. A more important selection involves incident particle direction. To be deflected, the particle must be incident within the critical angle for channeling along the particular plane being used. Even for the particles incident within the planar angle, those with large divergence will be lost more rapidly, as the critical curvature or the particle momentum are increased. This technique is very useful, especially for bending and focussing of the particle beam. *Baublis et. al.* [306)] reviewed regarding these bent crystal channeling experiments and preparation of the suitable crystals for these experiments.

1.4 Dechanneling by defects:

It is well known fact that real crystals are never perfect as they contain lattice defects which lead to **dechanneling**. The most general kinds of defects found in solids are vacancies, self interstitials, foreign atoms, stacking faults, grain boundaries, dislocations,

voids, gas bubbles, etc.. Even if the defects are not present before irradiation of the crystals, they are created during particle propagation and hence affect the propagation of the particles *selfconsistently*. This reflects the importance of the ion beam interaction with the defects.

A charged particle propagating through real solids can *see* the presence of the defects through the effects these defects will produce in the solids. Classically the particle can see the presence of defects by either direct obstruction of the particle path, or distortion produced in the crystals. When the projectile is affected by the potential of the defect, its trajectory is modified. These effects are of obstruction type. Examples are stacking faults, interstitial atoms, grain boundaries etc. If the defects give rise to distortion in a certain region of the crystal, disturbing the regularity of the material in that region, the effects are of distortion type, for example dislocations. These two kinds of defects give rise to obstruction dechanneling and distortion dechanneling respectively.

But the dechanneling may also be caused by the combination of the both, and in such cases this dechanneling is neither purely of obstruction type nor of distortion type and this phenomena is called composite dechanneling. This happens because of the fact that the defects produced in the solid are *not* uniquely of one type but a combination of different kinds of defects or because the defect itself gives rise partly to obstruction effects and partly to distortion effects, for example gas bubbles, Guinier-Preston zones etc. There are enormous applications of study of gas bubbles in nuclear reactors. During the process of nuclear fission, fragments are released into the fuel which have some atomic mass distribution and few of these fragments consist of inert gasses such as Kr, Xe. These inert gas atoms are not able to form compounds and take the form of an *agglomerate* provided their mobility in the solid is sufficient. These *agglomerates* are called gas bubbles. The effects of these gas bubbles on the channeled particles have been studied by *Quere et al.*[31]. Two main sources of dechanneling

by these gas bubbles are (i) The charged particle is scattered in the bubble by gas atoms which causes change in trajectory and transverse energy E_{\perp} of the particle. (ii) it may touch the exit surface and get dechanneled, though there is no change in ' ψ '. Another very important application of gas bubbles in materials science relevant to reactor physics is, in connection with blistering studies[32] where the escape gas bubbles from the material surface induces drastic changes in the surface properties. In contrary to these gas bubbles, another kind of imperfections namely *Guinier-Preston*(G.P.) zones distort the lattice and give rise to hardening. These zones are basically small clusters formed by super saturated solute atoms in several alloys. The dechanneling method is a fairly sensitive method for observing and studying the precipitation of these G.P. zones [33].

Channeling and back scattering experiments with energetic ions have been widely employed for defect analysis in *Ion-implanted semiconductors* [34]. In the aligned spectra, a well resolved disorder peak is usually observed at the range of the implanted ions, originating from the direct back scattering of the probe particles from the displaced atoms. However, aligned back scattering spectra from the ion bombarded metals indicated an increase in dechanneling yield and show no damage peak [35]. The simultaneous use of channeling, back scattering and TEM [36], is a promising procedure to correlate the dechanneling observations with damage configurations. In addition, dechanneling analysis itself is effective technique by which different types of defects may be separated out. This differentiation is possible on the basis of the qualitative energy dependence on dechanneling cross sections [37] and dechanneling yields obtained by defect analysis [38]. The qualitative energy dependence of these yields carry the information on the kind of defects present in the material. For example, \sqrt{E} dependence indicate dislocations, $E^0 \rightarrow$ stacking faults, gas bubbles [39] and $E^{-1} \rightarrow$ randomly distributed atoms.

1.5 Quantum-Mechanical Effects:

Lindhard's classical theory of channeling provides a complete description of channeling phenomena for relatively heavy ions. However when the work on electron microscopy especially TEM with crystalline materials was being extended to channeling phenomena, there were clear indications of quantum and diffractive effects dominating the patterns. The quantum mechanical treatments [40] indicated that it is the product of the mass of the particle and the strength of the interaction between the particle and the crystal which determines applicability of classical or quantum picture. The classical features start becoming dominant as this product increases. This product should be small for the validity of quantum mechanical treatments. These have been revealed in fact in electron and positron channeling; the angular dips for these particles show a fairly oscillating structure [41]. Thus protons and all other heavier ions behave classically whereas electrons, positrons, neutrons and mesons would be expected to behave quantum-mechanically [42]. *Chadderton* [43] outlined that even protons also exhibit wave particle nature when their energy is very low (\sim few keV). Though neutrons are as heavy as protons, the Fourier component of the potential strength is still weak so that the product of mass and potential strength remains small and hence diffraction effects are dominant.

Moreover, in order that diffractive effects to be observed, it is necessary that dimensions of the regions/obstacle, limiting the motion of the particle (normally this is \sim lattice period) must be appreciably larger than the de Broglie wave length associated with the particle [44], similar to the situations in wave optics. This de Broglie wave length can be estimated by the equation $\lambda = hc/E$ where, h is plank constant, c is speed of light and E is energy of the particle. This de Broglie wave length, say for example 12 MeV positrons is $\sim 10^{-3} \text{ \AA}$ [45]. It is well known that GeV electrons ($\lambda \sim 10^{-14} \text{ cm}$) are

used to study the nuclear structures, because these are of the dimensions of $\sim 10^{-12} \text{cm}$ and the particle wavelength here is much smaller than 10^{-12}cm .

Quantum mechanically, the longitudinal and transverse components are separated out [46], the transverse motion for positively charged particles (like positrons) is described by one dimensional Schrodinger equation with a harmonic oscillator potential where, the potential minima are located at middle axis of the axial/planar channel. For electrons, the potential minima are at the center of the atomic strings or planes and channeled electrons have an increased probability for hard collisions with atoms. So the transverse potential for electrons is approximated to one dimensional hydrogen atom [47]. This implies that channeling states for electrons are much less stable than for positrons [48] and the maximum number of quantum states supported by the transverse potential (say n_{max}) for positrons is smaller than that for the electrons. So the solutions of the corresponding Schrodinger equations for electron as well as positron, gives rise to quantized transverse energies. Hence number of quantum states are formed and the transverse energy assumes a series of discrete values. The maximum number of bound states supported by transverse continuum potential increases with the relativistic particle mass i.e., $n_{\text{max}} \propto \sqrt{\gamma m}$, where the Lorentz factor, $\gamma = 1/\sqrt{1 - v_z^2/c^2}$ and m is the rest mass of the particle.

The validity of classical or quantum picture has also been discussed on the basis of correspondence principle [49]. As mentioned earlier, when the particle energy or the mass of the particle increases, the number of quantum states supported by the transverse potential also increases ($n_{\text{max}} \propto \sqrt{\gamma m}$). So obviously, for heavy ions and high energy electrons/positrons, the motion becomes more classical. However quantum effects are dominant when the number of quantum states supported in the potential well is small and this is the case for light particles (electron/positron) of Mev energy. The assumption of separation of transverse and longitudinal motion is fairly accurate

and we continue to use it in our present Quantum descriptions also.

As mentioned in the earlier section, charged particle can be used as probe to study various defects present in the crystals. In this connection the light particles especially positrons are found to be very useful as they are more sensitive to probe various kinds of defects present in the solid [50]. More over these light particles can also be used for the possible construction of the three dimensional holography [51], which is another potential area of current research.

1.6 Outline of the Thesis:

The most of the work on dechanneling by defects is based on several simplifying assumptions restricting the validity of the results. For example, although qualitatively the results on energy dependence etc., are reliable, quantitatively the accuracy is poor. Therefore more work, possibly using quantum mechanical and/or field theoretical techniques is needed to treat the whole defect problem in a more accurate way. In this spirit quantum mechanical formulations have been made and theoretical descriptions for extended defects like stacking faults and dislocations are given.

In Chapter 2, we discuss about the evolution of dechanneling concept in quantum mechanical framework. We present a quantum mechanical formulation for effects of stacking faults on dechanneling. At the stacking fault boundary, the quantum states in the transverse potential make transitions for which probabilities have been calculated using sudden approximation. However, the continuum potentials in particular used in the discussion are in principle valid for infinite planes where in the case of stacking fault we had half planes i.e., those ending at the fault and those starting from the fault. So the transverse potential is slightly complicated just at the interface and one has to match the appropriate basis wave functions at the interface of the stacking fault

boundary. An estimation regarding the effects of periodicity of transverse potential on dechanneling probabilities is made.

In chapter 3, a quantum mechanical treatment of the effects of dislocations on planar dechanneling is given. The effects of channel distortion due to dislocation are incorporated through a relativistic centrifugal energy term. We evaluated the number of quantum states supported by this distorted channel and the transition probabilities among these states due to distortions in the planar channel; the resulting dechanneling probabilities for varying distortion are calculated using sudden approximation. The energy dependence of these dechanneling probabilities for initially well channeled particles has been estimated and we show that it varies linearly with energy for relativistic particles.

In chapter 4, a quantum mechanical formulation is developed by relaxing the sudden approximation used in the chapters 2 and 3, where bound - bound transitions are considered. In this chapter we consider the transitions from these bound states to scattering states due to lattice distortions in the planar channel, using time dependent perturbation theory. The resulting expressions for dechanneling probabilities and hence for dechanneling cross-section for initially well channeled particles has been estimated and qualitative features like dechanneling radius, energy dependence etc., are discussed.

Chapter 5 contains a summary of work, concluding remarks and comments on possible future directions of research work in this field.

References

1. M. von Lau *Historical Introduction to International Tables for X-ray Crystallography*, Vol. **1**, Eds. N. F. M. Henry and K. Lonsdale (Kynoch Press, 1952).
2. M. W. Thompson *Contemp. Phys.* **9**, 375 (1968).
3. J. Stark *Z. Phys.* **13**, 973 (1912);
J. Stark and G. Wendt *Ann. Phys.* **38**, 921 (1912).
4. J. A. Davies, J. Friesen and J. D. McIntyre *Can. J. Chem.* **38**, 1526 (1960);
J. A. Davies, J. D. McIntyre, R. L. Cushing and M. Lounsbury
Can. J. Chem. **38**, 1535 (1960).
5. P. K. Rol, J. M. Fluit, F. P. Vichbock and M. DeJong
Proc. Forth. Int. Conf. on Ionization Phenomena in Gases,
Ed: N. R. Nilsson, (North Holland, Amsterdam), pg. 257 (1960).
6. O. Almen and G. Bruce *Nucl. Instrum. Methods* **11**, 279 (1961).
7. Mark T. Robinson and Ordean S. Oen, *Phys. Rev. B* **132**, 2385 (1963).
8. a) H. O. Lutz and R. Sizmann *Phys. Lett.* **5**, 113 (1963);
G. R. Piercey, F. Brown, J. A. Davies and J. A. McCargo
Phys. Rev. Lett. **10**, 399 (1963).
b) W. Brandt, *Scientific American* **218**, 90 (1968).
9. J. Lindhard, *Phys. Lett.* **12**, 126 (1964);
K. Dan. Vidensk. Selsk. Mat. Fys. Medd. **34**, (No. 14) (1965).
10. C. Erginsoy, *Phys. Lett.* **15**, 360 (1965).

11. J. Lindhard, V. Nielsen and M. Scharff,
K. Dan. Vidensk. Selsk Mat. Fys. Medd. 36 (10) (1968);
D. J. O'Conner and J. P. Biersack, *Nucl.Instrum. Methods B* 15, 14 (1986).
12. I. M. Torrens, *Interatomic potentials* (Acad. Press, N.Y., 1972).
13. O. B. Firsov, *Sov. Phys. JETP* 5, 1192 (1957); 6, 534 (1958);
M. Born and J. E. Mayer, *Z. Phys.* 75, 1 (1932).
14. N. Bohr *K. Dan. Vidensk. Selsk. Mat. Fys. Medd.* 18, (No. 8) (1948).
15. J. Mory and Y. Quere, *Rad. Eff.* 13, 57 (1972).
16. J. Rosner, W. M. Gibson, J. A. Golovchenko, A. N. Goland and H. E. Wegner
Phys. Rev. B 18, 1066 (1978).
17. J. More, *J. Physique* 32, 41 (1971).
18. A. P. Pathak *J. Phys. C* 8, L439 (1975); *Rad. Eff.* 61, 1 (1982).
19. J. U. Andersen, O. Andreassen, J. A. Davies and E. Uggerhøj,
Rad. Eff. 7, 25 (1971); J. U. Andersen, E. Laegsgaard and L. C. Feldman
Rad. Eff. 12, 219 (1972); S. Nagata, S. Yamaguchi, H. Naramoto
and Y. Kazumata *Nucl.Instrum. Meth in Phys. Res. B* 48, 231 (1990).
20. John H. Barrett, *Nucl. Instrum. Methods* 149, 341 (1978);
S. T. Picraux, L. R. Dawson and G. C. Osbown
Appl. Phys. Lett. 43, 930 (1983);
S. T. Picraux, L. R. Dawson, G. C. Osbown, R. M. Biefeld and W. K. Chu
Appl. Phys. Lett. 43, 1020 (1983).

21. S. T. Picraux, *New uses of ion accelerators* (ed.) J. F. Ziegler; (Plenum, N. Y., 1973); D. V. Morgan (ed.), *Channeling* (Wiley, N. Y., 1973); L. C. Feldman, *Physica Scripta* 28, 303 (1983).
22. M. J. Algard, R. L. Swent, R. H. Patnell, B. L. Bermen, S. D. Bloom and S. Datz, *Phys. Rev. Lett.* 42, 1148 (1979).
23. R. H. Patnell and M. J. Alguard *J. Appl. Phys.* 50, 798 (1979); R. Wedell, *Phys. Stat. Sol. (b)* 99, 12 (1980); V. V. Beloshitsky and F. F. Komarov *Phys. Rep.* 93, 117 (1982); J. U. Andersen, E. Bonderup, E. Laegsgaard and A. H. Sørensen *Phys. Scripta* 28, 308 (1983); J. C. Kimball and N. Cue *Phys. Rev. Lett.* 52, 1747 (1984); Anand P. Pathak *Phys. Rev. B* 31, 1633 (1985); J. Lindhard *Phys. Rev. A* 43, 6032 (1991); L. V. Hau and J. U. Andersen *Phys. Rev. A* 47, 4007 (1993); Nikolai V. Laskin, Alexander I. Zhukov *Nucl. lustrum. Meth. in Phys. Res. B* 108, 251 (1996); Haakon A. Olesen and Yuri Kunashenko *Phys. Rev. A* 56, 527 (1997).
24. M. A. Kumakhov and R. Wedell *Phys. Stat. Sol. (b)* 84, 581 (1977).
25. R. L. Swent, R. H. Patnell, M. J. Alguard, B. L. Bermen, S. D. Bloom and S. Datz *Phys. Rev. Lett.* 43, 1723 (1979); M. Gouanare, D. Silloun, M. Spiighel, N. Chu, M. J. Gaillard, R. G. Kirsch, J. C. Poizat, J. Remillicux, B. L. Bermen, P. Catillon, L. Roussel, G. M. Temmer *Phys. Rev.* 38, 4352 (1988).
26. Henry Makowitz *Rad. Eff.* 106, 117 (1988).
27. E. A. Kovaleva and V. S. Malyshevsky *Rad. Eff.* 106, 47 (1988).
28. M. A. Khumakov, *Nucl. lustrum. Methods in Phys. Res. B* 48, 283 (1990).

29. S. Datz, C. Erginsoy, C. Liebfried and H. O.Lutz *Ann.Nucl.Sci.* 17, 129 (1967);
A. F. Elishev *et.al*, *Phys. Lett.* **88** B, 387 (1979).
Physics today, search and discovery, (May 1980).
R. A. Carrigan Jr., and J. A. Ellison (eds.) *Relativistic channeling*,
(NATO ASI Series B **165**), (Plenum, N. Y., 1987).
30. a) E. N. Tsyganov, Fermi lab **TM-682, TM-684**, Batavia, 1976.
b) V. V. Baublis, A. V. Khanzadeev, V. V. Kuryatkov, E. G. Lapin,
N. M. Miftakhov, S. R. Novikov, T. I. Prokofieva, V. M. Samsonov, G. P. Solodov,
B. B. Loginov, M. N. Strickhanov, R. A. Carrigan Jr., D. Chem, and C. T. Murphy
Nucl.Instrum.Meth.inPhys. Res. B 119, 308 (1996).
31. Y. Quere, *J. Nucl. Mat.* 53, 262 (1974); D. Polonsky, G. Desarmot,
N. Housseau and Y. Quere, *Rad. Eff.* 27, 81 (1975).
32. S. K. Das and M. Kaininsky in *Application of Ion beams to Metals*,
S. T. Pecraux, E. P. EerNisse and F. L. Vook (eds.) (Plenum press, N. Y., 1974)
and references there in.
33. G. Desarmot, *Phys. Lett.* 46 A, 159 (1973).
34. J. W. Mayer, L. Eriksson and J. A. Davies, *Ion Implantation in semiconductors*
(Academic press, N. Y., 1970).
35. P. P. Pronko, J. Bottiger, J. A. Davies and J. B. Mitchell
Rad. Eff. 21, 25 (1974).
36. W. F. Tseng, J. Gyulai, T. Koji, S. S. Lau, J. Roth and J. W. Mayer
Nucl. Instrum. Meth. 149, 615 (1978).
37. Y. Quere, *Rad. Eff.* **28**, 253 (1976).

38. E. Rimini, S. U. Campisano, G. Foti, P. Baeri and S. T. Picraux,
Ion beam surface layer analysis Eds. O. Mayer, G. Linker and F. Kappeler
(Plenum press, N. Y., 1976) pg. 597
39. Danuta Ronikier-polonsky, Goerges Desarmot, Nicole Housseau and Yves Quere
Rad. Eff. 27, 81 (1975).
40. R. E. DeWames, W. F. Hall and G. W. Lehman *Phys. Rev.* **148**, 181 (1966);
M. W. Thompson, *Contemp. Phys.* 9, 375 (1968); A. P. Pathak and M. Yussouf,
Phys. Rev. B 2, 4723 (1970); A. P. Pathak *Phys. Rev. B* 9, 2406 (1974).
41. J. U. Andersen, W. M. Augustyniak and E. Uggerhøj
Phys. Rev. B 3, 705 (1971)
42. D. S. Gemmel *Rev. Mod. Phys.* 46, 129 (1974); L.V. Hau, J. A. Golovchenko,
R. Haakenaasen, A. W. Hunt, J. P. Peng, P. Asoka- Kumar, K. G. Lynn,
M. Weinert, and J. C. Palathingal *Nucl.Instrum. Meth. in Phys. Res. B*,
119, 30 (1996).
43. L. T. Chadderton, *Phys. Lett.* 23, 303 (1966).
44. R. E. DeWames, W. F. Hall and G. W. Lehman *Phys. Rev.* **174**, 392 (1968);
F. Grasso, M. Lo Savio and E. Rimini *Rad. Eff.* 12, 149 (1972); A. P. Pathak
Phys. Rev. B 7, 4813 (1973); Philip Lervig, Jens Lindhard and Vibeka Nielsen
Nucl. Phys. A 96, 481 (1967).
45. D. terHaar, *Problems in quantum mechanics*, (pion ltd., London, 1975) pg 215.
46. R. Wedell *Phys. Stat. Sol. (b)* **99**, 11 (1980);
Zhirong Huang, Pisin Chen and Ronald D. Ruth
Phys. Rev. Lett. **74**, 1759 (1995).

47. S. Sathpathy and A. P. Pathak *Phys. Stat. Sol. (b)* **153**, 455 (1989).
48. J. U. Andersen, E. Bonderup and R. H. Patnell
Ann. Rev. Nucl. Part. Sci. 33, 453 (1983).
49. Leonard I. Schiff, Quantum Mechanics, *McGraw Hill* (1968);
Zhirong Huang, Pisin Chen and Ronald D. Ruth
Nucl. Instrum. Meth. in Phys. Res. B 119, 192 (1996).
50. Peter. J. Schultz, Guiti R. Massoumi and W. N. Lennard
Nuclear Instrum. and Meth. in Phys. Res. B **90**, 567 (1994);
M. J. Pusaka and C. Corbel *Phys. Rev. B* 38, 9874 (1988);
M. J. Pusaka, C. Corbel and R. M. Nieminen *Phys. Rev. B* 41, 9980 (1990).
for a review see, M. J. Pusaka and R. M. Nieminen,
Rev. Mod. Phys. 66, 841 (1994).
51. Akira Tonomura *Rev. Mod. Phys.* 59, 639 (1987).

Chapter 2

Quantum description of dechanneling by stacking faults

2.1 Introduction to quantum dechanneling theory:

In the introductory chapter, we outlined the possible usages of the classical descriptions and also discussed the need for quantum mechanical treatments, especially for dechanneling of electrons and positrons. Classically, dechanneling effects caused by the defects are explained on the basis of the transverse energy. The presence of the defect in the vicinity of the projectile leads to significant modification in trajectory of the particle, increasing its transverse energy. When this transverse energy exceeds a *critical value* ($E_{\perp}^c \sim E\psi_c^2$), the particle is no longer confined to its actual path and eventually gets dechanneled. Most of the classical treatments of dechanneling theory are based on the diffusion equation for the transverse energy [1]. This yielded diffusion coefficients [2] where the effects of the defects are suitably incorporated through various quantities. These include momentum transfer, its gradient along the direction of propagation, electronic part as well as nuclear contributions. The integration over all the possible transverse energies give *dechanneling probability* (x). Owing to the amplitude and the phase of the approaching particle, the amount of dechanneling caused by the defect is calculated. Furthermore, one can realize the difficulty in predicting these quantities precisely. So dechanneling probability is obtained by averaging all the

possible phase co-ordinates and we say that the particle is dechanneled when its amplitude exceeds the *critical amplitude* A_c (the maximum amplitude beyond which the particle gets dechanneled). Even though these classical dechanneling results especially on energy dependence are reliable, detailed dynamics of the particle during its passage through defected region is not so clear. Hence it is important to have a complete description of the particle during its passage through the defected region. So quantum mechanical approach is better choice, particularly for electron/positron dechanneling studies. This is mainly because of its inbuilt structure which enables effective handling of these dechanneling processes. The utility of quantum mechanics lies in the fact that it provides various analytical techniques which can be used appropriately.

Moreover the quantized nature of the transverse motion of few Mev electrons/positrons has been nicely revealed through the *channeling radiation spectroscopy* [3], where the discreteness is reflected through the number of bound states available in the phase space. So one can realize the importance and need of full quantum mechanical framework, especially to investigate *inherent symmetries* involved in the defect problem, because these symmetries contain much physics to give better insight into the actual problem. The quantum mechanical methods have already been used in the light of channeling radiation to understand various properties like monochromaticity, tuning by variation of the energy associated with the channeled particle and the polarization; many papers and review articles have already been published especially for electron and positron channeling radiation [4]. However, in addition to their usefulness in channeling radiation spectroscopy, these particles are very sensitive in probing various defects present in the crystals. So more research work has to be done in physics as well as application view point of electron and positron propagations in the pure and defective crystals.

In quantum mechanical framework, the transverse energy is quantized. Initially, depending upon the angle of incidence, the particle occupies any one of these quantum states supported by the transverse potential well. If the particle is injected into the crystal with an angle greater than ψ_c , it gets dechanneled at the entry surface itself. This is because of the fact that the transverse energy of the particle in this case is much higher than the *critical transverse energy* ($E\psi_c^2$), implying that there are no bound states supported by the transverse potential well. However, those particles with small incident angle refers to initially channeled particles which carry the signature of the presence of the defect. Owing to the influence of the defect, the particle goes to any one of the excited states and this is again as a result of increase in the transverse energy. If this influence is strong enough to cause a transition to an *above barrier state* (state near the top of the potential well), the particle is no longer bounded; it goes to continuum of states and this leads to dechanneling. So quantum mechanically dechanneling means transition from a *bound state* to *scattering state* due to increase in the transverse energy. This is analogous to classical interpretation of dechanneling phenomena, where we notice that transition from *aligned* beam to *random* beam [5]. In the quantum description, the presence of the defect is taken as perturbation which induce transitions to various states. The dechanneling probability is obtained by evaluation of the transition amplitudes corresponding to appropriate wavefunctions; incorporated suitably in various regions of obstruction/distortion.

2.1.1 Electron and Positron Channeling:

For electron channeling, the electrons in the ground state of the transverse energy spectrum are dechanneled faster than those in excited states. Hence, the electrons corresponding to lower transverse energy states, oscillate around the atomic planes with a smaller amplitude so that overall they spend larger fraction of their time in the vicinity of atomic planes and hence get dechanneled at a faster rate than those corresponding to higher transverse energy, i.e., excited states. Both these mechanisms will tend to dechannel the ground state in the transverse energy spectrum electrons much faster. The propagation of the electron and its *rosette-motion* [6] can also be seen in the Fig. (2.1).

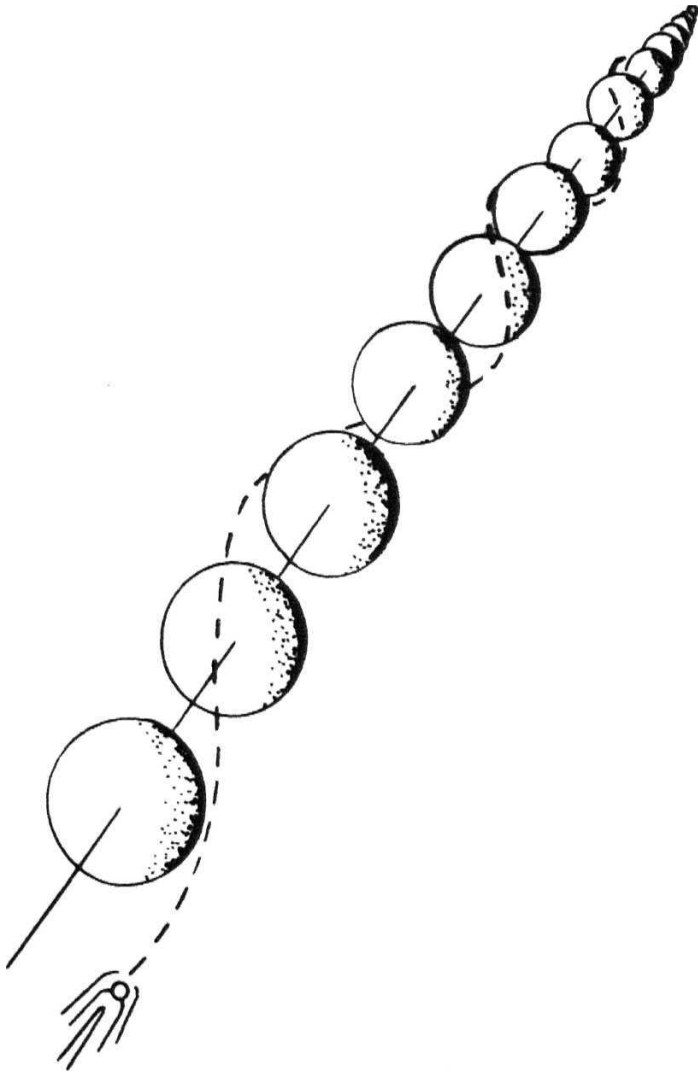


Fig. 2.1: Channeling trajectory of electron along a string of atoms in the crystal. The electron is trapped due to its interaction with the atomic string.

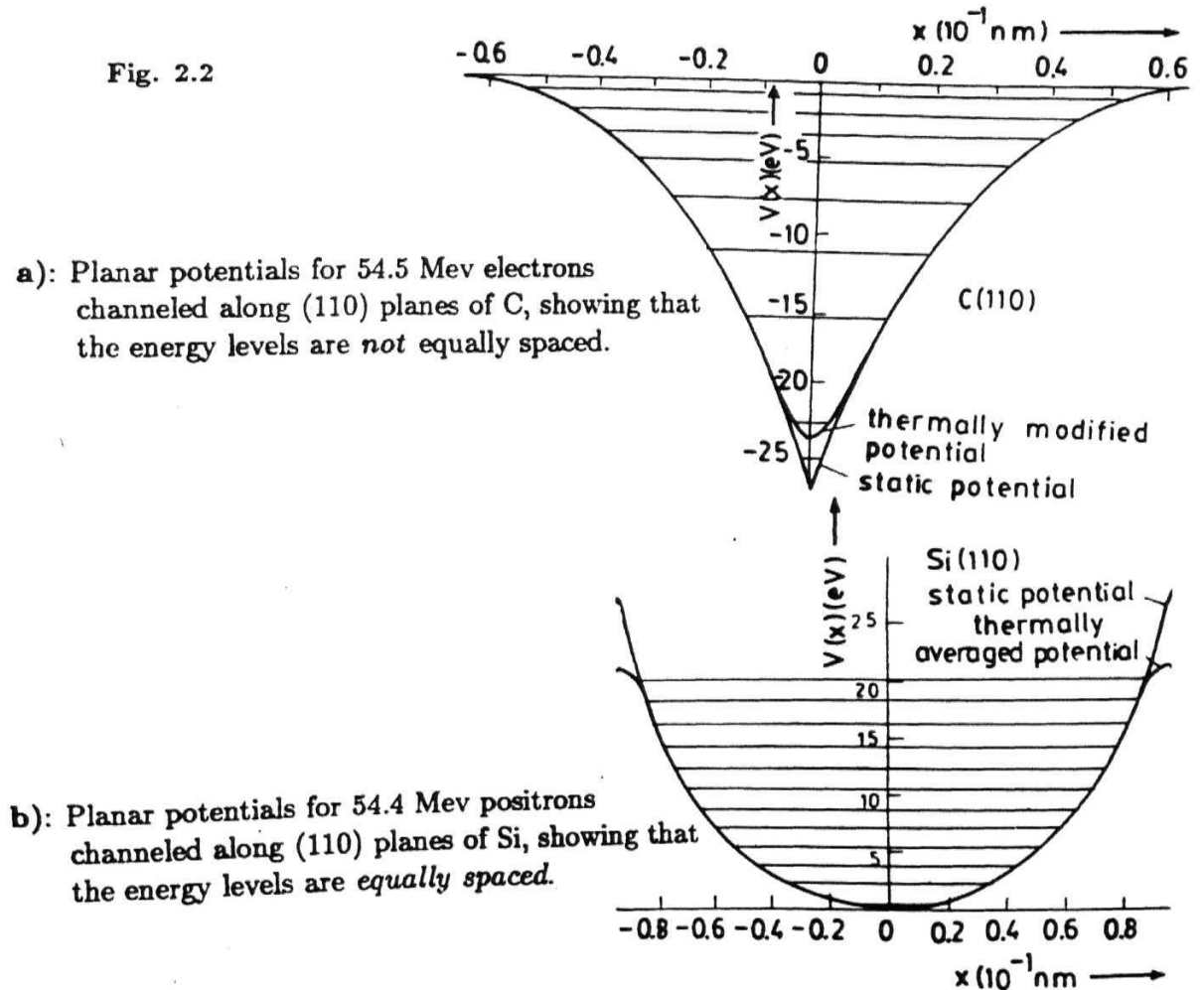
Hence the transverse potential for electrons is expected to be of the form

$$V(x) = A \exp(-|x|) + B \quad (\text{as shown in Fig. (2.2a)})$$

For the positrons because of opposite charge, situation is quite opposite to that described above [7] and the transverse potential for positrons is well approximated by simple harmonic oscillator given by

$$V(x) = V_o + \frac{1}{2} K x^2$$

As shown in Fig. 2.2 b), the ground state wavefunction of the positron is strongly localized about the channel axis ($x = 0$) and this enables the particle to confine itself along this axis. These particles refer to well-channeled configuration as they have less tendency to hit the atomic plane directly. On the other hand, the excited states will have more tendency to cause dechanneling, as expected.



2.1.2 Basis of the present model:

For particles channeled along major **crystallographic** planes or axes, the longitudinal component of the particle velocity remains nearly along incident direction and the transverse motion of the particle accounts for a very small fraction of the incident energy and to a good approximation remains constant.

As the particle energy increases the *critical angle* decreases because of $E^{-1/2}$ dependence so that even for relativistically fast particles the transverse energy $E\psi^2$ remains **non-relativistic**; the transverse motion of the channeled particle is described by usual Schrodinger equation with rest mass of the particle replaced by relativistic mass. The spin effects can be neglected as they are not important for the transverse motion [8] and it is possible to separate out the transverse and longitudinal motions [9]. The corresponding Schrodinger equation governing the transverse motion is given by

$$\left[\frac{-\hbar^2}{2\gamma m} \nabla^2 + V(\mathbf{r}) \right] \psi = E_{\perp} \psi$$

where γm is the relativistic mass of the particle [10]. $V(r)$ is the continuum potential due to strings or planes depending only on transverse coordinate x for planar channeling and two dimensional transverse space co-ordinate for axial channeling.

Through out the thesis, we concentrate on planar dechanneling of positrons for which we continue to use the potential discussed in the chapter 1.

We have

$$V(x) = 2\pi Z_1 Z_2 e^2 C a_{T.F.}^2 N_p \left(\frac{1}{l + a_{T.F.} - x} + \frac{1}{l + a_{T.F.} + x} \right)$$

This can be expanded around $x = 0$ to get equivalent potential in the harmonic approximation [11] which is given by

$$V(x) = V_o + \frac{1}{2} k_1 x^2$$

$$\text{where, } k_1 = \frac{2V_o}{(l + a_{T.F.})^2} \quad ;$$

$$V_o = \frac{4\pi Z_1 Z_2 e^2 C a_{T.F.}^2 N_p}{(l + a_{T.F.})}$$

Substitution of this potential in the Schrodinger equation described above, yields quantized transverse energy spectrum which is given by

$$E_n = (n + \frac{1}{2})\hbar\omega; \quad \omega = \sqrt{k_1/\gamma m}. \quad (2.1)$$

A stacking fault (S.F.) is an example of obstruction without any distortion as shown in Fig. (2.3 a)). At the stacking fault, the potential valleys present on the one side of the fault (say left) are completely shifted w.r.t the potential hills on the other side (say right), as shown in Fig. (2.3 b)). The amount of this stacking shift is denoted by a_s . For any charged particle passing through the stacking fault, the longitudinal component of energy is not much effected but the transverse energy undergoes a change. So basically it is a transition from one harmonic potential (left part of the fault) to other similar potential (right side of the fault), shifted by a_s .

In this chapter, we present a model quantum mechanical calculation for the case of stacking faults in otherwise perfect crystals. We discuss and compare the present results with existing classical results.

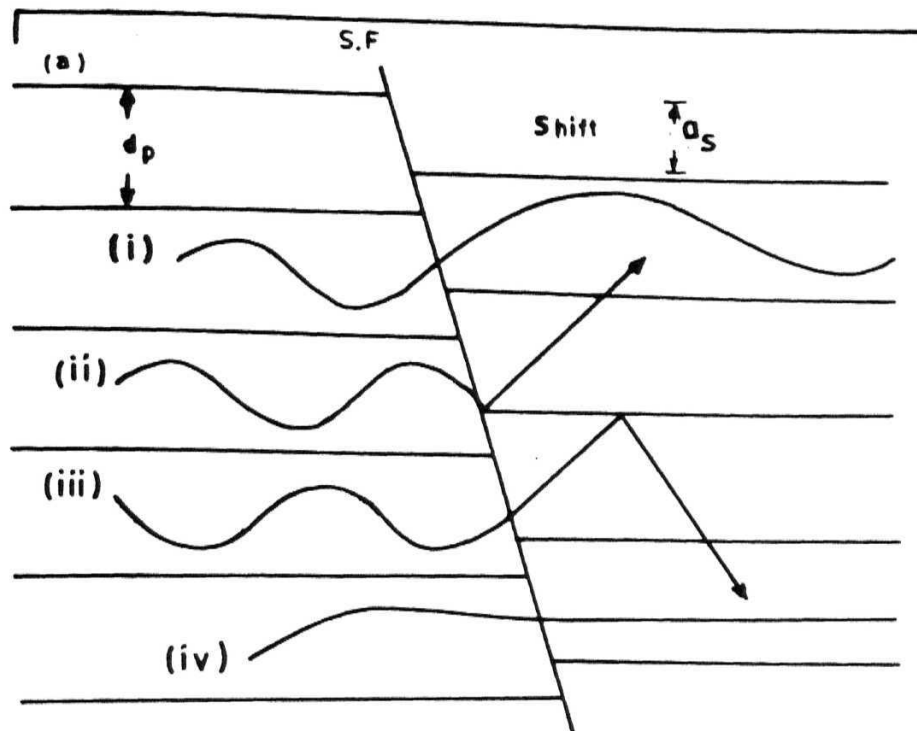


Fig. 2.3 a) : The stacking fault situation involving (i) improved channeling (ii) dechanneling at the fault (iii) dechanneling after the fault (iv) the particle becoming well channeled (with zero amplitude) due to various phases in approaching the fault, on the left hand side.

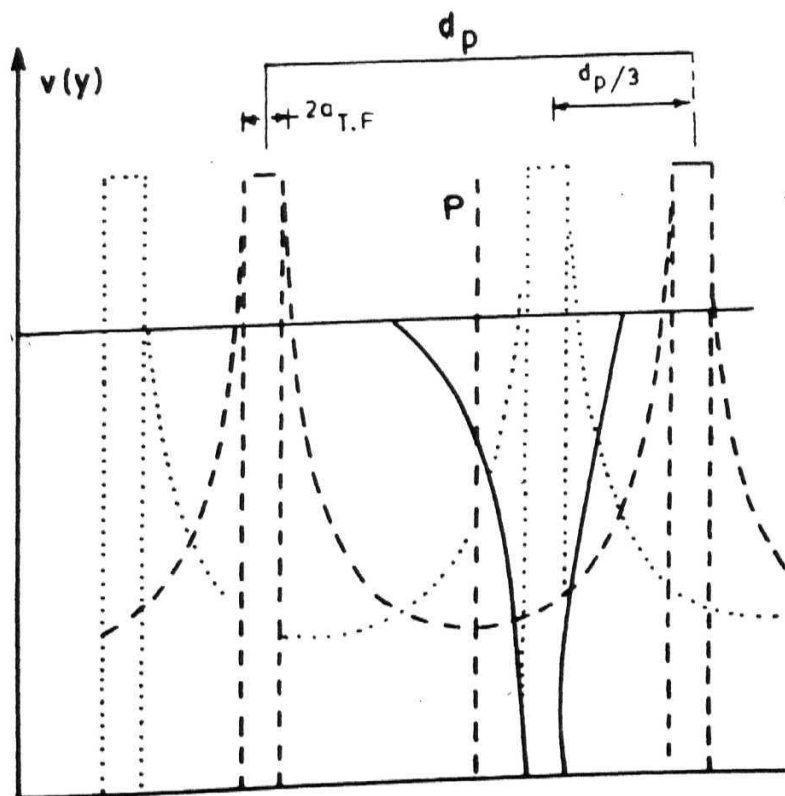


Fig. 2.3 b) : The obstruction of the potential valleys present on one side of the fault by the potential hills on the other side, where $a_s = dp/3$.

2.2 Theory and formulation:

The channeling phenomena under this situation is governed by the matrix element of the wave functions corresponding to left channel and right channel. Here the coupling constant α , appearing in the harmonic oscillator ($= \sqrt{\gamma m \omega / \hbar}$) will change to α' , just at the boundary between the two channels i.e., left channel and right channel. Hence the initial and final states of the particle are taken as

$$\psi_i(x) = |n\rangle, \quad \psi_f(x) = |m\rangle$$

$$\psi_i = \psi_L = \left(\frac{\alpha}{\sqrt{\pi} 2^n n!} \right)^{1/2} \exp\left(-\frac{\alpha^2 x^2}{2}\right) H_n(\alpha x) \quad (2.2)$$

$$\psi_f = \psi_R = \left(\frac{\alpha'}{\sqrt{\pi} 2^m m!} \right)^{1/2} \exp\left(-\frac{\alpha'^2 (x + a_s)^2}{2}\right) H_m(\alpha' x + \alpha' a_s) \quad (2.3)$$

where α, α' are coupling terms corresponding to left channel and the channel at the stacking fault respectively.

The matrix element is given by

$$\begin{aligned} \langle \psi_f | \psi_i \rangle &= \int_{-\infty}^{\infty} \psi_m^*(x) \psi_n(x) dx \\ &= \left(\frac{\alpha \alpha'}{\pi 2^{m+n} m! n!} \right)^{1/2} \int_{-\infty}^{\infty} \exp\left(-\frac{1}{2}[\alpha^2 x^2 + \alpha'^2 (x + a_s)^2]\right) \\ &\quad \times H_n(\alpha x) H_m(\alpha' x + \alpha' a_s) dx = \left(\frac{\alpha \alpha'}{\pi 2^{m+n} m! n!} \right)^{1/2} I_{n,m} \end{aligned}$$

where

$$I_{n,m} = \int_{-\infty}^{\infty} \exp\left(-\frac{1}{2}[\alpha^2 x^2 + \alpha'^2 (x + a_s)^2]\right) H_n(\alpha x) H_m(\alpha' x + \alpha' a_s) dx \quad (2.4)$$

The generating function for Hermite polynomial is given by

$$\begin{aligned} \sum_n \frac{z^n}{n!} H_n(x) &= \exp(2xz - z^2) \\ \Rightarrow \sum_{n=0}^{\infty} \frac{z^n}{n!} H_n(\alpha x) &= \exp(2\alpha xz - z^2) \\ \text{and } \sum_{m=0}^{\infty} \frac{s^m}{m!} H_m(\alpha' x + \alpha' a_s) &= \exp[2(\alpha' x + \alpha' a_s)s - s^2] \\ \Rightarrow \sum_{m,n} \left(\frac{z^n}{n!} \frac{s^m}{m!} \right) H_n(\alpha x) H_m(\alpha' x + \alpha' a_s) &= \exp[2x(\alpha z + \alpha' s) + 2\alpha' s a_s - (s^2 + z^2)] \end{aligned} \quad (2.5)$$

Multiplying both sides with $\exp\{\frac{1}{2}[\alpha^2 x^2 + \alpha'^2(x + a_s)^2]\}$ and integrating w.r.t x

$$\begin{aligned} \Rightarrow \sum_{m,n} \left(\frac{z^n}{n!} \frac{s^m}{m!} \right) I_{n,m} &= \exp\{2\alpha' s a_s - (s^2 + z^2)\} \left\{ \int_{-\infty}^{\infty} \exp\left\{-\frac{1}{2}[\alpha^2 x^2 + \alpha'^2(x + a_s)^2] + 2x(\alpha z + \alpha' s)\right\} dx \right\} \\ &= \exp\{2\alpha' s a_s - (s^2 + z^2)\} \left\{ \int_{-\infty}^{\infty} \exp\left\{-\frac{1}{2}[\alpha^2 x^2 + \alpha'^2(x + a_s)^2] + 2x(\alpha z + \alpha' s)\right\} dx \right\} \end{aligned} \quad (2.6)$$

$$\begin{aligned} \Rightarrow \sum_{m,n} \frac{z^n}{n!} \frac{s^m}{m!} I_{n,m} &= C_{n,m} \sqrt{\left(\frac{2\pi}{\alpha^2 + \alpha'^2} \right)} \exp\left\{ \left(\frac{\alpha^2 - \alpha'^2}{\alpha^2 + \alpha'^2} \right) (z^2 - s^2) \right. \\ &\quad \left. + \frac{4\alpha\alpha'}{\alpha^2 + \alpha'^2} sz + \frac{2\alpha\alpha'}{\alpha^2 + \alpha'^2} a_s(\alpha s - \alpha' z) \right\} \exp\left[\frac{-\alpha'^4 a_s^2}{2(\alpha^2 + \alpha'^2)} \right] \end{aligned} \quad (2.7)$$

where $C_{n,m} = (\alpha\alpha'/\pi 2^{m+n} m!n!)^{1/2}$; Let $\alpha' = \tau\alpha$, τ being the transition parameter

$$\begin{aligned} \Rightarrow \sum_{n,m} \frac{z^n}{n!} \frac{s^m}{m!} I_{n,m} &= \left[\frac{2\tau}{(1 + \tau^2)(2^{m+n} m!n!)} \right]^{1/2} \exp\left\{ -\frac{\tau^4 \alpha^2 a_s^2}{2(1 + \tau^2)} \right\} \\ &\quad \times \exp\left\{ \left(\frac{1 - \tau^2}{1 + \tau^2} \right) (z^2 - s^2) + \frac{4\tau}{1 + \tau^2} sz + \frac{2\tau}{1 + \tau^2} \alpha a_s (s - \tau z) \right\} \end{aligned} \quad (2.8)$$

2.2.1 Sudden Approximation:

Since the energy of the incident particle is high, the time spent by the charged particle at the interface between the two channels is very small compared to the over all time spent by it in any of the channels i.e., (left or right). Hence we use sudden approximation [12] where the wave functions are identical in coupling terms. That means the particle can not “see” the discontinuity at the boundary during its passage and the transition parameter V becomes unity.

Under sudden approximation the overlap integral $\langle \psi_n | \psi_m \rangle$ becomes

$$\begin{aligned} & \frac{\alpha}{\sqrt{\pi 2^{m+n} m! n!}} \int_{-\infty}^{\infty} \exp \left\{ -\frac{1}{2} [\alpha^2 x^2 + \alpha^2 (x + a_s)^2] \right\} H_n(\alpha x) H_m(\alpha x + \alpha a_s) dx \\ &= \frac{1}{\sqrt{\pi 2^{m+n} m! n!}} \exp \left\{ -\alpha^2 a_s^2 / 4 \right\} \int_{-\infty}^{\infty} \exp \left\{ -\left(t + \frac{b}{2}\right)^2 \right\} H_n(t) H_m(t + b) dt \end{aligned} \quad (2.9)$$

where $b = \alpha a_s$; $\alpha x = t$.

$$\Rightarrow \sum_{n,m} \left(\frac{z^n s^m}{n! m!} \right) I_{n,m} = \left(\frac{1}{2^{m+n} m! n!} \right)^{1/2} \exp \left\{ -\frac{\alpha^2 a_s^2}{4} \right\} \exp \{ 2sz + \alpha a_s (s - z) \} \quad (2.10)$$

Comparing the coefficients of the parameters z, s is still difficult hence we use abstract notation to handle this overlap integral.

2.2.2 Operator formalism:

As we know, the displaced wavefunction $\psi(x + a_s)$ can be expanded in Taylor series as

$$\psi(x + a_s) = \psi(x) + a_s \frac{\partial}{\partial x} \psi(x) + \frac{a_s^2}{2!} \frac{\partial^2}{\partial x^2} \psi(x) + \frac{a_s^3}{3!} \frac{\partial^3}{\partial x^3} \psi(x) + \dots \infty = \exp \left(a_s \frac{\partial}{\partial x} \right) \psi(x).$$

Here, $\frac{\partial}{\partial x}$ appearing in the above exponential is basically momentum operator in co-ordinate basis, hence it can be expressed in terms of *creation* and *annihilation* operators and we write

$$\langle \psi_f(x) | \psi_i(x) \rangle = \langle m | \exp \left\{ \frac{a_s \alpha}{\sqrt{2}} (a - a^\dagger) \right\} | n \rangle. \quad (2.11)$$

where, $a^\dagger a|n\rangle = n|n\rangle$, $a|n\rangle = \sqrt{n}|n-1\rangle$ and $a^\dagger|n\rangle = \sqrt{n+1}|n+1\rangle$.

The Matrix element M_{mn} becomes

$$\begin{aligned} M_{mn} &= \langle m | \exp \left\{ \frac{a_s \alpha}{\sqrt{2}} (a - a^\dagger) \right\} | n \rangle \\ &= \exp(-\alpha^2 a_s^2 / 4) \langle m | \exp(\lambda a^\dagger) \exp(-\lambda a) | n \rangle \end{aligned}$$

where the dimensionless quantity, $A = \alpha a_s / \sqrt{2}$; $|n\rangle$, $|m\rangle$ are the eigenstates of harmonic potential well corresponding to initial state (left part of the channel before the fault) and final state (after the fault) respectively. The details of these calculations are given in the APPENDIX. The general expression so obtained is given by

$$\langle n | m \rangle = \frac{\exp(-\alpha^2 a_s^2 / 4)}{\sqrt{2^{m+n} m! n!}} \left(\sum_{r=\max(0, m-n)}^m (-1)^{n-m+r} 2^{m-r} m_{cr} \frac{n!}{(n-m+r)!} (b)^{n-m+2r} \right) \quad (2.12)$$

This general expression is extremely useful in various fields [15]. It reduces enormous machine time in computing various matrix elements, particularly when the transitions involving higher quantum numbers.

The transition/channeling probability in general, is then obtained through the expression $p_{m \rightarrow n} = M_{nm} = |\langle n | m \rangle|^2 = |\langle m | n \rangle|^2 = M_{mn} = p_{n \rightarrow m}$. The transition amplitude for $p_{0 \rightarrow m}$ is obtained by using above general expression to reproduce the expression given in Ref. [12]. However, a general expression for arbitrary values of n and m is not obtained so far. After so much of analytical effort, by intuition, I could obtain the above general expression. This formula for the overlap integral $\langle n | m \rangle$ is deduced by making advantage of the *annihilation* and *creation* operator formalism. One can appreciate the effectiveness of this approach as compared to conventional way of integration procedure for these displaced harmonic oscillator wavefunctions.

2.2.3 Evaluation of number of states in the continuum potential well:

In this work we have taken specific example of quantum description of positrons with incident energy 12.75 Mev (7=25) channeled along $Al(111)$ planes with stacking faults. The number of quantum states in the harmonic potential well is calculated by equating the total quantized transverse energy to the depth of the potential well [14] and this is given by

$$(n_{\max} + \frac{1}{2})\hbar\omega = \frac{1}{2}k_1x_{\max}^2 \quad (2.13)$$

$$\Rightarrow \left(n_{\max} + \frac{1}{2}\right)\hbar\omega = \frac{1}{2} \left[\frac{8\pi Z_1 Z_2 e^2 C a_{T.F.}^2 N_p}{(l + a_{T.F.})^3} \cdot (l - a_{T.F.})^2 \right]$$

$$\Rightarrow n_{\max} = \frac{1}{2} \left[\sqrt{\frac{\gamma m 8\pi Z_1 Z_2 e^2 C a_{T.F.}^2 N_p}{(l + a_{T.F.})^3} \frac{(l - a_{T.F.})^2}{\hbar}} - 1 \right] \quad (2.14)$$

For positron $Z_1 = 1$; for Aluminium $Z_2 = 13$; N = bulk density of atom in the crystal given by

$$N = \frac{\rho N_o}{A} / cm^3$$

ρ =density of the target; N_o =Avagadro number = 6.023×10^{23} ; A =mass number; For Aluminium $\rho = 2.70 \text{ gm/cm}^3$

$$A_{Al} = 26.982$$

$$\text{Thomas-Fermi screening } a_{T.F.} = \frac{0.8853a_o}{\sqrt{1^{2/3} + 13^{2/3}}} = 0.3466437 a_o$$

$$d_p(111) = 2.3383371\text{\AA} = 4.4188182 a_o$$

$$\Rightarrow l = 2.2094091 a_o; \quad x_{\max} = 1.8627654 a_o$$

The planar concentration is calculated in atomic units which given by

$$N_p = 0.0394649/a_o^2$$

Substituting these values in Eqn. (2.14) and using atomic units (i.e., $\hbar = 1$, electron charge(e) = 1), we get $n_{\max} = 3$.

Initial state of the particle is fixed (in the left part of channel). It can go and occupy any one of the states in the right side channel (after fault). The possible transitions are

$$\begin{aligned} 0 &\longrightarrow 0 ; & 0 &\longrightarrow 1 ; & 0 &\longrightarrow 2 ; & 0 &\longrightarrow 3 \\ 1 &\longrightarrow 0 ; & 1 &\longrightarrow 1 ; & 1 &\longrightarrow 2 ; & 1 &\longrightarrow 3 \\ 2 &\longrightarrow 0 ; & 2 &\longrightarrow 1 ; & 2 &\longrightarrow 2 ; & 2 &\longrightarrow 3 \\ 3 &\longrightarrow 0 ; & 3 &\longrightarrow 1 ; & 3 &\longrightarrow 2 ; & 3 &\longrightarrow 3 \end{aligned}$$

Since the harmonic oscillator wave functions are real $|\langle i|j\rangle|^2 = |\langle j|i\rangle|^2$ and this implies $p_{i \rightarrow j} = p_{j \rightarrow i}$, and the actual number of matrix elements to be evaluated is reduced to 9. This shows the directional symmetry inbuilt in the problem reflecting that it does not matter whether the particle is injected from the left channel or right channel.

The probability that a particle with initial state $|i\rangle$, to occupy any one of the available final states (i.e., the probability for particle to remain channeled after the fault) is obtained by

$$p_i = \sum_{f=0}^3 |\langle i|f\rangle|^2 \quad (2.15)$$

The initial state of the particle $|i\rangle$ is fixed, it can be 0, 1, 2, or 3. $|i\rangle = |0\rangle$ corresponds to initially well channeled particle. Here we show explicit calculation of the matrix elements using integral form directly. However the calculation using the operator method is furnished in the APPENDIX, at the end of this chapter. To evaluate individual matrix elements (i.e., the integral 2.9) we need the Hermite functions, which can be obtained by using the Rodrigue's formula. $H_n(x) = (-1)^n e^{x^2} \frac{d^n}{dx^n} e^{-x^2}$.

These polynomials, so obtained are

$$H_0(x) = 1 ; \quad H_1(x) = 2x ; \quad H_2(x) = 4x^2 - 2 ; \quad H_3(x) = 8x^3 - 12x \text{ etc.} \quad (2.16)$$

The individual transition amplitudes are evaluated as follows:

i) $|\langle 1|0\rangle|^2$:

$$= \left| \frac{1}{\sqrt{2}} \exp\{-\alpha^2 a_s^2/4\} \int_{-\infty}^{\infty} \exp\left\{-\left(t + \frac{b}{2}\right)^2\right\} H_1(t) H_0(t+b) dt \right|^2$$

$$\Rightarrow \frac{1}{2} \alpha^2 a_s^2 \exp(-\alpha^2 a_s^2/2)$$

$$\boxed{p_{1 \rightarrow 0} = |\langle 1|0\rangle|^2 = \frac{\alpha^2 a_s^2}{2} \exp\{-\alpha^2 a_s^2/2\}} \quad (2.17)$$

ii) $|\langle 1|1\rangle|^2$:

$$= \left| \frac{1}{\sqrt{4\pi}} \exp\{-\alpha^2 a_s^2/4\} \int_{-\infty}^{\infty} \exp\left\{-\left(t + \frac{b}{2}\right)^2\right\} H_1(t) H_1(t+b) dt \right|^2.$$

Substituting H_1 and evaluating the integral we get

$$|\langle 1|1\rangle|^2 = \left| \frac{2 - \alpha^2 a_s^2}{2} \exp\{-\alpha^2 a_s^2/4\} \right|^2$$

$$\Rightarrow |\langle 1|1\rangle|^2 = \left(\frac{2 - \alpha^2 a_s^2}{2} \right)^2 \exp\{-\alpha^2 a_s^2/2\}$$

$$\boxed{p_{1 \rightarrow 1} = \left(\frac{2 - \alpha^2 a_s^2}{2} \right)^2 \exp\{-\alpha^2 a_s^2/2\}} \quad (2.18)$$

iii) $|\langle 1|2\rangle|^2$:

$$= \left| \frac{1}{\sqrt{16\pi}} \exp\{-\alpha^2 a_s^2/4\} \int_{-\infty}^{\infty} \exp\left\{-\left(t + \frac{b}{2}\right)^2\right\} H_1(t) H_2(t+b) dt \right|^2$$

Substituting H_1 ; H_2 and integrating one gets:

$$\begin{aligned}
 |\langle 1|2\rangle|^2 &= \left| \frac{\exp(-\alpha^2 a_s^2/4)}{2} \left(2\alpha a_s - \frac{\alpha^3 a_s^3}{2} \right) \right|^2 \\
 \Rightarrow |\langle 1|2\rangle|^2 &= \frac{1}{4} \exp(-\alpha^2 a_s^2/2) \left(2\alpha a_s - \frac{\alpha^3 a_s^3}{2} \right)^2 \\
 \therefore \boxed{p_{1 \rightarrow 2} = \frac{1}{4} \exp(-\alpha^2 a_s^2/2) \left(2\alpha a_s - \frac{\alpha^3 a_s^3}{2} \right)^2} & \quad (2.19)
 \end{aligned}$$

iv) $|\langle 1|3\rangle|^2$:

$$\begin{aligned}
 &= \left| \frac{1}{\sqrt{2^4 \cdot 6\pi}} \exp[-\alpha^2 a_s^2/4] \int_{-\infty}^{\infty} \exp[-(t + \frac{b}{2})^2] H_1(t) H_3(t + b) dt \right|^2 \\
 \Rightarrow |\langle 1|3\rangle|^2 &= \frac{1}{96} \exp(-\alpha^2 a_s^2/2) (6\alpha^2 a_s^2 - \alpha^4 a_s^4)^2 \\
 \boxed{p_{1 \rightarrow 3} = \frac{1}{96} \exp(-\alpha^2 a_s^2/2) (6\alpha^2 a_s^2 - \alpha^4 a_s^4)^2} & \quad (2.20)
 \end{aligned}$$

v) $|\langle 2|0\rangle|^2$:

$$\begin{aligned}
 &= \left| \frac{1}{\sqrt{8\pi}} \exp(-\alpha^2 a_s^2/4) \int_{-\infty}^{\infty} \exp[-(t + \frac{b}{2})^2] H_2(t) H_0(t + b) dt \right|^2 \\
 \Rightarrow |\langle 2|0\rangle|^2 &= \frac{\alpha^4 a_s^4}{8} \exp(-\alpha^2 a_s^2/2) \\
 \boxed{p_{2 \rightarrow 0} = \frac{1}{8} \alpha^4 a_s^4 \exp(-\alpha^2 a_s^2/2)} & \quad (2.21)
 \end{aligned}$$

vi) $|\langle 2|2\rangle|^2$:

$$\begin{aligned}
&= \left| \frac{1}{\sqrt{2^6\pi}} \exp(-\alpha^2 a_s^2/4) \int_{-\infty}^{\infty} \exp(-(t + \frac{b}{2})^2) H_2(t) H_2(t + b) dt \right|^2 \\
\Rightarrow |\langle 2|2\rangle|^2 &= \left(\frac{\alpha^4 a_s^4}{8} - \alpha^2 a_s^2 + 1 \right)^2 \exp(-\alpha^2 a_s^2/2) \\
\boxed{p_{2 \rightarrow 2} &= \left(\frac{\alpha^4 a_s^4}{8} - \alpha^2 a_s^2 + 1 \right)^2 \exp(-\alpha^2 a_s^2/2)} \\
&\hspace{15em} (2.22)
\end{aligned}$$

vii) $|\langle 2|3\rangle|^2$:

$$\begin{aligned}
&= \left| \frac{1}{\sqrt{2^6 \cdot 6\pi}} \exp(-\alpha^2 a_s^2/4) \int_{-\infty}^{\infty} \exp(-(t + \frac{b}{2})^2) H_2(t) H_3(t + b) dt \right|^2 \\
\Rightarrow |\langle 2|3\rangle|^2 &= \frac{\exp(-\alpha^2 a_s^2/2)}{6} \left(\frac{\alpha^5 a_s^5}{8} - \frac{3\alpha^3 a_s^3}{2} + 3\alpha a_s \right)^2 \\
\boxed{p_{2 \rightarrow 3} = |\langle 2|3\rangle|^2 &= \frac{\exp(-\alpha^2 a_s^2/2)}{6} \left(\frac{\alpha^5 a_s^5}{8} - \frac{3\alpha^3 a_s^3}{2} + 3\alpha a_s \right)^2} \\
&\hspace{15em} (2.23)
\end{aligned}$$

viii) $|\langle 3|0\rangle|^2$:

$$\begin{aligned}
&= \left| \frac{1}{\sqrt{2^4 \cdot 3\pi}} \exp(-\alpha^2 a_s^2/4) \int_{-\infty}^{\infty} \exp(-(t + \frac{b}{2})^2) H_3(t) H_0(t + b) dt \right|^2 \\
\boxed{p_{3 \rightarrow 0} = |\langle 3|0\rangle|^2 &= \frac{\alpha^6 a_s^6}{48} \exp(-\alpha^2 a_s^2/2)} \\
&\hspace{15em} (2.24)
\end{aligned}$$

ix) $|\langle 3|3\rangle|^2$:

$$= \left| \frac{\exp(-\alpha^2 a_s^2/4)}{\sqrt{2^6 (3!)^2 \pi}} \int_{-\infty}^{\infty} \exp[-(t + \frac{b}{2})^2] H_3(t) H_3(t + b) dt \right|^2$$

$$= \left| \frac{1}{3} \left(3 - \frac{9}{2} \alpha^2 a_s^2 + \frac{9}{8} \alpha^4 a_s^4 - \frac{\alpha^6 a_s^6}{16} \right) \exp(-\alpha^2 a_s^2/4) \right|^2$$

$$\boxed{p_{3 \rightarrow 3} = |\langle 3|3 \rangle|^2 = \frac{1}{9} \left(3 - \frac{9}{2} \alpha^2 a_s^2 + \frac{9}{8} \alpha^4 a_s^4 - \frac{\alpha^6 a_s^6}{16} \right)^2 \exp(-\alpha^2 a_s^2/2)}$$
(2.25)

The dechanneling probability is defined as

$$\chi_i = 1 - p_i$$

$$\chi_i = 1 - \sum_{j=0}^3 |\langle i|f \rangle|^2$$
(2.26)

Eqns. (2.15) and (2.26) gives $\chi_0 = 1 - p_0$; $\chi_1 = 1 - p_1$; $\chi_2 = 1 - p_2$ and $\chi_3 = 1 - p_3$.

The dechanneling probabilities are computed by incorporating corresponding matrix elements appropriately and these results are given in Table I (a). In classical description, the corresponding dechanneling probability is obtained by incorporating that the particle with position x and angle ψ before the fault takes new values x' and ψ' after the fault. The expression for χ_1 is derived for a stacking shift $dp/3$. This classical expression is given by [16, 17]

$$\chi = \frac{a'}{x_c} \cdot \left[\int_{-d_p/6}^{(d_p/6)-a'} g(x) dx - \int_{d_p/6}^{(d_p/2)-a'} g(x) dx + \int_{(d_p/6)+a'}^{d_p/3} g(x) dx - \int_{d_p/3}^{(d_p/2)-a'} g(x) dx \right]$$
(2.27)

Here $g(x) = \sqrt{[(x_c^2 - x^2)/(L^2 - x^2)]}$, with $x_c = l - a_{T,F}$, $L = l + a_{T,F}$. Here $a' = a_{T,F} + \rho_{\perp}$; thermal correction term to screening function (ρ_{\perp}) is to include effects of temperature on χ due to thermal vibration of the atomic planes.

By neglecting the temperature effects (that means $\rho_{\perp} = 0$), we calculated the dechanneling probability and compare with present quantum mechanical calculation and these results are given in Table I(b), showing good agreement

TABLE I

(a):

Variation of Dechanneling Probabilities for Positrons in Al with stacking shift for various initial states

Shift in units of l	Dechanneling Probabilities			
	X_0	X_1	X_2	X_3
0.00	0.00	0.00	0.00	0.00
0.10	0.00	0.07	0.07	0.17
0.20	0.00	0.21	0.29	0.46
0.30	0.00	0.33	0.57	0.56
0.40	0.01	0.38	0.71	0.51
0.50	0.04	0.38	0.62	0.52
0.60	0.10	0.37	0.43	0.60
0.70	0.22	0.36	0.32	0.63
0.80	0.39	0.35	0.37	0.61
0.90	0.56	0.38	0.48	0.63
1.00	0.72	0.47	0.56	0.69

(b):

A comparison of Dechanneling Probabilities for a stacking shift of $d_p/3$ obtained for classical calculation with present Quantum description

Classical calculation [16]	present quantum calculations			
	X_0	X_1	X_2	X_3
0.28	0.17	0.36	0.34	0.63

2.2.4 Dechanneling effects at the stacking fault:

The continuum potentials in particular used in the discussion are in principle valid for infinite planes where as in the case of stacking fault we had half planes i.e., those ending at the fault and those starting from the fault. Hence the potential is slightly complicated just at the interface.

In quantum mechanical treatment we start with a wave function describing the incident particle(ψ_L) coming from the left. This wavefunction is of the form of wavepacket along longitudinal direction (z) and harmonic oscillator in transverse direction (x). When this packet reaches the fault, the transverse planar potential is described by the expression of the form

$$V(z, x) = \frac{1}{2}k_1x^2H(z_0 - z) + \frac{1}{2}k_1(x + a_s)^2H(z - z_0)$$

where $H(z)$ is step function which equals '1' for positive arguments and zero for negative arguments. The solution of the Schrodinger equation in this potential is different in two parts of the crystal (i.e., for $z < z_0$ and $z > z_0$). At the boundary $z = z_0$, part of the incident flux is reflected and the rest is transmitted. Hence the total wavefunction in the left part of the channel is of the form

$$\psi_L(z, x) = (A \exp(ikz) + B \exp(-ikz)) \varphi_n(x)$$

Similarly the wave function corresponding to transmitted particle after the fault will take the form

$$\psi_R(z, x) = C \exp(ik'z) \varphi_m(x + a_s)$$

So we match the wave functions at the stacking fault ($z = z_0$) to get the reflected flux (N_r) and transmitted flux (N_t) in terms of incident flux (N_i) at the fault. We have

$$N_i = \frac{\hbar k}{m}|A|^2, N_r = \frac{\hbar k}{m}|B|^2 \text{ and } N_t = \frac{\hbar k'}{m}|C|^2.$$

By incorporating the boundary conditions in these wavefunctions, one gets

$$\begin{aligned}(A \exp(ikz_0) + B \exp(-ikz_0)) \langle m|n \rangle &= C \exp(ik'z_0) \\ k(A \exp(ikz_0) - B \exp(-ikz_0)) \langle m|n \rangle &= C k' \exp(ik'z_0)\end{aligned}$$

The transmission and reflection co-efficients are obtained as

$$T = \frac{N_t}{N_i} = \frac{k'}{k} \left| \frac{C}{A} \right|^2 ; R = \frac{N_r}{N_i} = \left| \frac{B}{A} \right|^2 = \left(\frac{k - k'}{k + k'} \right)^2 \quad (2.28)$$

with $\left| \frac{C}{A} \right|^2 = \frac{4k^2}{(k + k')^2} |\langle m|n \rangle|^2$. Hence the reflection and transmission coefficients are given by [18]

$$R = \frac{N_r}{N_i} = \left(\frac{k - k'}{k + k'} \right)^2 ; T = \frac{N_t}{N_i} = \frac{4kk'}{(k + k')^2} |\langle m|n \rangle|^2 \quad (2.29)$$

It is evident from the above expressions that there are some particles which are neither in the left part of the channel nor in the right. These particles will not experience the standard harmonic potential since they already came out of the channel. These may be dechanneled particles which hit the fault and get deflected away from the channel. This situation corresponds to dechanneling at the fault. So one can define dechanneling coefficient (D) in terms of dechanneled flux $N_d (= N_i - (N_r + N_t))$ as

$$(2.30)$$

Since the total energy of the positron is very high, it can not recognize the presence of the fault during its passage through the fault unless it hits the fault directly. The longitudinal momentum is therefore likely to be un-altered so that ' k' ' equals to ' k ' and $R = 0$. So in this high energy limit we could reproduce previous results based on the sudden approximation, described in above sections.

2.2.5 The effects of periodicity in the transverse space:

The transverse potential in principle is a periodic function with period d_p , hence the wave functions are of Bloch type. One can estimate the periodicity effect due to remaining wells by evaluating the dipole momentum. An estimate is given here for the contribution of remaining wells at $n = 1$ using Eqn(3.8) of Ref. [19] and we have

$$\bar{\alpha}_x - \alpha_x = \sqrt{\pi} C_1 C_0 \sum_{\nu' \neq 0} e^{-ik\nu'} \left(1 - 8 \frac{m_{rel}\omega}{4\hbar} (\nu' d_p)^2 \right) \exp\left(-\frac{m_{rel}\omega}{4\hbar}\right) (\nu' d_p)^2 \quad (2.31)$$

Here C_0 & C_1 are the normalization constants for $|0\rangle$ and $|1\rangle$ respectively. By denoting $z = \frac{1}{2} \sqrt{\frac{m_{rel}\omega}{\hbar}} (d_p \nu')$, the summation in the above equation is evaluated as follows:

$$\begin{aligned} &\Rightarrow \sum_{\nu'=-\infty}^{-1} e^{-ik\nu'} (1 - 8z^2) e^{-z^2} + \sum_{\nu'=1}^{\infty} e^{-ik\nu'} (1 - 8z^2) e^{-z^2} \quad \text{changing the parity,} \\ &\Rightarrow \sum_{\nu'=1}^{\infty} \exp(ikd_p \nu') (1 - 8z^2) e^{-z^2} + \sum_{\nu'=1}^{\infty} \exp(-ikd_p \nu') (1 - 8z^2) e^{-z^2} \\ &= \sum_{\nu'=1}^{\infty} \{ \exp(ikd_p \nu') + \exp(-ikd_p \nu') \} (1 - 8z^2) e^{-z^2} \\ &= 2 \sum_{\nu'=1}^{\infty} \cos\left(\frac{2\pi}{d_p} \cdot d_p \nu'\right) (1 - 8z^2) e^{-z^2} \\ &= 2 \sum_{\nu'=1}^{\infty} \cos(2\pi \nu') (1 - 8z^2) e^{-z^2} = 2 \sum_{\nu'=1}^{\infty} (1 - 8z^2) e^{-z^2} \end{aligned} \quad (2.32)$$

This gives $\bar{\alpha}_x - \alpha_x = -0.0010511$. Therefore the contribution of the other wells to the dipole momentum ($\bar{\alpha}_x$) is negligibly small when compared to dipole momentum corresponding to single well ($\alpha_x \approx 1.001$), hence the periodicity effects are likely to be negligible for our channeling/dechanneling probability calculations.

2.3 Results and Discussion:

We have studied the quantum aspects of the processes related with effects of defects (specially stacking faults) on channeled particles with specific reference to positrons. The number of quantum states present in the transverse potential well is proportional to $\gamma^{1/2}$ (Eqn. 2.14). If the incident particle energy is very high, the level spacing corresponding to the transverse energy becomes smaller and some times even leads to classical behaviour.

Restricting to positron channeling, on the specific assumption that the crystal is otherwise pure and clean, channeling and dechanneling probabilities corresponding to stacking fault situations have been studied using sudden approximation. The dechanneling probabilities obtained from quantum mechanical treatments shown in Eqn. (2.26) are not having explicit energy dependence as was also seen from classical description represented by Eqn. (2.27)

The dechanneling probabilities for various initial states i.e., χ_0, χ_1, χ_2 and χ_3 as a function of the stacking shift are given in Figs. (2.4) & (2.5). The dechanneling probabilities will depend on the initial state. If the particle after passing through the fault goes to a state which is same as initial state (i.e., remain in the same state), the transition probability is maximum corresponding to shift $a_s=0$, as expected. This is of course trivial result for the situation of faultless crystal.

There are some states which lead to maximum dechanneling. These states, may be called *dechanneling states*. If the particle happens to be in these dechanneling states, whatever the shift may be, there is very high tendency for the particle to get dechanneled. As shown in Figs. (2.6 & 2.7), $1 \leftrightarrow 3$; $2 \leftrightarrow 0$; $3 \leftrightarrow 0$ exhibit this kind of behaviour. For a given initial state the channeling probability is very sensitive to stacking shift.

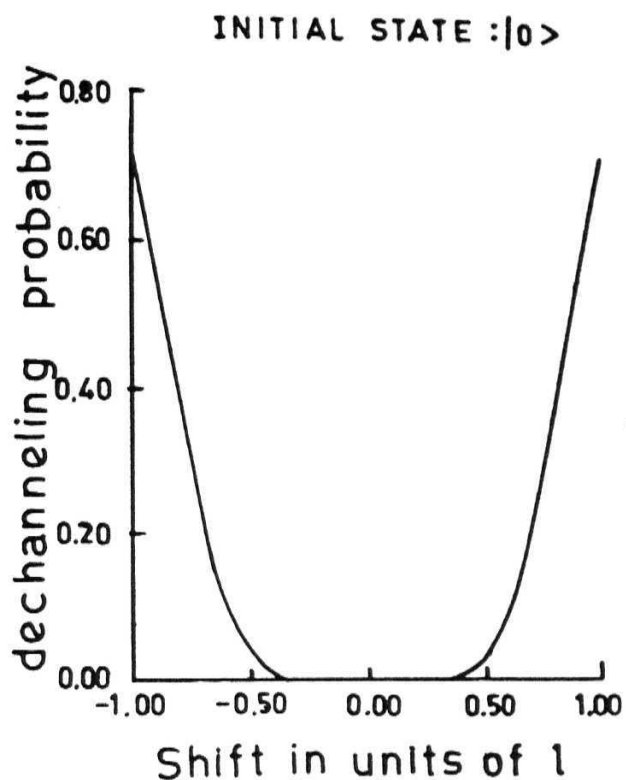


Fig. 2.4 a): The variation of dechanneling probability with the stacking shift ' a_s ' corresponding to the initial state $|0\rangle$ in the left hand channel.

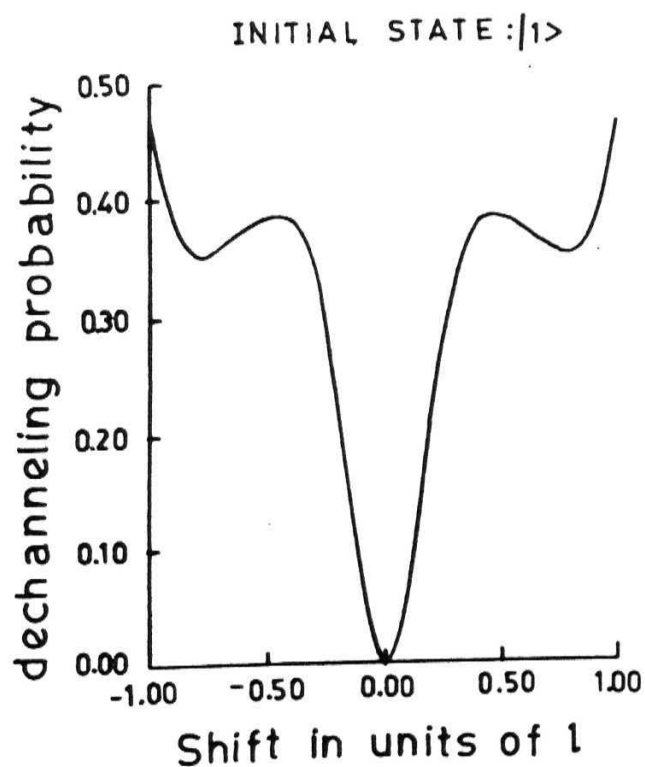


Fig. 2.4 b): The variation of dechanneling probability with the stacking shift ' a_s ' corresponding to the initial state $|1\rangle$ in the left hand channel.

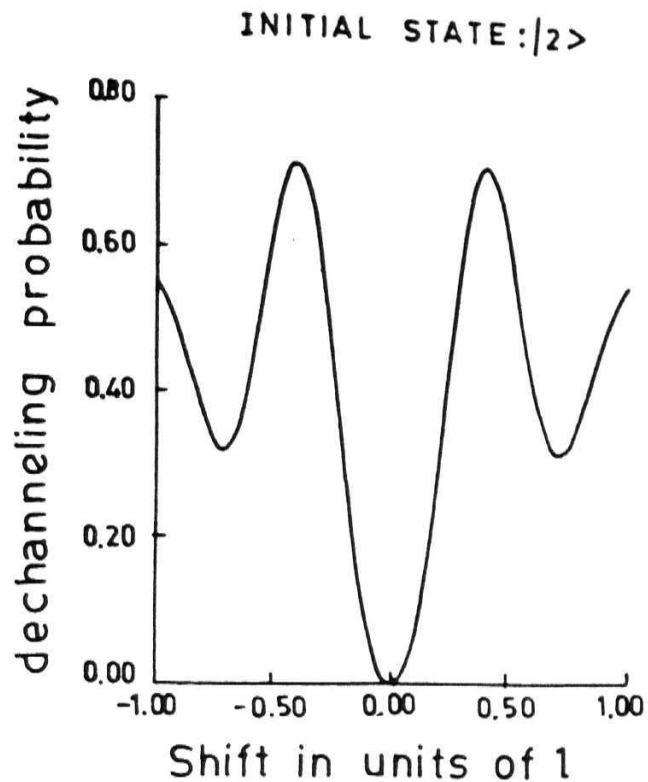


Fig. 2.5 b): The variation of dechanneling probability with the stacking shift ' a_s ' corresponding to the initial state $|3\rangle$ in the left hand channel.

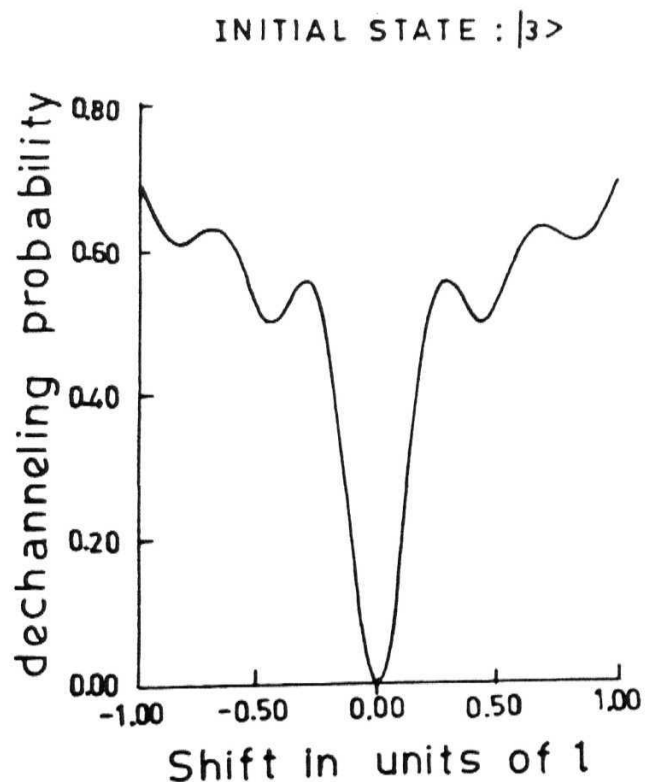


Fig. 2.5 b): The variation of dechanneling probability with the stacking shift ' a_s ' corresponding to the initial state $|3\rangle$ in the left hand channel.

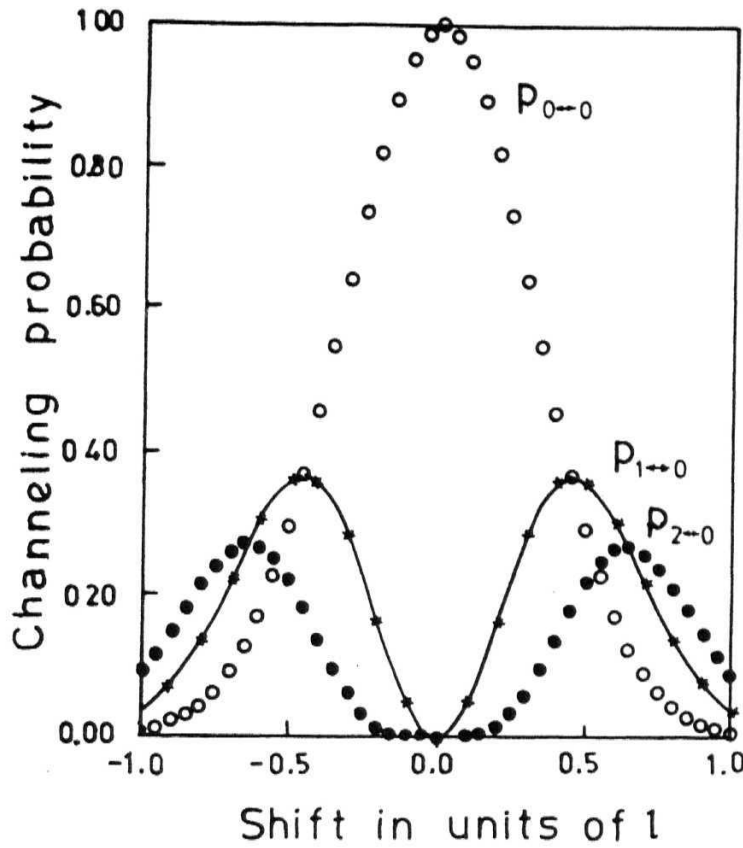


Fig. 2.6 a): The channeling probability as a function of the stacking shift ' a_s ' in units of ' l '. Here various matrix elements are symbolically denoted as $\circ : |\langle 0|0\rangle|^2$; $\star : |\langle 1|0\rangle|^2$; $\bullet : |\langle 2|0\rangle|^2$

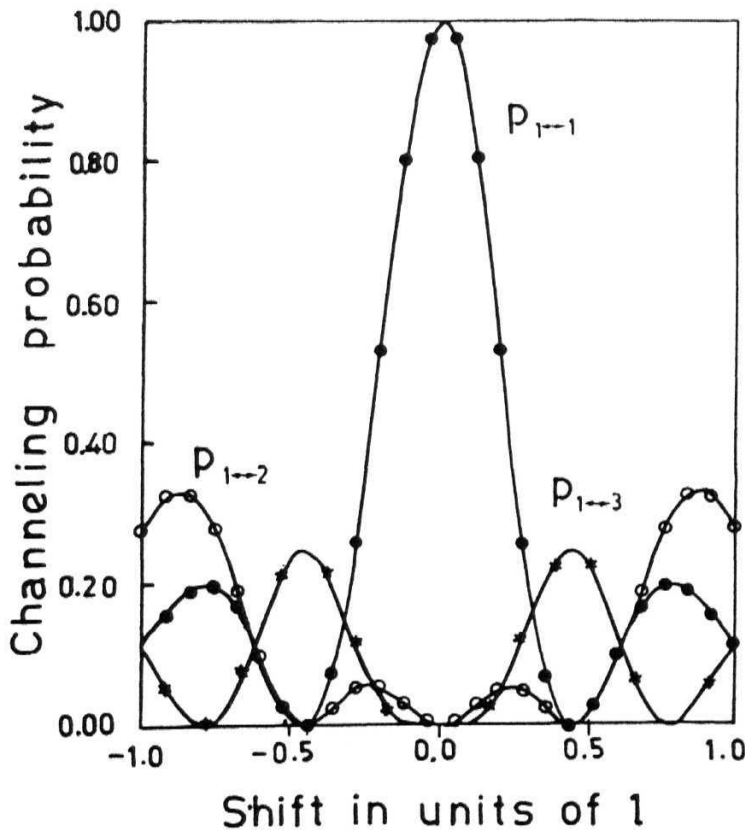


Fig. 2.6 b): The channeling probability as a function of the stacking shift ' a_s ' in units of ' l '. Here various matrix elements are symbolically denoted as $\circ : |\langle 1|2\rangle|^2$; $\star : |\langle 1|3\rangle|^2$; $\bullet : |\langle 1|1\rangle|^2$

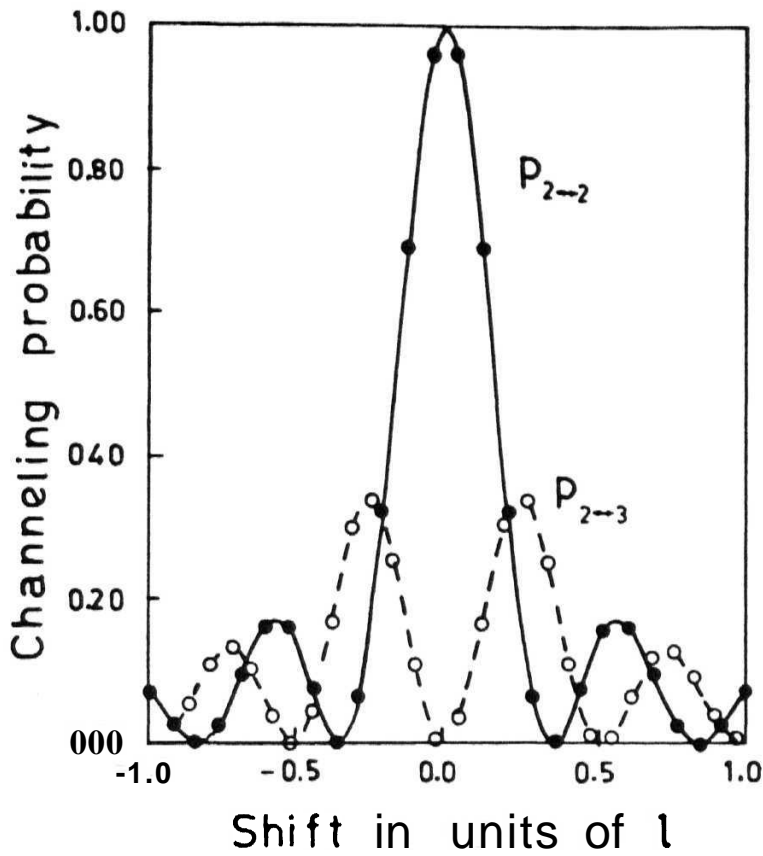


Fig. 2.7 a): The channeling probability as a function of the stacking shift ' a_s ' in units of ' l '. Here various matrix elements are symbolically denoted as $\circ : |\langle 2|3 \rangle|^2$; $\bullet : |\langle 2|2 \rangle|^2$

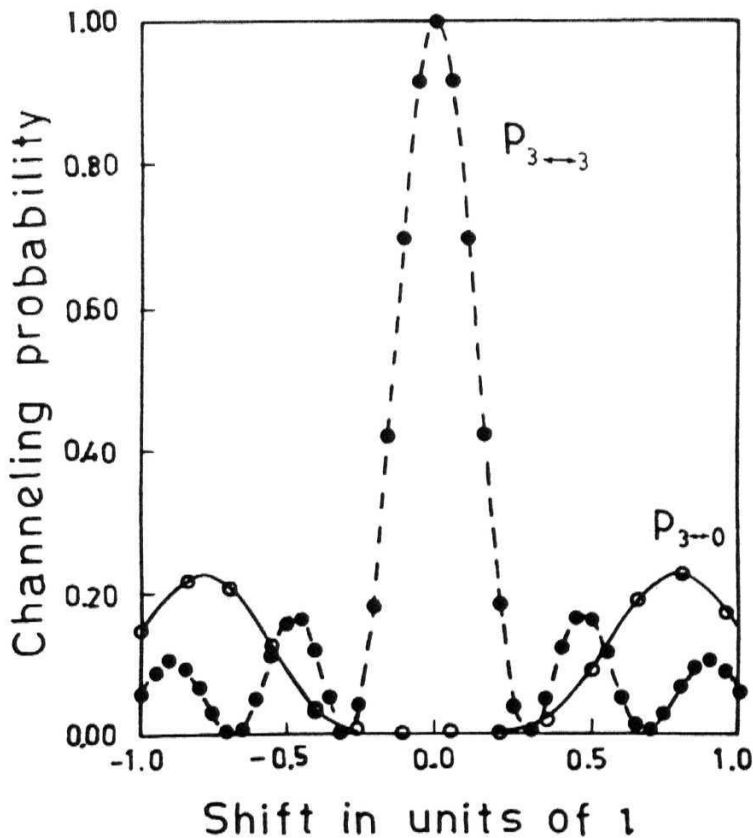


Fig. 2.7 b): The channeling probability as a function of the stacking shift ' a_s ' in units of ' l '. Here various matrix elements are symbolically denoted as $\circ : |\langle 3|0 \rangle|^2$; $\bullet : |\langle 3|3 \rangle|^2$

If the final state is much different from the initial state, the transition/channeling probability drastically oscillates as a function of stacking shift; this oscillatory behaviour can be noticed from these figures.

In classical description, it is required to have the amount of stacking shift to calculate dechanneling probability using expression (2.27). But in quantum description, a general expression is obtained for dechanneling probabilities for a general value of stacking shift and one can calculate the variations in a more general and straight forward manner.

These points indicate that there is another important parameter i.e., phase of the particle with which it is approaching the stacking fault boundary. This can also be seen explicitly from the Eqn. (2.30) which tells that the dechanneling at the fault will depend upon the final state in to which the particle is going to be. The non-diagonal matrix elements vanish for zero shift, implying that the well-channeled (min. amplitude) particle suddenly can not exhibit oscillatory behaviour in the absence of stacking faults. The fate of the particle after the fault will be decided by the amount of the shift and the phase with which it approaches the fault. This kind of dependence on phase of approaching particle was also discussed in classical analysis [15].

J. Mory et. al. [15] had discussed some experimental results of ' χ ' using classical description. An attempt was made to discuss those results using present quantum description but for that case, n_{\max} turns out to be as large as 278. It clearly shows that for their α -particle dechanneling situation, classical treatment will be good enough as far as the channeling aspects are concerned. From Fig. (2.8), one can notice that the dechanneling probability for well-channeled particles (xo) increases with thermal correction ρ_{\perp} and this behaviour is almost linear, similar to that noticed in classical calculations [17].

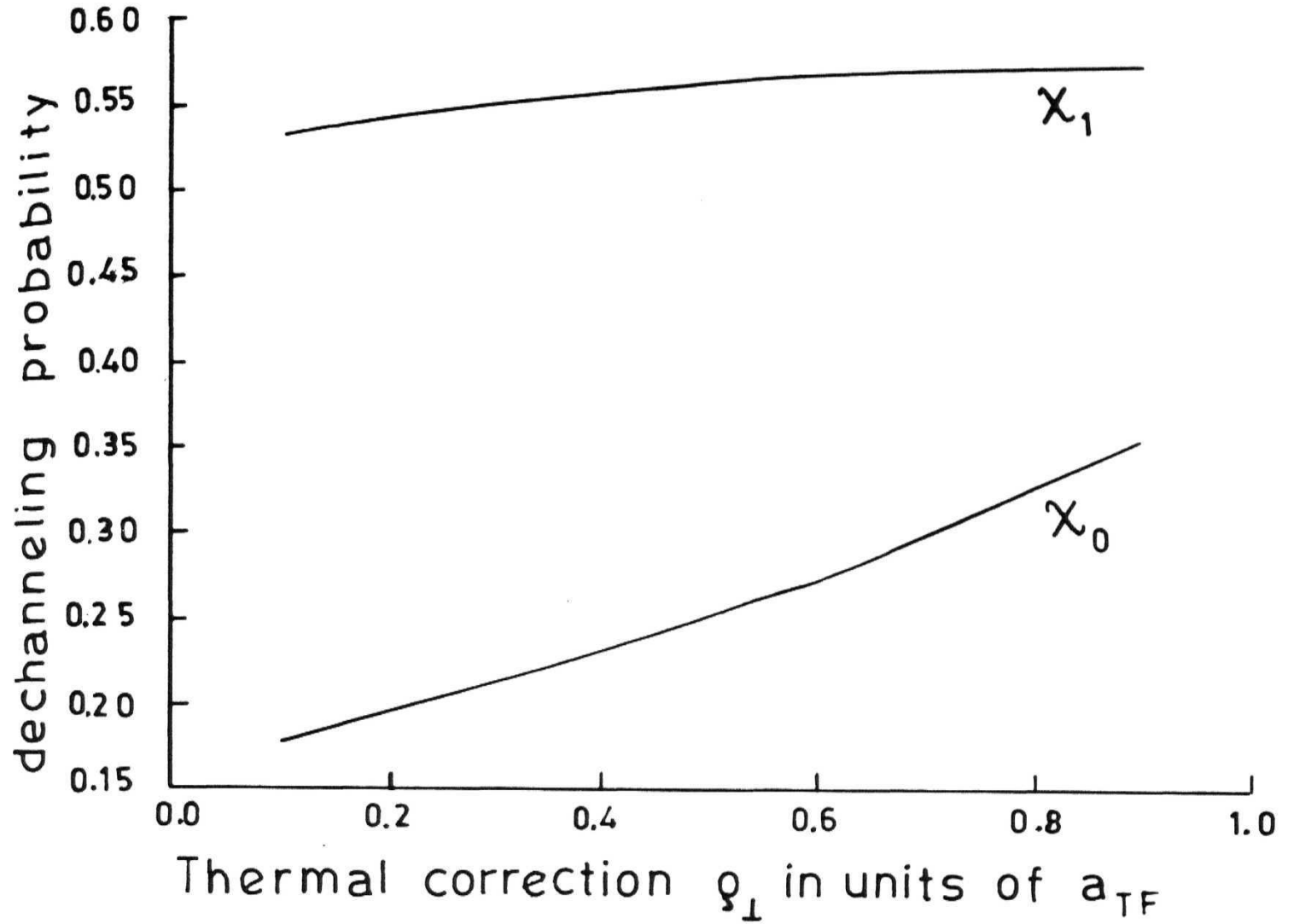


Fig. 2.8 : The variation of dechanneling probability with ' ρ_{\perp} ' for initially well-channeled particles ($|i\rangle = |0\rangle$)

In conclusion a general expression for the overlap integral $\langle n|m\rangle$ for arbitrary values of ' n ' and ' m ' is given for the *first time* which is having remarkable physical significance, and reduces laborious analytical calculations involving **Hermite** functions, in particular the higher states and this general expression can be used elsewhere.

The usefulness and completeness of this quantum mechanical formulation, lies in the fact that it is helpful for numerical calculations involving higher quantum numbers to reduce enormous computational time. This is because of the fact that one has to calculate higher order derivatives in extracting the Hermite functions. Since this analytical expression is a simple summation, the accuracy also high.

Since the wavefunctions are real, there is an interesting *left-right symmetry* inbuilt in the problem which is not clearly realized in classical description, i.e., whether the charged particle injected into channel from left or right, it does not matter as far as the dechanneling and channeling are concerned. The estimate of the effects of periodicity on dechanneling shown to be not significant and probably these features might be important in the case of low energy particles. However, more refined experiments on electron/positron dechanneling are needed to verify these results and confirm the utility of the present quantum description. We do not expect the classical results to be valid for positron and electron dechanneling.

APPENDIX

Here we show, how the operator method is used to evaluate the transition amplitudes.

For example, consider $p_{5 \rightarrow 5}$:

$$\begin{aligned}
 p_{5 \rightarrow 5} &= |\langle 5 | \exp(\lambda a^\dagger) \exp(-\lambda a) | 5 \rangle|^2 \exp(-\alpha^2 a_s^2 / 2) \\
 &= \langle 5 | \exp(\lambda a^\dagger) \left(|5\rangle - \lambda \sqrt{5} |4\rangle + \frac{\lambda^2}{2!} \sqrt{5 \cdot 4} |3\rangle - \frac{\lambda^3}{3!} \sqrt{5 \cdot 4 \cdot 3} |2\rangle \right. \\
 &\quad \left. + \frac{\lambda^4}{4!} \sqrt{5 \cdot 4 \cdot 3 \cdot 2} |1\rangle - \frac{\lambda^5}{5!} \sqrt{5!} |0\rangle \right)^2 \exp(-\alpha^2 a_s^2 / 2) \\
 &= \left[1 - 5\lambda^2 + 20 \left(\frac{\lambda^2}{2!} \right)^2 - 60 \left(\frac{\lambda^3}{3!} \right)^2 + 120 \left(\frac{\lambda^4}{4!} \right)^2 - 120 \left(\frac{\lambda^5}{5!} \right)^2 \right]^2 \exp(-\alpha^2 a_s^2 / 2) \\
 &= \left(1 - \frac{5}{2} \alpha^2 a_s^2 + \frac{5}{4} \alpha^4 a_s^4 - \frac{5}{24} \alpha^6 a_s^6 + \frac{5}{384} \alpha^8 a_s^8 - \frac{\alpha^{10} a_s^{10}}{3840} \right)^2 \exp(-\alpha^2 a_s^2 / 2)
 \end{aligned} \tag{2.33}$$

Now, consider the general expression

$$\begin{aligned}
 |\langle n | n \rangle|^2 &= \frac{\exp(-\alpha^2 a_s^2 / 2)}{2^{n+n} n! n!} \left(\sum_{r=0}^n (-1)^{n-n+r} 2^{n-r} {}^n c_r \frac{n!}{(n-n+r)!} (b)^{n-n+2r} \right)^2 \\
 \Rightarrow p_{n \rightarrow n} &= \frac{\exp(-\alpha^2 a_s^2 / 2)}{2^{2n} n!^2} \left(\sum_{r=0}^n (-1)^r 2^{n-r} {}^n c_r \frac{n!}{r!} b^{2r} \right)^2 \\
 &= \frac{\exp(-\alpha^2 a_s^2 / 2)}{2^{2n} n!^2} \left(\sum_{r=0}^n (-1)^r 2^{n-r} {}^n c_r \frac{n!}{r!} (\alpha a_s)^{2r} \right)^2 \\
 &= \exp(-\alpha^2 a_s^2 / 2) \left(\sum_{r=0}^n (-1)^r 2^{-r} {}^n c_r \frac{1}{r!} (\alpha a_s)^{2r} \right)^2
 \end{aligned}$$

$$= \left[\sum_{r=0}^n (-1)^r \left(\frac{\alpha^2 a_s^2}{2} \right)^r \frac{1}{r!} {}^n c_r \right]^2 \exp(-\alpha^2 a_s^2/2) \quad (2.34)$$

$$\Rightarrow p_{5 \rightarrow 5} = \left[\sum_{r=0}^5 (-1)^r \left(\frac{\alpha^2 a_s^2}{2} \right)^r \frac{1}{r!} {}^5 c_r \right]^2 \exp(-\alpha^2 a_s^2/2)$$

The summation is expanded as

$$\begin{aligned} &= 1 - 5 \frac{\alpha^2 a_s^2}{2} + \left(\frac{\alpha^2 a_s^2}{2} \right)^2 \frac{1}{2} {}^5 c_2 - \left(\frac{\alpha^2 a_s^2}{2} \right)^3 \frac{1}{3!} {}^5 c_3 + \left(\frac{\alpha^2 a_s^2}{2} \right)^4 \frac{1}{4!} {}^5 c_4 - \left(\frac{\alpha^2 a_s^2}{2} \right)^5 \frac{1}{5!} \\ &\Rightarrow \left(1 - \frac{5}{2} \alpha^2 a_s^2 + \frac{5}{4} \alpha^4 a_s^4 - \frac{5}{24} \alpha^6 a_s^6 + \frac{5}{384} \alpha^8 a_s^8 - \frac{\alpha^{10} a_s^{10}}{3840} \right)^2 \exp(-\alpha^2 a_s^2/2) \end{aligned} \quad (2.35)$$

So the expression obtained by the operator method calculation is reproduced from the formula $\langle n|n \rangle$. (i.e., Eqns. 2.33 and 2.35 are identical.)

Now consider the integral form of this matrix element

Other interesting features of this general expression $\langle n|m \rangle$:

Consider $|i\rangle = 0$, to obtain an expression for $p_{0 \rightarrow n}$. We have

$$\begin{aligned} p_{m \rightarrow n} &= |\langle n|m \rangle|^2 = |\langle n| \exp(\lambda a^\dagger) \exp(-\lambda a) |m \rangle|^2 \exp(-\alpha^2 a_s^2/2) \\ &= \frac{\exp(-\alpha^2 a_s^2/4)}{\sqrt{2^{m+n} m! n!}} \left(\sum_{r=\max(0, m-n)}^m (-1)^{n-m+r} 2^{m-r} m_{c_r} \frac{n!}{(n-m+r)!} (b)^{n-m+2r} \right)^2 \end{aligned}$$

when $m = n$ from the Eqn.2.34, we have

$$p_{n \rightarrow n} = \left[\sum_{r=0}^n (-1)^r \left(\frac{\alpha^2 a_s^2}{2} \right)^r \frac{1}{r!} {}^n c_r \right]^2 \exp(-\alpha^2 a_s^2/2)$$

$$p_{0 \rightarrow n} = \frac{\alpha^{2n} a_s^{2n}}{2^n n!} \exp(-\alpha^2 a_s^2 / 2), \text{ (i.e., expression } |\langle n|0 \rangle|^2) \quad (2.36)$$

$$\Rightarrow \sum_{n=0}^{\infty} p_{0 \rightarrow n} = \exp\left(\frac{\alpha^2 a_s^2}{2}\right) \exp\left(-\frac{\alpha^2 a_s^2}{2}\right) = 1, \text{ as expected}$$

$$\Rightarrow \exp\left(\frac{\alpha^2 a_s^2}{2}\right) \cdot 2^r p_{0 \rightarrow r} = \frac{\alpha^{2r} a_s^{2r}}{r!} \quad (2.37)$$

$$\boxed{p_{n \rightarrow n} \Rightarrow \exp\left(\frac{\alpha^2 a_s^2}{2}\right) \left[\sum_{r=0}^n (-1)^r {}^n c_r p_{0 \rightarrow r} \right]^2}$$

Thus the amplitude $p_{n \rightarrow n}$ can be expanded in terms of

intermediate transitions (i.e., $p_{0 \rightarrow r}$). Consider the operator form,

$$p_{n \rightarrow n} = |\langle n | \exp(\lambda a^\dagger) \exp(-\lambda a) | n \rangle|^2 \exp(-\alpha^2 a_s^2 / 2); \text{ This } \langle n | \exp(\lambda a^\dagger) \exp(-\lambda a) | n \rangle \text{ is}$$

$$= 1 - \lambda \sqrt{n} \lambda a^\dagger |n-1\rangle + \frac{\lambda^2}{2!} \sqrt{n(n-1)} \frac{\lambda^2}{2!} (a^\dagger)^2 |n-2\rangle + \dots$$

$$+ \frac{\lambda^r}{r!} (a^\dagger)^r \left[(-1)^r \frac{\lambda^r}{r!} \sqrt{n(n-1)(n-2) \dots (n-r+1)} |n-r\rangle \right] \dots \dots$$

$$\Rightarrow p_{n \rightarrow n} = \left[\sum_{r=0}^n (-1)^r \frac{\lambda^{2r}}{r!} \cdot \frac{n!}{(n-r)! r!} \right]^2 \exp(-\alpha^2 a_s^2 / 2)$$

$$= \left(\sum_{r=0}^n (-1)^r \frac{\lambda^{2r}}{r!} {}^n c_r \right) \exp(-\alpha^2 a_s^2 / 2)$$

$$\equiv \left(\sum_{r=0}^n (-1)^r \left(\frac{\alpha^2 a_s^2}{2} \right)^r \frac{1}{r!} {}^n c_r \right)^2 \exp(-\alpha^2 a_s^2 / 2) \text{ same as 2.34}$$

References

- [1] E. Bonderup, H. Esbensen, J. U. Andersen and H. E. Schi0tt
Rad. Eff. **12**, 261 (1972);
 K. Björkqvist, B. Cartling and B. Domeij *Rad. Eff.* **12**, 267 (1972);
 N. Matsunami and L. M. Howe *Rad. Eff.* **51**, 111 (1980);
 Yu. V. Kononets and V. A. Ryabov
Nucl. Instrum. Meth. in Phys. Res. B **48**, 187 (1990).
- [2] Y. H. Ohtsuki, T. Omura, H. Tanaka and M. Kitagawa
Nucl. Instrum. Meth. **149**, 361 (1978);
 H. Nitta and Y. U. Ohtsuki *Phys. Rev. B* **38**, 4404 (1988)
- [3] L. V. Hau, E. Laegsgaard and J. U. Andersen
Nucl. Instrum. Meth. in Phys. Res. B **48**, 244 (1990)
- [4] M. A. Kumakhov, and R. Wedell, eds.,
Radiation of relativistic light particles during interaction with single crystals;
 (spektrum Akademischer verlag, 1991)
 R. L. Swent, R. H. Patnell, H. Park, J. O. Kephart R. K. Klein, S. Datz,
 R. H. Fearick and B. L. Berman *Phys. Rev. B* **29**, 52 (1984);
 V. V. Beloshitsky and A. A. Bobrov
Nucl. Instrum. Meth. in Phys. Res. B **72**, 395 (1992);
 M. Gouanere *et. al*, *Phys. Rev. B* **38**, 4352 (1988);
 J. Augustin, A. Schafer and W. Greiner *Phys. Rev. A* **51**, 1367 (1995).
 B. L. Berman *Rad. Eff. and Defects in Solids* **122-123**, 277 (1991) and other
 papers in this issue.
- [5] A. Corciovei and A. Visinescu *Rad. Eff.* **55**, 141 (1981)
- [6] A. Tamura and Y. H. Ohtsuki *Phys. Stat. Sol. (b)* **62**, 477 (1974)
- [7] A. P. Pathak and S. Satpathy, *Nucl. Instrum. Meth.* **B 33**, 39 (1988);
 S. Satpathy and A. P. Pathak *Phys. Stat. Sol. (b)* **153**, 455 (1989);
 R. H. Patnell and R. L. Swent *Appl. Phys. Lett.* **35**, 910 (1979);
 H. D. Dulman *et al*, *Phys. Rev. B* **48**, 9 (1993).
- [8] H. Pilkuhn in : — *Relativistic channeling*
 Ed. Richard A. Carrigan, Jr., and James A. Ellison,
 NATO ASI series B **165** 185 (1986) (plenum, N. Y.).

- [9] V. V. Belowshitski and F. F. Komarov *Phys. Rep.* 93, **117** (1982);
J. U. Andersen, E. Bonderop, E. Leagsgaard and A. H. Sørensen
Phys. Scripta 28, 308 (1983).
- [10] R. Wedell *Phys. Stat. Sol. (b)* 99, 11 (1980).
- [11] B. Rath and A. P. Pathak *Rad. Eff.* 63, 227 (1982).
- [12] Leonard I. Schiff, Quantum Mechanics, *McGraw Hill* (1968).
- [13] Lewis M. Branscomb *Phys. Rev. B* **148**, 11 (1966).
- [14] D. S. Gemmell *Rev. Mod. Phys.* 46, 129 (1974).
- [15] J. Mory and Y. Quere, *Rad. Effects.* 13, 57 (1972).
- [16] A. P. Pathak *Rad. Effects.* 61, 1 (1982).
- [17] J. Mory, *J. Physique* 32, 41 (1971); CEA report No. R-4745 (1976)
- [18] L. N. S. Prakash Goteti and Anand P. Pathak
J. Phys. Cond. Matter 9, 1709 (1997).
- [19] M. A. Kumakhov, and R. Wedell, *Phys. Stat. Sol. (b)* **84**, 581 (1977).

Chapter 3

Quantum description of dechanneling by Dislocations

3.1 Introduction:

Dislocations [1] are formed either by **strain** relaxation in the fabrication of semiconductor devices [2] or due to complete missing of atomic planes during the process of crystal growth or ion-implantation. As a result of this, one may notice distortion in the crystallographic channels. This distortion decreases with increasing distance from the *dislocation core*. The crystallographic channels in the vicinity of the dislocation are distorted heavily. However, as shown in Fig, (3.1), the channels outside a particular region of radius r_0 around the dislocation core (called *dechanneling cylinder*), are distorted to a lesser extent and result in only moderate modification in the motion of the channeled particles. These distortions affect the spectrum of channeled flux, even though the energy loss of well channeled particles is not significantly affected [3].

The effects of dislocations on charged particle propagation along major crystallographic directions and planes have been studied for some time. Dechanneling induced by the isolated linear dislocations was first studied by *Quere* [4]. From the balance of the restoring force due to the continuum potential of the atomic strings and the centrifugal deflecting force arising from the bending of the planar channel, he derived a simple analytical expressions for the diameter of the **dechanneling** cylinder, around

the dislocation core.

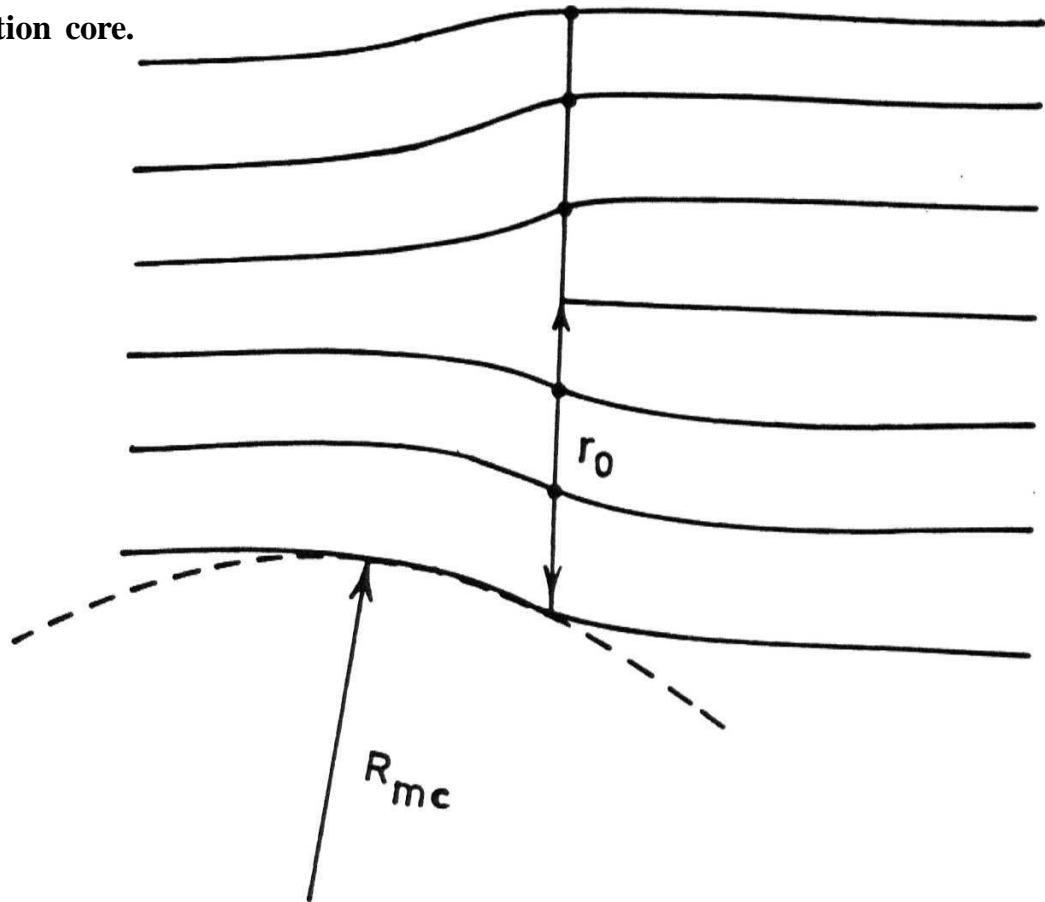


Fig. 3.1 : The planar channels that are distorted due to presence of a dislocation. Here R_{mc} is minimal radius of curvature of a typical channel situated at a distance r_0 from the dislocation.

This classical treatment was successfully refined in a series of studies which describe the effect of the ion trajectories and extended them to the case of dislocation loops [5], formed due to higher dislocation concentration. The results of such theories apply to the characterization of the defective layers, if the defects actions simply superpose with out interacting. This classical approach has been used extensively and shown to describe experimental results [6], reasonably well.

However, as discussed in the previous chapters, the dechanneling of light particles due to presence of the defects should be described quantum mechanically [7, 2], because they cannot be regarded as being localized but rather as an extended wave in

the crystal [9]. In case of point defects, the related effects due to impurity scattering **have** been studied by evaluating quantum mechanically the corresponding scattering cross-sections [1]. Similar quantum treatment for the effects of extended defects like dislocations has not been given so far. In chapter 2, we studied the dechanneling effects due to stacking faults, quantum mechanically, where the effects of obstruction are suitably incorporated in transition matrix elements of wavefunctions. The model gave reasonable description of dechanneling. This stimulated us for further development of these models to handle the distortion effects of the planar channel due to dislocations. Here one requires much more rigorous treatment of the dechanneling problem. At the same time, these quantum dechanneling calculations involve complicated analytical as well as numerical calculations. In this chapter, we restrict ourselves to the simplest case of *screw dislocations* of low concentrations so that there is no nucleation of dislocation loops. We present a model quantum mechanical calculation for the dechanneling effects due to distortions of the planar channel situated away from the dislocation core and there by we evaluate the dechanneling probabilities due to these dislocations.

3.2 Basis of the present model:

For the case of stacking faults, the effects on the propagating particle are of obstruction type and the treatment was simple whereas for the case of dislocations the channels are distorted. Hence these distortion effects on channeling are incorporated by introducing an energy term $(- \frac{E}{R} x^2)$ due to transverse deflecting centrifugal force. Here 'E' is average energy in the curved part of the channel with radius of curvature 'R' and 'x' is the position of the particle in transverse direction.

As shown in Fig. (3.2), the standard displacement equations for the case of screw dislocation are given by

$$u_1 \equiv u_2 \equiv 0, \text{ and } u_3 \equiv \frac{b}{2\pi} \theta.$$

The corresponding critical distance r_0 of such a channel (say A) from the dislocation core with Burger's vector 'b' is calculated by taking the displacement perpendicular to A i.e., with $u = u_3 \cos \varphi$. Choosing the channel along the z - direction (which is same as direction of propagation of the particle), the corresponding curvature was estimated from the second derivative of this displacement equation given by

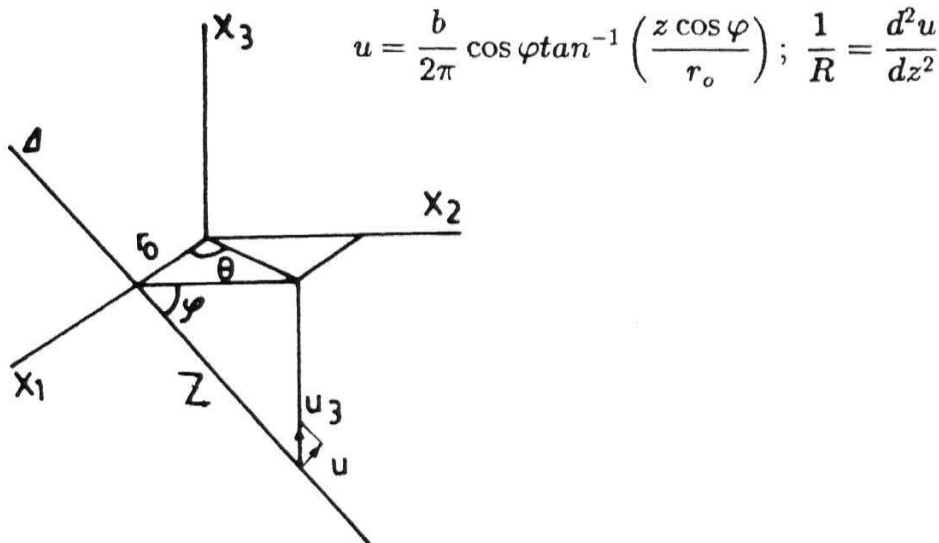


Fig. 3.2 : The displacements of a channel A situated at a distance of r_0 from a screw dislocation along the axis x_3 . Here φ is the angle made by the channel with x_1x_2 plane.

By solving the above displacement equations for screw dislocation, the mean dechanneling radius is obtained in terms of minimal radius of curvature which is given by [4]

$$r_0 = \sqrt{\left(\frac{bR_{mc}}{10}\right)} \quad (3.1)$$

with ' \mathbf{b} ' as the Burgers vector. Here, the critical minimum radius of curvature R_{mc} of channels (below which the particle will dechannel completely) is obtained by equating the deflecting centrifugal force to the restoring force due to planar potential, evaluated at the minimum distance of approach $a_{T.F.}$ [11]. The amount of distortion present in a channel depends on the average concentration of the dislocations ' n ', one can make an estimate for the farthest distance from the dislocation in terms of dislocation concentration ($r_o^{\max} = 1/2(n^{1/2})$).

3.2.1 Relativistic expression for the curvature:

The analytical expression (for curvature) so obtained in the previous section is appropriate for non-relativistic heavy ions like protons, α - particles, etc. So it is quite obvious that above expression is no longer valid for relativistic particles, hence these relativistic effects are to be incorporated suitably to obtain an equivalent relativistic expression for the curvature. Here we consider the motion of the positrons described in the *rest frame* of the particle. In this frame the particle "sees" continuum potential $\gamma V(x)$ in the transverse direction because of the fact that for the relativistic energies, the continuum potential in the transverse space is enhanced by a factor of γ ($= 1/\sqrt{1 - v_z^2/c^2}$), due to length contraction in the direction of propagation. We denote the longitudinal co-ordinate in this relativistic case as (Z) ($= z/\gamma$ with z being that in non-relativistic case). When the particle enters into the distorted portion, the motion of the particle is modified due to the influence of the curvature and in this distorted part of the channel, the corresponding relativistic displacement equation along Z is obtained as follows:

$$Z \rightarrow \frac{z}{\gamma} \Rightarrow \frac{d}{dz} = \frac{d}{dZ} \frac{dZ}{dz} \Rightarrow \frac{d^2}{dZ^2} = \gamma^2 \frac{d^2}{dz^2} \Rightarrow \frac{1}{R} = \frac{d^2 u}{dZ^2} = \gamma^2 \frac{d^2 u}{dz^2} \Big|_{z=\gamma Z} \quad (3.2)$$

So the modified continuum potential as “seen” by the particle becomes 7
this is given by

$$\gamma V_{eff} = \gamma V(x) - \gamma^2 m v_z^2 \left\{ \frac{b}{\pi} \cdot \frac{r(\gamma Z)}{(r^2 + \gamma^2 Z^2)^2} \right\} x \quad (3.3)$$

The expression for dechanneling radius r_0 in terms of minimal critical radius of curvature R_{mc} is obtained by equating the restoring force ($-\gamma \frac{dV}{dy}$) to the maximum value of the deflecting force due to curvature ($\gamma^2 \frac{2E}{R_{mc}}$). Using this procedure [11] and Eqn. (1.20), we have

$$\begin{aligned} V(y) &= \frac{2V_0 a_{T.F}}{(y + a_{T.F})} \quad \text{with } V_0 = \pi Z_1 Z_2 e^2 C a_{T.F} N_p \\ &\Rightarrow -\gamma \frac{dV}{dy} \Big|_{a_{T.F}} = \gamma \frac{V_0}{2a_{T.F}} \\ -\gamma \frac{dV}{dy} &= \gamma^2 \frac{2E}{R_{mc}} \Rightarrow \frac{V_0}{2a_{T.F}} = 2E \frac{\gamma}{R_{mc}} \Rightarrow \frac{R_{mc}}{\gamma} = \frac{4E}{\pi Z_1 Z_2 e^2 C N_p} \Rightarrow R_{mc} \rightarrow \frac{R_{mc}}{\gamma} \end{aligned}$$

The deflection force term on the other hand leads to modification in r_0 given by

$$r_0 = \sqrt{\gamma^2 \frac{b}{10} \frac{R_{mc}}{\gamma}} \Rightarrow r_0 \rightarrow \sqrt{\frac{\gamma b R_{mc}}{10}} = \sqrt{\gamma} r_0$$

One may notice that, due to these relativistic effects r_0 in Eqn. (3.1) is enhanced by a factor of $\sqrt{\gamma}$. Here we evaluate dechanneling probabilities and discuss their variation with channel distance r_0 (given by Eqn. (3.1)) from the dislocation core.

Like in the stacking fault case, the quantum description requires as to calculate the *transition probability* among the energy levels in the transverse continuum potential. These transitions are induced by the distortion created due to dislocations. As before, we use harmonic oscillator model for transverse potential and sudden approximation for transitions. The coupling constant α (appearing in the normal harmonic oscillator model potential $\alpha = \sqrt{\frac{m_{\perp} \omega}{\hbar}}$) will change to α' in the distorted portion because the oscillation frequency of the particle gets modified in this distorted portion, due to modification of net force constant.

The centrifugal energy term in the distorted portion is to be added to the well known continuum potential (surrounding the channel), which acts as **restoring** force [12, 11]. The channels within that critical region are distorted heavily, which eventually leads to dechanneling of most of the particles arriving in that region. However, the regions outside that *core region* are only moderately affected; channeling and continuum model is still valid and used extensively by incorporating the effects of distortion through above mentioned centrifugal force term. The situation in these regions is similar to that found in the bending of beams by *bent crystal channeling* [15] explained with continuum model. The condition is that bending should be less than critical angle for channeling. The force constant in the distorted channel is different from that in the straight channel and as a result of that, all the particles coming in the channels with radius of curvature less than R_{mc} will get dechanneled. This modified force constant is obtained with the consideration of the harmonic approximation to above effective planar potential in the distorted part. This analysis is appropriate for the channels that are situated far away from the dislocation which in turn implies that we are dealing with crystals of low dislocation concentrations (typically 10^6 to 10^8 per cm^2).

Classically, the initially well-channeled particle in undistorted region starts oscillating about the axis of the distorted channel. Once it enters into the distorted portion, the potential minimum (about which the particle oscillates) is shifted due to curvature, reducing the available space for transverse motion in the channel. The expression for this shift (say ' a_r ') in the distorted channel is obtained with an approximation namely, neglecting fourth and higher order terms of $\frac{x}{L}$ which implies that we are dealing with those channel which are not heavily distorted (i.e., not very close to dislocation axis). This in turn introduces a maximum error of about 6%. The effects of distortion on the continuum potential will be discussed in the following section

3.2.2 Effects of distortion on the force constant:

The effective potential in the distorted part of the channel is given by [12]

$$V_{\text{eff}} = \frac{4V_0La_{T.F}}{L^2 - x^2} - \frac{2E}{R}x \quad (3.4)$$

Expanding this around the shifted minimum, a_r

$$V_{\text{eff}}(x) = V_{\text{eff}}(a_r) + (x - a_r) \left. \frac{dV_{\text{eff}}}{dx} \right|_{x=a_r} + \frac{1}{2}(x - a_r)^2 \left. \frac{d^2V_{\text{eff}}}{dx^2} \right|_{x=a_r}$$

$$\frac{dV_{\text{eff}}}{dx} = 0 \Rightarrow a_r = \sqrt{\left(\frac{B^2}{L^2}\right) + \frac{L^2}{2}} - \frac{B}{L}; B = \frac{RV_0a_{T.F}}{E}, L = l + a_{T.F}$$

$$\Rightarrow V_{\text{eff}}(x) = V_{\text{eff}}(a_r) + \frac{1}{2}(x - a_r)^2 \left. \frac{d^2V_{\text{eff}}}{dx^2} \right|_{x=a_r} \quad (3.5)$$

The effective force constant is obtained as

$$k_1^{\text{eff}} = \frac{8V_0a_{T.F}L}{(L^2 - a_r^2)^3} [L^2 + 3a_r^2]$$

Hence the maximum number of bound states in the distorted part (j_{max}) is obtained as

$$j_{\text{max}} = \frac{1}{2} \left[\sqrt{\frac{\gamma m 8V_0a_{T.F}L}{(L^2 - a_r^2)^3} (L^2 + 3a_r^2)} \frac{(l - a_{T.F} - a_r)^2}{\hbar} - 1 \right] \quad (3.6)$$

From the prescription given in the previous chapter, we have

$$N_p = 0.0394649a_o^{-2}; V_0 = \pi Z_1 Z_2 e^2 C a_{T.F} N_p = 0.9671975 \text{ a.u.}$$

$$L = l + a_{T.F} = 2.2094091a_o + 0.3466437a_o = 2.5560528a_o; l - a_{T.F} = 1.8627654a_o.$$

$$\Rightarrow j_{\text{max}} = \frac{1}{2} \left[\sqrt{\frac{171.39505}{(6.5334059 - a_r^2)^3} (6.5334059 + 3a_r^2)} (1.8627654 - a_r)^2 - 1 \right]$$

As a consequence of change in the force constant of harmonic motion in the distorted portion, coupling constant gets modified to α' . So from the Eqn. (3.6),

$$\alpha'^2 = \sqrt{\gamma m 8V_0a_{T.F}L \frac{L^2 + 3a_r^2}{(L^2 - a_r^2)^3}} = \sqrt{\frac{\gamma m 8V_0a_{T.F}}{L^3} \left\{ \frac{1 + 3(a_r/L)^2}{1 - (a_r/L)^2} \right\}}$$

$$= \tau^2 \alpha^2 \text{ where } \alpha^2 = \sqrt{\frac{\gamma m 8 V_0 a_{T.F}}{L^3}} \text{ and } \tau^2 = \sqrt{\left\{ \frac{1 + 3(a_r/L)^2}{1 - (a_r/L)^2} \right\}}$$

When $a_r \rightarrow 0$, we notice $\alpha' \rightarrow \alpha$ indicating that the shift in the potential (induced by the curvature) reflects in the modification of resulting force constant. This is as expected because when the channel becomes straight the coupling term will be as it was in the straight channel. Here we introduce a transition parameter $\tau (= \alpha'/\alpha)$ as we did in the earlier chapter. As shown in Fig. (3.3), $r \rightarrow 1 \Rightarrow a_r \rightarrow 0$ and this happens when the channel becomes straight (radius of curvature $R \rightarrow \infty$). Here onwards we call this ' τ ' as *distortion parameter* to take care of distortion effects.

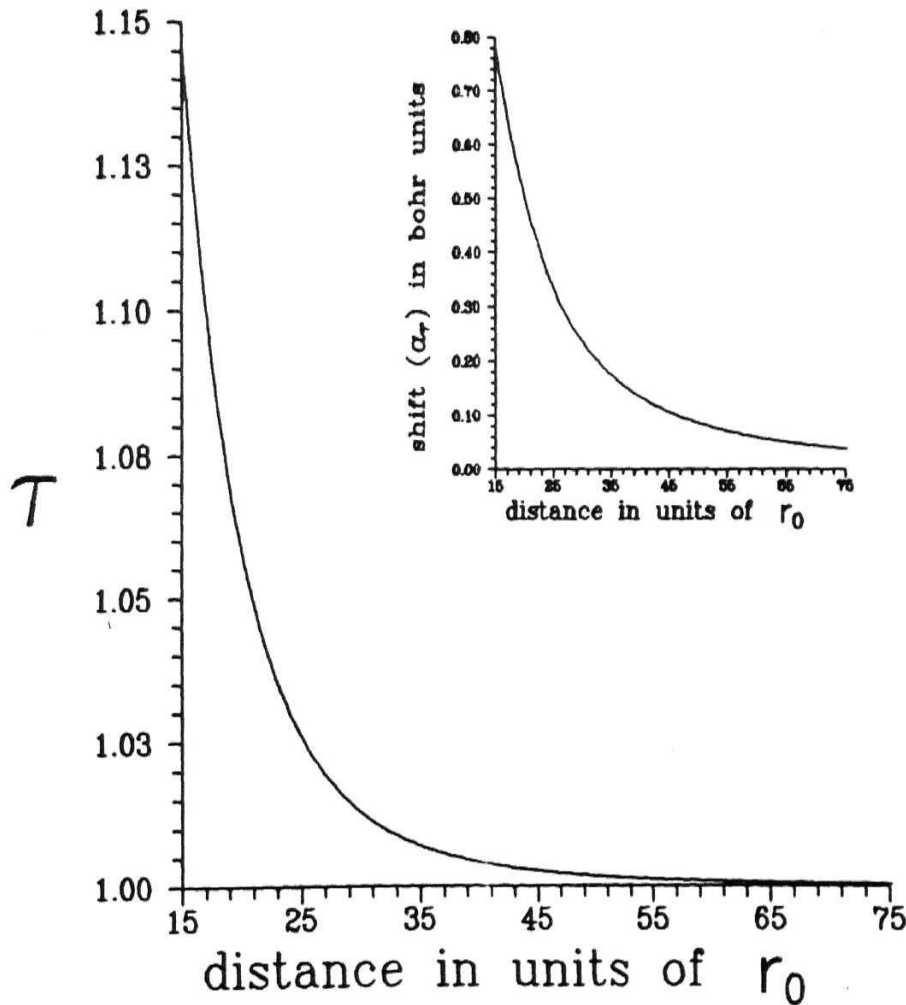


Fig. 3.3 : The variation of distortion parameter τ ($r = \alpha'/\alpha$) as a function of distance from the dislocation.

3.3 Theory and formulation:

Using those concepts discussed in the previous sections, a quantum mechanical formulation is developed for the effects of dislocations on planar dechanneling of positrons, with specific reference to screw dislocations. Here we use analysis similar to that given in the previous chapter and corresponding bound states in the straight channel are considered with $n_{\max} = i_{\max}$. This i_{\max} is calculated by equating total transverse energy to the depth of the continuum potential well; these details are given in forthcoming sections. The channeling/dechanneling phenomena under this situation is governed by the overlap integrals of the appropriate wave functions in various regions of distortion. As shown in Fig. (3.4), there are three *boundaries*, which the particle has to cross during its passage through the distorted channel, to find itself again in straight channel.

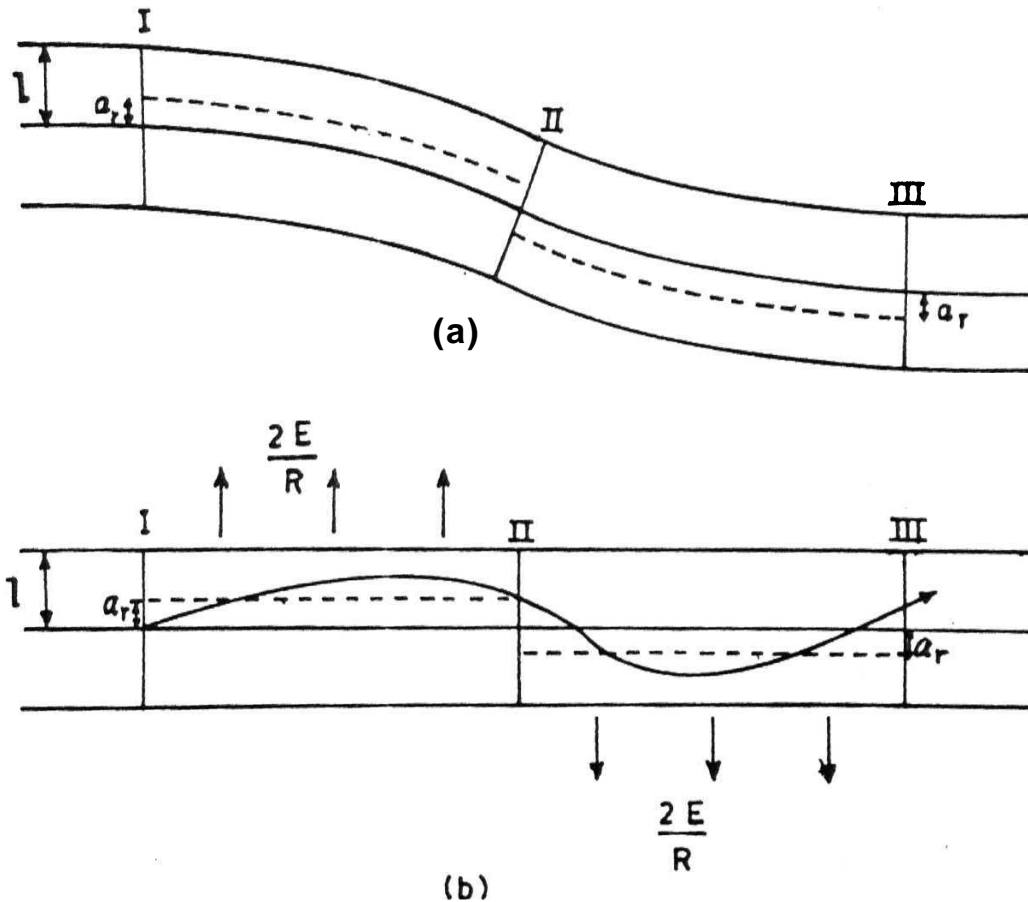


Fig. 3.4 : a) Typical planar channel of some finite curvature R , ' a_r ' is the shift in equilibrium position due to distortion.
 b) Straight model channel replacing the channel of part (a).
 Here I, II, III are various portions of distortion and ' a_r ' is the equilibrium position about which the particle will oscillate.

These boundaries are not so sharply well defined. However, for simplicity of the present (model) calculations, we use sudden approximation to calculate the transition probabilities across these three boundaries and in what follows, we will identify these boundaries as 3 interfaces (denoted by I, II, & III). The wavefunction of the particle in different regions may be written as,

$$\psi_i = \psi_L = \left(\frac{\alpha}{\sqrt{\pi} 2^i i!} \right)^{1/2} \exp \left\{ -\frac{\alpha^2 x^2}{2} \right\} H_i(\alpha x) \quad (3.7)$$

$$\psi_j^{(1)} = \psi_I = \left(\frac{\alpha'}{\sqrt{\pi} 2^j j!} \right)^{1/2} \exp \left\{ -\frac{\alpha'^2 (x + a_r)^2}{2} \right\} H_j(\alpha' x + \alpha' a_r) \quad (3.8)$$

$$\psi_k^{(2)} = \psi_{II} = \left(\frac{\alpha'}{\sqrt{\pi} 2^k k!} \right)^{1/2} \exp \left\{ -\frac{\alpha'^2 (x - a_r)^2}{2} \right\} H_k(\alpha' x - \alpha' a_r) \quad (3.9)$$

$$\psi_f = \psi_R = \left(\frac{\alpha}{\sqrt{\pi} 2^f f!} \right)^{1/2} \exp \left\{ -\frac{\alpha^2 x^2}{2} \right\} H_f(\alpha x) \quad (3.10)$$

As described in section 2.2 of previous chapter, the maximum number of quantum states supported by a planar channel (surrounded by two planes) is estimated from the equation given by

$$\left(i_{\max} + \frac{1}{2} \right) \hbar \omega = \frac{1}{2} k_1 x_{\max}^2. \quad (3.11)$$

The maximum number of quantum states in undistorted continuum potential $i_{\max} = f_{\max}$ is taken as 3. However, the number of quantum states available in the distorted portions '1' and '2' is estimated using Eqn. (3.6) which is found to be $i_{\max}^{(1)} = k_{\max}^{(2)} = 1$, corresponding to a channel situated at a distance of $15r_0$ from the dislocation (r_0 obtained from Eqn.(3.1) and for the present case of Al(111), b is taken as **2.86Å**). As shown in Fig. (3.5), this $j_{\max}^{(1)}$ approaches to i_{\max} for those channels at the farthest distance from the **core**.

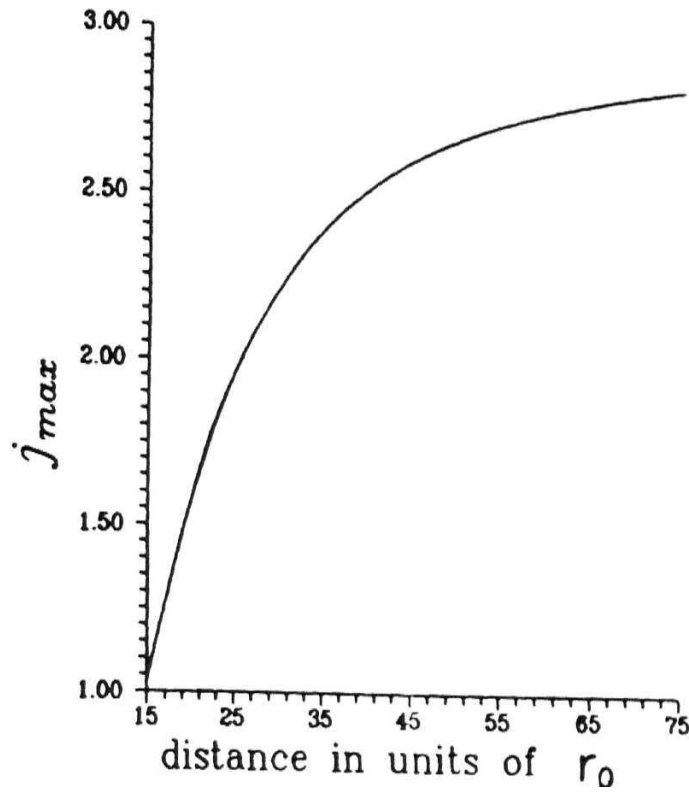


Fig. 3.5 : The variation of number of states supported by a planar channel with channel distortion, where these effects are expressed in units of r_0

3.3.1 Channeling probabilities across(I) interface:

The channeling probability of the particle with initial state $|i\rangle$ to cross first interface and to be in state $|j\rangle$ in distorted part, can be defined as

$$p_{i \rightarrow j} = |\langle \psi_j^{(1)} | \psi_i \rangle|^2 \quad (3.12)$$

where subscript '1' on the state denotes the relevant wave function corresponds to distorted channel after I interface.

We have

$$\begin{aligned} |\langle j^{(1)} | i \rangle|^2 &= \left(\frac{\alpha \alpha'}{\pi 2^{j^{(1)}+i} j^{(1)}! i!} \right) \exp \left\{ - \left(\frac{\alpha'^2}{\alpha^2 + \alpha'^2} \right) \alpha^2 a_r^2 \right\} \\ &\times \left| \int_{-\infty}^{\infty} \exp \left\{ - \frac{1}{2} (\alpha^2 + \alpha'^2) \left[x + \frac{\alpha'^2}{\alpha^2 + \alpha'^2} a_r \right] \right\} H_j(\alpha' x + \alpha' a_r) H_i(\alpha x) \right|^2 dx \end{aligned}$$

For example consider,

i) $|\langle 0^{(1)}|0\rangle|^2$:

$$\begin{aligned}
 &= \left(\frac{\alpha\alpha'}{\pi} \right) \exp \left\{ - \left(\frac{\alpha'^2}{\alpha^2 + \alpha'^2} \right) \alpha^2 a_r^2 \right\} \\
 &\quad \times \left| \int_{-\infty}^{\infty} \exp \left\{ -\frac{1}{2} (\alpha^2 + \alpha'^2) \left[x + \frac{\alpha'^2}{\alpha^2 + \alpha'^2} a_r \right] \right\} H_0(\alpha'x + \alpha'a_r) H_0(\alpha x) \right|^2 \\
 &= \frac{2\alpha\alpha'}{\alpha^2 + \alpha'^2} \exp \left\{ - \left(\frac{\alpha'^2}{\alpha^2 + \alpha'^2} \right) \alpha^2 a_r^2 \right\} \\
 |\langle 0^{(1)}|0\rangle|^2 &\Rightarrow 2 \left(\frac{\tau}{1 + \tau^2} \right) \exp \left\{ -\frac{\tau^2}{1 + \tau^2} \alpha^2 a_r^2 \right\}
 \end{aligned}$$

ii) $|\langle 1^{(1)}|0\rangle|^2$:

$$\begin{aligned}
 &= \left(\frac{\alpha\alpha'}{2\pi} \right) \exp \left\{ - \left(\frac{\alpha'^2}{\alpha^2 + \alpha'^2} \right) \alpha^2 a_r^2 \right\} \\
 &\quad \times \left| \int_{-\infty}^{\infty} \exp \left\{ -\frac{1}{2} (\alpha^2 + \alpha'^2) \left[x + \frac{\alpha'^2}{\alpha^2 + \alpha'^2} a_r \right] \right\} H_1(\alpha'x + \alpha'a_r) H_0(\alpha x) \right|^2 \\
 &= \left(\frac{4\alpha\alpha'}{\alpha^2 + \alpha'^2} \right) (\alpha'^2 a_r^2) \left(\frac{\alpha^2}{\alpha^2 + \alpha'^2} \right)^2 \exp \left\{ - \left(\frac{\alpha'^2}{\alpha^2 + \alpha'^2} \right) \alpha^2 a_r^2 \right\} \\
 |\langle 1^{(1)}|0\rangle|^2 &\Rightarrow \left(\frac{4\tau}{1 + \tau^2} \right) \left(\frac{\tau}{1 + \tau^2} \right)^2 \alpha^2 a_r^2 \exp \left\{ -\frac{\tau^2}{1 + \tau^2} \alpha^2 a_r^2 \right\}
 \end{aligned}$$

iii) $|\langle 2^{(1)}|0\rangle|^2$:

$$\begin{aligned}
 &= \left(\frac{\alpha\alpha'}{8\pi} \right) \exp \left\{ - \left(\frac{\alpha'^2}{\alpha^2 + \alpha'^2} \right) \alpha^2 a_r^2 \right\} \\
 &\quad \times \left| \int_{-\infty}^{\infty} \exp \left\{ -\frac{1}{2} (\alpha^2 + \alpha'^2) \left[x + \frac{\alpha'^2}{\alpha^2 + \alpha'^2} a_r \right] \right\} H_2(\alpha'x + \alpha'a_r) H_0(\alpha x) \right|^2 \\
 &= \frac{\alpha\alpha'}{4(\alpha^2 + \alpha'^2)} \left[2 \left(\frac{\alpha^2 - \alpha'^2}{\alpha^2 + \alpha'^2} \right) + 4\alpha^2 a_r^2 \left(\frac{\alpha'^2}{\alpha^2 + \alpha'^2} \right)^2 \right]^2 \exp \left\{ - \left(\frac{\alpha'^2}{\alpha^2 + \alpha'^2} \right) \alpha^2 a_r^2 \right\} \\
 |\langle 2^{(1)}|0\rangle|^2 &\Rightarrow \left(\frac{\tau}{4(1 + \tau^2)} \right) \left[\left(\frac{\tau^2}{1 + \tau^2} \right)^2 4\alpha^2 a_r^2 + 2 \left(\frac{1 - \tau^2}{1 + \tau^2} \right) \right]^2 \exp \left\{ -\frac{\tau^2}{1 + \tau^2} \alpha^2 a_r^2 \right\} \\
 &= |\langle 0^{(1)}|2\rangle|^2
 \end{aligned}$$

By incorporating appropriate Hermite functions in the overlap integral one **can** obtain the other expressions for these transition amplitudes. The details of these expressions are given in the APPENDIX. Here it can easily be verified that $|\langle i|j^{(1)}\rangle|^2 = |\langle j^{(1)}|i\rangle|^2$. The Corresponding probability for the particle with initial state $|i\rangle$ (in the straight part of the channel), to occupy any one of the states $|j^{(1)}\rangle (j_{\max} < i_{\max})$ in the distorted portion I is:

$$p_i^I = \sum_{j=0}^{j_{\max}} |\langle j^{(1)}|i\rangle|^2 \quad (3.13)$$

So the dechanneling probability at (I) is $\chi_i^I = 1 - p_i^I$ •

3.3.2 Channeling probabilities across (II) interface:

The channeling probability of the particle with intermediate state $|j\rangle$ to cross second interface and to occupy a state $|k\rangle$ can be defined as

$$p_{j \rightarrow k} = |\langle \psi_k^{(2)} | \psi_j^{(1)} \rangle|^2 \quad (3.14)$$

Here subscript '2' denotes the wave function in second part of distorted channel after crossing 'II' interface.

Corresponding probability of the particle to occupy any one of the states $|k\rangle$ ($k_{\max} < i_{\max}$) is:

$$p_{j(i)}^{II} = \sum_{k=0}^{k_{\max}} |\langle k^{(2)} | j^{(1)} \rangle|^2; \chi_{j(i)}^{II} = 1 - p_{j(i)}^{II} \quad (3.15)$$

To evaluate various matrix elements in this case, we make use of the general expression obtained for $(j|k)$ in the previous chapter and one may notice here that $|\langle k^{(2)} | j^{(1)} \rangle|^2 = |\langle j^{(2)} | k^{(1)} \rangle|^2$. These details are given in APPENDIX - II

3.3.3 Channeling probabilities across (III) interface:

The channeling probability of the particle with intermediate state $|k\rangle$ to cross third interface and to occupy any one of the states $|f\rangle$ ($f < i$) is:

$$p_k^{III} = \sum_{f=0}^3 |\langle f|k^{(2)}\rangle|^2; \chi_k^{III} = 1 - p_k^{III} \quad (3.16)$$

with

$$p_{k^{(3)} \rightarrow f} = |\langle f|k^{(2)}\rangle|^2 \quad (3.17)$$

For Example,

$$p_{0^{(2)} \rightarrow 0}^{(3)} = |\langle 0|0^{(2)}\rangle|^2 = 2 \frac{\tau}{1 + \tau^2} \exp \left\{ -\frac{\tau^2}{1 + \tau^2} \alpha^2 a_r^2 \right\} = |\langle 0^{(1)}|0\rangle|^2$$

The details of these expressions are given in the APPENDIX - I. Further, it can be shown that $|\langle f|k^{(2)}\rangle|^2 = |\langle j^{(1)}|i\rangle|^2$ for the same quantum numbers of ' k ' and ' j '. The transition probability for the passage of initially well channeled particle through dislocation will be product of the transition probabilities across various parts of the channel, where the effects of distortion are suitably incorporated. The general expression for the total channeling probability of the particle with a specific initial state $|i\rangle$ so that the particle feels itself again in the straight channel with final state $|f\rangle$ (after passing through the various portions of distortion) has been obtained and is given by [15]

$$p_{i \rightarrow f} = \sum_{k^{(2)}=0}^{k_{max}^{(2)}} \left(p_{k^{(2)} \rightarrow f} \left[\sum_{j^{(1)}=0}^{j_{max}^{(1)}} p_{i \rightarrow j^{(1)}} \times p_{j^{(1)} \rightarrow k^{(2)}} \right] \right) = p_{f \rightarrow i} \quad (3.18)$$

The total channeling probability for initially well channeled particle, to find itself again in the straight channel after passing through various portions of the distortions is given by

$$p_0 = \sum_{f=0}^{f_{max}=3} (p_{0 \rightarrow f}); \chi_0 = 1 - p_0 \quad (3.19)$$

These probabilities are calculated by incorporating the above equations and results are given in Fig. (3.6 - 3.8)

3.4 Results and Discussion:

We have developed a quantum theory of dechanneling due to defects with special reference to dislocations. The theory is valid as long as the number of quantum states supported by the transverse potential due to the two planes is small and is the case of light particles (like positrons) in MeV range. We studied the dechanneling processes by continuous distortions of the planar channels, mapping to three distinct regions and corresponding displaced and modified wavefunctions. This happens for channels far away from the dislocation which in turn implies applicability of present calculation to lower concentrations (i.e. no interaction between dislocations). On the other hand the channels close to the dislocation axis, the distortion is so heavy that one can not talk of crystallographic channels.

In Fig. 3.3, we show the variation of the distortion parameter ' τ ' with r_0 . We notice that, for larger r_0 the radius of curvature (R) of distorted planar channel increases to infinity, $a_r \rightarrow 0$ and $r \rightarrow 1$ as expected because the coupling terms in the wavefunctions are identical, the particle recognizes the absence of distortions in those regions and obviously the non-diagonal matrix elements vanish for $a_r = 0$, implying that a well-channeled particle cannot suddenly go to oscillatory behaviour in an undistorted channel. In Fig. 3.5, we have shown variation of maximum number of allowed states in the distorted channel as a function of distance from the dislocation. The atomic planes at considerably larger distances from the core are distorted slightly and thus ' r_0 ' carries the signature of the distortion effects. We notice that j_{\max} approaches asymptotically to $i_{\max}(= 3)$ as r_0 increases (i.e. the channel is almost straight). As mentioned earlier this depends on the concentration of dislocations, thus for lower concentrations we have a family of channels through which a particle can propagate successfully with out much dechanneling. We consider the channels starting from $15r_0$ (this corresponds to a

concentration $\approx 3 \times 10^8$ dislocations/cm², below this the channels are distorted heavily leading to formation of dislocation loops) to a farthest distance $50r_0$ (this dislocation concentration is typically $\approx 2 \times 10^7$ /cm²).

The results for channeling probabilities obtained from expressions (3.18) and (3.19) have been plotted in Figs. (3.6 & 3.7) for initially well channeled particle (i.e. ground state) and first excited state respectively. One may notice that at some values of r_0 , there is sharp increase in the probability for individual transitions. This is result of change in the number of states supported in the distorted portions of channel (i.e., after I & II interfaces). This is also reflected in the overall dechanneling probabilities χ_0 and χ_1 respectively, because corresponding channeling probabilities approaches unity for the channels situated at the farthest from the dislocation axis, which means that slight dissociation of dislocations reduces their long range distortion as discussed in classical analysis.

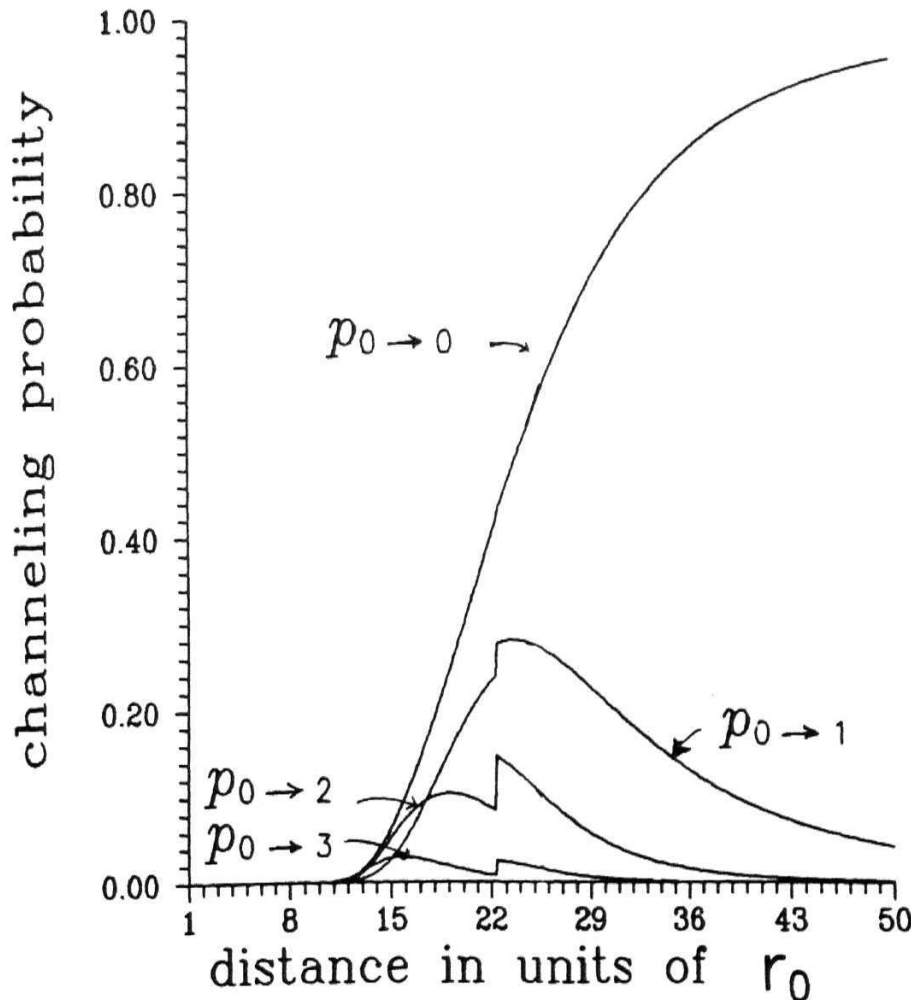


Fig. 3.6 : Influence of channel distance from the dislocation on channeling probabilities corresponding to initially well channeled particle ($i = |0\rangle$).

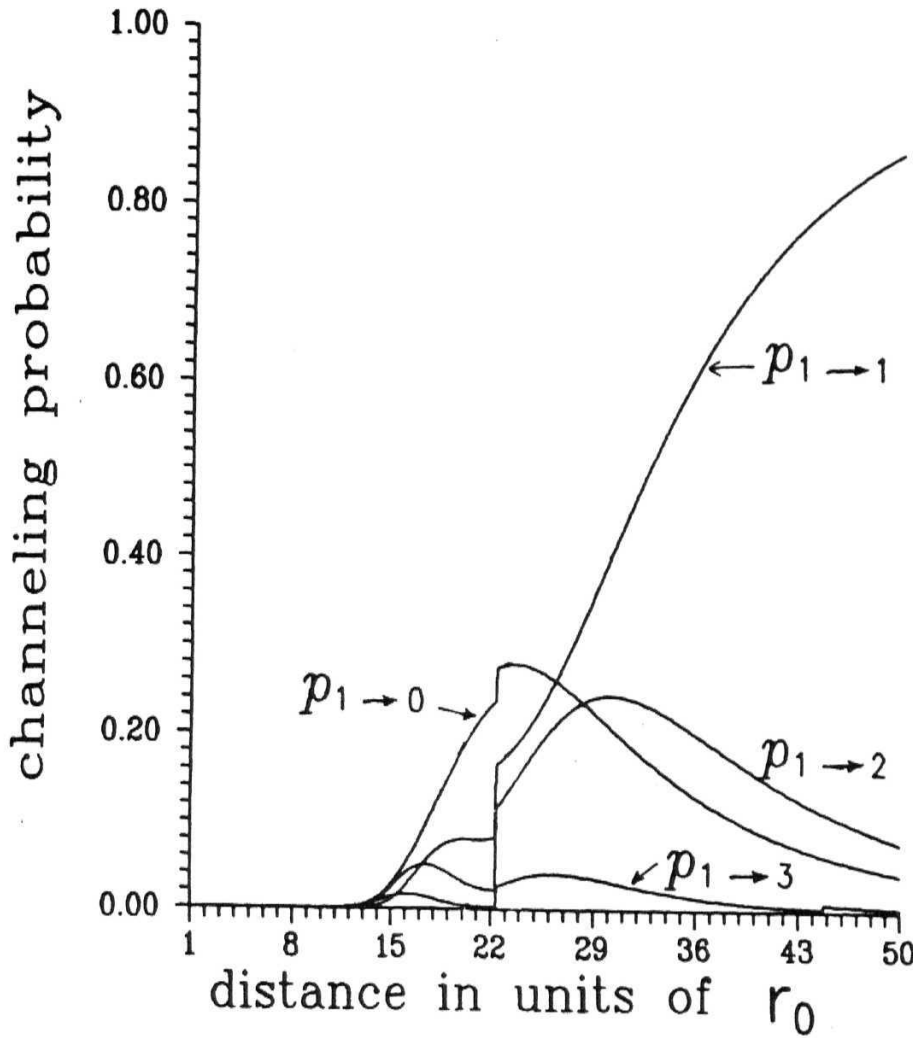


Fig. 3.7 : Influence of the channel distance from the dislocation on channeling probabilities corresponding to initial state $|1\rangle$.

As shown in Fig. (3.8), the overall dechanneling probabilities for initially well channeled particle (xo) always less for any channel as compared to χ_1 (particle initially in first excited state) because well channeled particle, even after making transitions to other excited states in distorted portions of the channel, manages to remain channeled for higher curvatures (lesser radii of curvatures) than does the initially excited (oscillating) particle. In the present simple model calculation these effects are manifested in natural way.

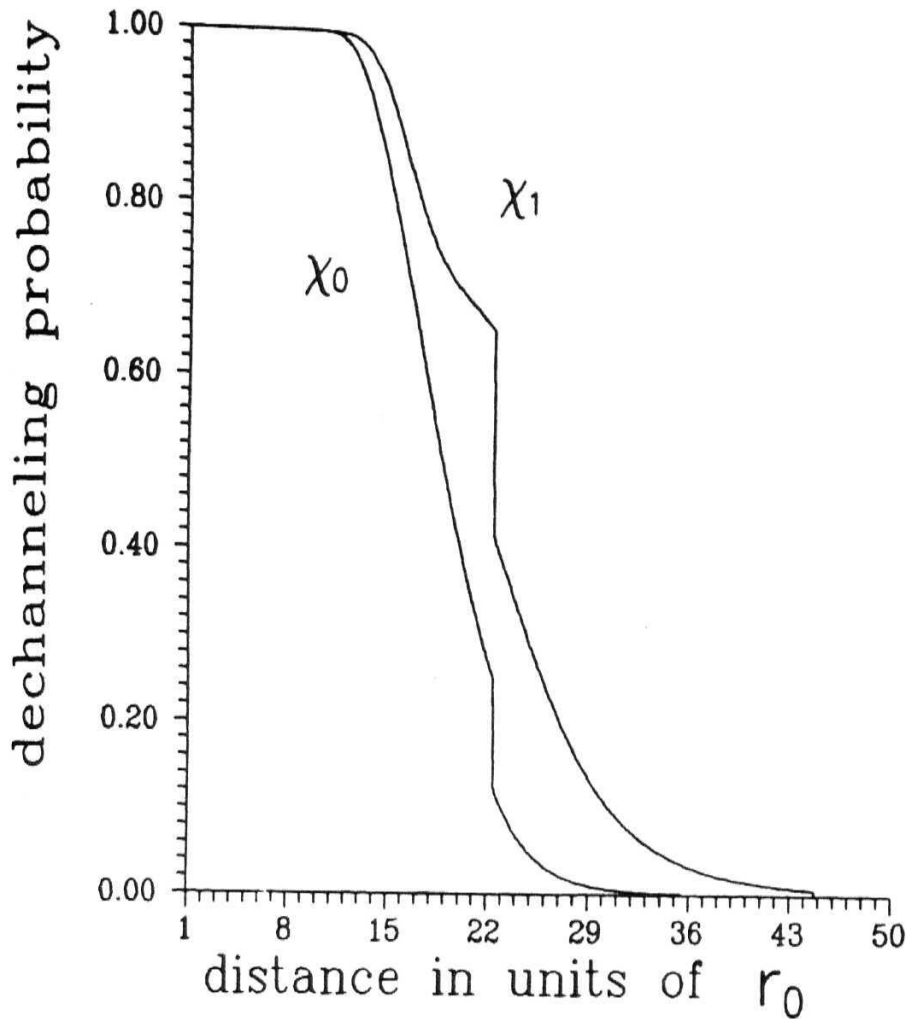


Fig. 3.8 : Influence of the channel distance from the dislocation on total dechanneling probabilities for initial state $|0\rangle$ and $|1\rangle$ denoted by χ_0 and χ_1 respectively.

If the particle after passing through various portions of distortions goes to a state which is same as initial state, corresponding channeling/transition probability is much higher as compared to other transitions. This is expected and can also be seen through the asymmetric nature of the planar channel. The channeling probabilities corresponding to different initial and final states combination are very low, and approach zero as channel distance increases from the dislocation. So the dechanneling probability depends upon final state of the particle which in turn reflects the phase dependence of the approaching particle, near the distortion.

The equation (3.18) carries the signature of interesting left-right symmetry inbuilt in the problem which is not clearly realized in classical descriptions. Fig. (3.9) shows the energy dependence of dechanneling probabilities, for initially well channeled particles. At the lower end of these relativistic energies, it is linear variation and as energy increases to higher side of relativistic energy, the energy dependence tends to be slower than linear.

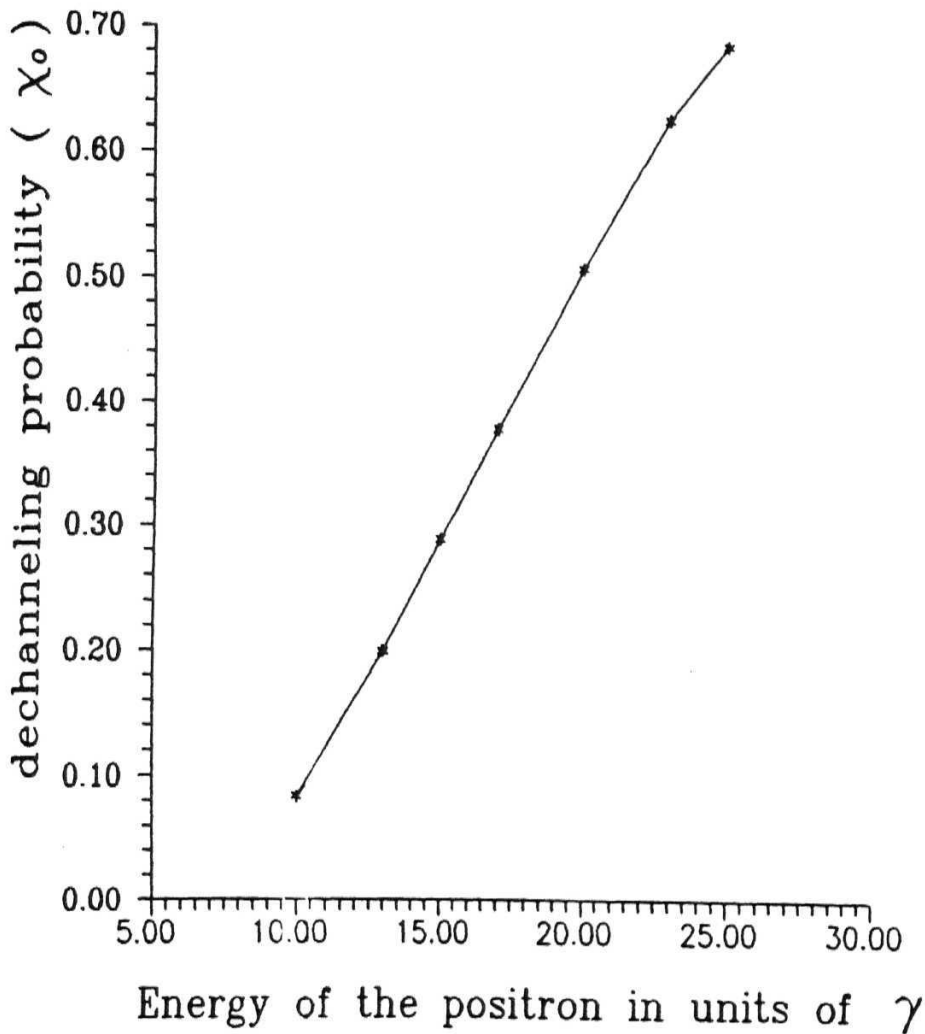


Fig. 3.9 : Energy dependence of total dechanneling probability of initially well channeled particle ' χ_0 '.

APPENDIX -

Evaluation of individual transition amplitudes: $|\langle j^{(1)}|i\rangle|^2$

Here we denote $\beta = \frac{\tau}{1+\tau^2}$; $\xi = \frac{\tau^2}{1+\tau^2}$, and $Ex = \exp\{-\xi\alpha^2 a_r^2\}$; this notion makes the final expressions for transition amplitudes more compact. By substituting the Hermite functions corresponding to various states and evaluating the integrals, the expressions for individual transition amplitudes are obtained as:

$$\begin{aligned}
|\langle 0^{(1)}|0\rangle|^2 &= 2\beta Ex \\
|\langle 1^{(1)}|0\rangle|^2 &= 4\beta^3 \alpha^2 a_r^2 Ex \\
|\langle 2^{(1)}|0\rangle|^2 &= \frac{\beta}{4} \left[4\beta^2 \alpha^2 a_r^2 + 2 \left(\frac{1-\tau^2}{1+\tau^2} \right) \right]^2 Ex \\
|\langle 3^{(1)}|0\rangle|^2 &= \frac{\beta}{24} \left[\alpha a_r (24\tau\xi^2 - 36\tau\xi + 12\tau) + \alpha^3 a_r^3 (8\tau^3\xi^3 + 24\tau\xi^2 - 8\tau^3) \right]^2 Ex \\
|\langle 0^{(1)}|1\rangle|^2 &= 4\beta\xi^2 \alpha^2 a_r^2 Ex \\
|\langle 1^{(1)}|1\rangle|^2 &= 8\beta^3 [1 - \xi\alpha^2 a_r^2]^2 Ex \\
|\langle 2^{(1)}|1\rangle|^2 &= \frac{\beta}{8} \left[\alpha a_r (24\xi^2 - 20\xi) + \alpha^3 a_r^3 (8\tau^2\xi^3 - 16\tau^2\xi^2 + 8\tau^2\xi) \right]^2 Ex \\
|\langle 3^{(1)}|1\rangle|^2 &= \frac{\beta}{48} \left[(48\beta\xi - 24\beta) + \alpha^2 a_r^2 (96\tau\xi^3 - 168\tau\xi^2 + 72\tau\xi) \right. \\
&\quad \left. + \alpha^4 a_r^4 (16\tau^3\xi^4 + 48\tau\xi^3 - 16\tau^3\xi) \right]^2 Ex \\
|\langle 0^{(1)}|2\rangle|^2 &= \frac{\beta}{4} \left[2 \left(\frac{1-\tau^2}{1+\tau^2} \right) + 4\xi^2 \alpha^2 a_r^2 \right]^2 Ex \\
|\langle 1^{(1)}|2\rangle|^2 &= \frac{\beta}{8} \left[8\beta\xi^2 \alpha^3 a_r^3 + 4\beta\alpha a_r - 24\beta\xi\alpha a_r \right]^2 Ex \\
|\langle 2^{(1)}|2\rangle|^2 &= \frac{\beta}{32} \left[48\beta^2 + \alpha^2 a_r^2 (96\tau^2\xi^3 - 96\xi^2 + 8\tau^2\xi + 16\xi - 8\tau^2) \right. \\
&\quad \left. + \alpha^4 a_r^4 (16\tau^2\xi^4 - 32\tau^2\xi^3 + 16\tau^2\xi^2) - 4 \right]^2 Ex
\end{aligned}$$

$$\begin{aligned}
|\langle 3^{(1)}|2\rangle|^2 &= \frac{\beta}{192} \left[\alpha a_r \left(-480\beta\xi^2 + 432\beta\xi + 48\tau\xi^2 - 48\beta - 72\tau\xi + 24\tau \right) \right. \\
&\quad + \alpha^3 a_r^3 \left(-320\tau\xi^4 + 624\tau\xi^3 - 336\tau\xi^2 + 16\tau^3\xi^3 + 32\tau\xi + 48\tau\xi^2 - 16\tau^3 \right) \\
&\quad \left. + \alpha^5 a_r^5 \left(-32\tau^3\xi^5 - 96\tau\xi^4 + 32\tau^3\xi^2 \right) \right]^2 Ex \\
|\langle 0^{(1)}|3\rangle|^2 &= \frac{\beta}{24} \left[12\xi\alpha a_r - 24\beta^2\alpha a_r - 8\xi^3\alpha^3 a_r^3 \right]^2 Ex \\
|\langle 1^{(1)}|3\rangle|^2 &= \frac{\beta}{48} \left[24 \left(\frac{1-\tau^2}{1+\tau^2} \right) \beta + 96\beta\xi^2\alpha^2 a_r^2 - 48\beta\xi\alpha^2 a_r^2 - 16\beta\xi^3\alpha^4 a_r^4 + 24\beta\xi\alpha^2 a_r^2 \right]^2 Ex \\
|\langle 2^{(1)}|3\rangle|^2 &= \frac{\beta}{192} \left[\alpha a_r \left(144\xi^2 - 480\beta^2\xi - 120\xi + 240\beta^2 \right) \right. \\
&\quad + \alpha^3 a_r^3 \left(-320\xi^4 + 48\tau^2\xi^3 + 400\xi^3 - 96\xi^2 - 96\tau^2\xi^2 + 48\tau^2\xi \right) \\
&\quad \left. + \alpha^5 a_r^5 \left(-32\tau^2\xi^5 - 32\tau^2\xi^3 + 64\tau^2\xi^4 \right) \right]^2 Ex \\
|\langle 3^{(1)}|3\rangle|^2 &= \frac{\beta}{1152} \left[\left(960\beta^3 - 288\beta\xi - 144\beta \left(\frac{1-\tau^2}{1+\tau^2} \right) \right) \right. \\
&\quad + \alpha^2 a_r^2 \left(2880\beta\xi^3 - 3456\beta\xi^2 + 1008\tau\xi^2 + 864\beta\xi - 576\tau\xi^3 - 432\tau\xi \right) \\
&\quad + \alpha^4 a_r^4 \left(960\tau\xi^5 - 2016\tau\xi^4 - 96\tau^3\xi^4 + 288\tau^3\xi^3 + 1248\tau\xi^3 - 192\tau\xi^2 \right. \\
&\quad \left. - 288\tau^3\xi^2 + 96\tau^3\xi \right) + \alpha^6 a_r^6 \left(64\tau^3\xi^6 - 192\tau^3\xi^5 + 192\tau^3\xi^4 - 64\tau^3\xi^3 \right) \left. \right]^2 Ex
\end{aligned}$$

APPENDIX - II

Channeling probabilities across interface (II):

The wavefunctions in the regions (1) and (2) are given by $\varphi_j(\alpha'x + \alpha'a_s)$ and $\varphi_k(\alpha'x - \alpha'a_s)$ respectively. This is equivalent to shifting the origin so that the wavefunctions are about $x = 0$ and $x = 2a_s$ respectively. This enables us to make use of the general expression given in chapter 2. This can be shown mathematically as follows

We have

$$\int_{-\infty}^{\infty} \varphi_j^*(x + a_s) \varphi_k(x - a_s) dx$$

Put $x - a_s = t$ (another variable)

$$\Rightarrow \int_{-\infty}^{\infty} \varphi_j^*(t + 2a_s) \varphi_k(t) dt$$

This expression is in the form of overlap integral, discussed in the chapter 2.

By replacing α with α' and a_s with $2a_s$ in the results of the previous chapter, we obtain

$$\begin{aligned} |\langle 0^{(2)} | 0^{(1)} \rangle|^2 &= \exp \left\{ -2\tau^2 \alpha^2 a_r^2 \right\} \\ |\langle 1^{(2)} | 0^{(1)} \rangle|^2 &= 2\tau^2 \alpha^2 a_r^2 \exp \left\{ -2\tau^2 \alpha^2 a_r^2 \right\} \\ |\langle 2^{(2)} | 0^{(1)} \rangle|^2 &= 2\tau^4 \alpha^4 a_r^4 \exp \left\{ -2\tau^2 \alpha^2 a_r^2 \right\} \\ |\langle 3^{(2)} | 0^{(1)} \rangle|^2 &= \frac{4\tau^6 \alpha^6 a_r^6}{3} \exp \left\{ -2\tau^2 \alpha^2 a_r^2 \right\} \\ |\langle 0^{(2)} | 1^{(1)} \rangle|^2 &= |\langle 1^{(2)} | 0^{(1)} \rangle|^2 \\ |\langle 1^{(2)} | 1^{(1)} \rangle|^2 &= \left(1 - 2\tau^2 \alpha^2 a_r^2 \right)^2 \exp \left\{ -2\tau^2 \alpha^2 a_r^2 \right\} \\ |\langle 2^{(2)} | 1^{(1)} \rangle|^2 &= \left(4\tau \alpha a_r - 4\tau^3 \alpha^3 a_r^3 \right)^2 \frac{\exp \left\{ -2\tau^2 \alpha^2 a_r^2 \right\}}{4} \\ |\langle 3^{(2)} | 1^{(1)} \rangle|^2 &= \left(24\tau^2 \alpha^2 a_r^2 - 16\tau^4 \alpha^4 a_r^4 \right)^2 \frac{\exp \left\{ -2\tau^2 \alpha^2 a_r^2 \right\}}{96} \end{aligned}$$

$$|\langle 0^{(2)} | 2^{(1)} \rangle|^2 = |\langle 2^{(2)} | 0^{(1)} \rangle|^2$$

$$|\langle 1^{(2)} | 2^{(1)} \rangle|^2 = |\langle 2^{(2)} | 1^{(1)} \rangle|^2$$

$$|\langle 2^{(2)} | 2^{(1)} \rangle|^2 = \left(2\tau^4 \alpha^4 a_r^4 - 4\tau^2 \alpha^2 a_r^2 + 1 \right)^2 \exp \{ -2\tau^2 \alpha^2 a_r^2 \}$$

$$|\langle 3^{(2)} | 2^{(1)} \rangle|^2 = \left(4\tau^5 \alpha^5 a_r^5 - 12\tau^3 \alpha^3 a_r^3 + 6\tau \alpha a_r \right)^2 \frac{\exp \{ -2\tau^2 \alpha^2 a_r^2 \}}{6}$$

$$|\langle 0^{(2)} | 3^{(1)} \rangle|^2 = |\langle 3^{(2)} | 0^{(1)} \rangle|^2$$

$$|\langle 1^{(2)} | 3^{(1)} \rangle|^2 = |\langle 3^{(2)} | 1^{(1)} \rangle|^2$$

$$|\langle 2^{(2)} | 3^{(1)} \rangle|^2 = |\langle 3^{(2)} | 2^{(1)} \rangle|^2$$

$$|\langle 3^{(2)} | 3^{(1)} \rangle|^2 = \left(3 - 18\tau^2 \alpha^2 a_r^2 + 18\tau^4 \alpha^4 a_r^4 - 4\tau^6 \alpha^6 a_r^6 \right)^2 \frac{\exp \{ -2\tau^2 \alpha^2 a_r^2 \}}{9}$$

One can easily notice here that $|\langle j^{(1)} | i \rangle|^2 = |\langle i | j^{(1)} \rangle|^2 \Rightarrow p_{i \rightarrow j^{(1)}} = p_{j^{(1)} \rightarrow i}$.

So we have

$$|\langle 1 | 0^{(2)} \rangle|^2 = |\langle 0^{(1)} | 1 \rangle|^2; \quad |\langle 2 | 0^{(2)} \rangle|^2 = |\langle 0^{(1)} | 2 \rangle|^2;$$

$$|\langle 3 | 0^{(2)} \rangle|^2 = |\langle 0^{(1)} | 3 \rangle|^2; \quad |\langle 0 | 1^{(2)} \rangle|^2 = |\langle 1^{(1)} | 0 \rangle|^2;$$

$$|\langle 1 | 1^{(2)} \rangle|^2 = |\langle 1^{(1)} | 1 \rangle|^2; \quad |\langle 2 | 1^{(2)} \rangle|^2 = |\langle 1^{(1)} | 2 \rangle|^2$$

and

$$|\langle 3 | 1^{(2)} \rangle|^2 = |\langle 1^{(1)} | 3 \rangle|^2.$$

References

- [1] F. R. N. Nabarro *Adv. in Phys.* 1, 269 (1952);
J. Friedel, *Dislocations* (Pergamon, N. Y.), 1964.
- [2] A. Kozanecki, J. Kaczanowski, B. J. Sealy and W. P. Gillin
Nuclear Inst. and Meth. in Phys. Res. **B** 118, 640 (1996)
for a review, see for example J. W. Mayer, *Rad. Eff.* 12, 183 (1972).
- [3] P. K. Bhattacharya, J. Chevallier, E. Uggerhøj, J. More and Y. Quere
Rad. Eff. **51**, 127 (1980); A. P. Pathak, *Phys. Lett.* 55A, 104 (1975);
57A, 467 (1976).
- [4] Y. Quere *Phys. Stat. Sol.* 30, 713 (1968).
- [5] D. Van Vliet, *Phys. Stat. Sol. (b)* 2, 571 (1970);
Hiroshi Kudo *J. Phys. Soc. Jpn.* 40, 1640 (1976); *Phys. Rev. B* 18, 5995 (1978).
- [6] S. T. Picraux, E. Rimini, G. Foti and S. Campisano *Phys. RevB* **18**, 2078 (1978).
- [7] F. Grasso, M. Lo Savio and E. Rimini *Rad. Eff.* 12, 149 (1972);
M. A. Kumakhov, and R. Wedell *Phys. Stat. Sol. (b)* 84, 581 (1977).
- [8] L. N. S. Prakash Goteti and Anand P. Pathak
J. Phys. Cond. Matter 9, 1709 (1997).
- [9] R. E. DeWames, W. F. Hall and G. W. Lehman *Phys. Rev.* **148**, 181 (1968);
174, 392 (1968) and A. P. Pathak *Phys. Rev. B* 7, 4813 (1973).
- [10] Azher M. Siddiqui, V. Harikumar, L. N. S. Prakash Goteti and
Anand P. Pathak *Modem. Phys. Lett. B* 10, 745 (1996).
- [11] Anand P. Pathak *Rad. Eff.* 30, 193 (1976);
- [12] A. P. Pathak *Phys. Rev. B* 13, 4688 (1976);
J. Mory and Y. Quere *Rad. Eff.* 13, 57 (1972).
- [13] A. P. Pathak *Rad. Eff.* 61, 1 (1982);
A. P. Pathak and S. Satpathy *Nucl. Instrum. Meth. B* 33, 39 (1988).

- [14] Richard A. Carrigan Jr., Timothy E. Toohing and Edica N. Tsyganov
Nuclear Inst. and Meth. in Phys. Res. B 48, 167 (1990);
M.A. Khumakov, *Nuclear Instrum. and Meth. in Phys. Res. B* 48, 167 (1990);
W. E. Gibson, I. J. Kim, M. Pisharody, S. M. Salman, C. R. Sun
G. H. Wang and R. Wijayawardana, J. S. Forster and I. V. Mitchell,
T. S. Nigmanov and E. N. Tsyganov, S. I. Baker, R.A. Carrigan Jr.,
and T.E. Toohig, V. V Avdeichikov, J. A. Ellison, P. Siffert
Nuclear Instrum. and Meth. in Phys. Res. B 2, 54 (1984).
- [15] L. N. S. Prakash Goteti and Anand P. Pathak *Phys. Rev. B* 58, 5243 (1998).

Chapter 4

Time dependent Formulation for dechanneling by Dislocations

4.1 Introduction:

In the earlier chapters of this thesis, we have used sudden approximation to treat the dechanneling problem for stacking faults and dislocations where we obtained dechanneling probabilities corresponding to various initial states. The dechanneling mechanism for the stacking defect is studied by incorporating the effects of obstruction [1] and that for the dislocation case is described in terms of distortions created due to curvature in the channel. It was also assumed that the curvature in the dislocation affected planar channels is nearly constant. For the dislocation problem we studied the dechanneling process, in the frame of *bound-bound transitions* in the planar channel induced by the sudden appearance of the curved channel[2]. However, this linear regime ceases to be valid at high defect concentrations and important deviations occur [3] with respect to the standard energy dependence of the dechanneling probabilities and cross-section. Here we improve upon that *static curvature* approach to a more realistic model by relaxing the sudden approximation and using the time dependent perturbation theory. These calculations show that scattering states play a vital role in dechanneling because of the occurrence of additional bound states in the planar channel with change in curvature. Eventhough, the constant curvature model and the sudden approximation helped

in better quantum mechanical understanding of the dechanneling mechanism, the consideration of non-uniformity of the curvature during the propagation of the particle is obviously more appropriate.

4.2 Basis of the time dependent approach:

In the previous chapter, the effects of channel curvature on charged particle propagation, are studied on the basis of harmonic approximation to the resultant transverse planar potential in the distorted part; this is done by incorporating these effects through respective wavefunctions in various regions of distortion. However, one can realize that above approximation is not valid for large distortions as in that regime the deflection force due to distortion dominates the restoring force (due to actual transverse potential) hence the motion of the particle in transverse space is no longer bounded. As a result of that, the particle gets dechanneled and what we call it as the scattering of the particle from the *bound state* to *continuum*(scattering state). Quantum mechanically this dechanneling probability can be obtained by using perturbation methods. As we notice, due to asymmetric nature of the distortion term V_R (described in the previous chapter), the first order perturbation theory will not give any shift in energy, hence the effect of dislocation on positron is small for sufficiently small curvatures. On the other hand, it induces a transition from a bound state to scattering state provided, the dislocation density is high. Moreover, the curvature of the distorted channel is non-uniform particularly when the channels are close to the dislocation, as shown in Fig. 4.1. In that case the constant curvature model may not be appropriate because, there will be imbalance in the magnitude of the centrifugal force $2E/R$ in the regions II and III of Fig. 3.2 as the bending may not be a smooth $\sim \neg$ shape.

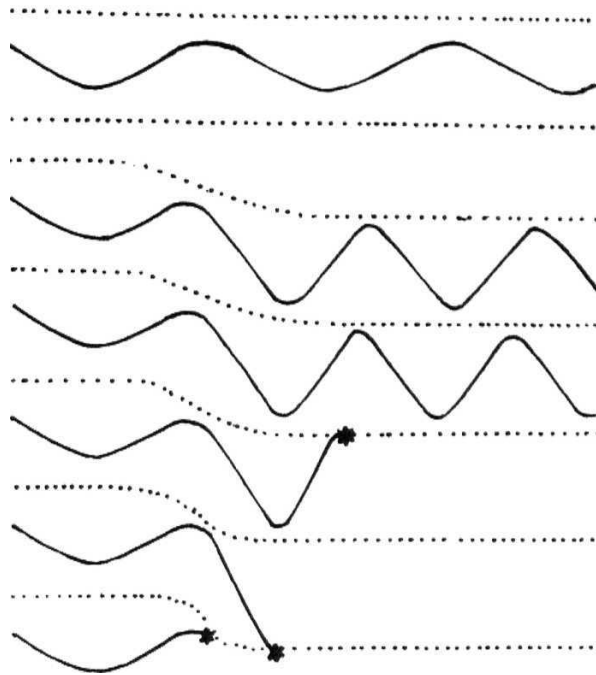


Fig. 4.1 : The dechanneling of the particle in the heavily distorted channels near the dislocation. It can also be seen that these effects are reduced considerably for the channels far away from the dislocation.

In classical analysis of time dependent approach [4], the dechanneling process is studied by writing the equations of motion which yield an expression for time dependent position in the transverse space co-ordinate $x(t)$. Invoking that the particle gets dechanneled when its oscillating amplitude exceeds the critical transverse amplitude, the resulting dechanneling cross-section is obtained by averaging over all possible phase co-ordinates and initial amplitudes. Similar treatment for the axial case was done by *Gartner et. al.* [5]. However, more detailed calculations are needed to understand this basic phenomena, especially to study the qualitative features like for **example**, the variation of dechanneling probability with distance from the dislocation axis and its energy

dependence etc. Here also we start with the well-known centrifugal energy term which has been used excessively in the context of dislocation dechanneling. The usefulness and completeness of this approach lies in the fact that it is derived from the displacement function obtained by the elastic continuum theory [6, 7]. We invoke time dependence in that term to obtain an equivalent expression and the dechanneling phenomena under this situation is governed by the transition probability of the particle from a well-defined bound state (harmonic oscillator) to a scattering state (plane wave). In this time dependent calculation, the modified centrifugal energy term is given by [3]

$$V_R(x, t) = 2E \frac{\partial^2 u_{\perp}}{\partial Z^2} \Big|_{Z=\gamma v_z t} = -\frac{mb}{\pi} \frac{\gamma^3 v_z^3 r t}{(r^2 + \gamma^2 v_z^2 t^2)^2} x \quad (4.1)$$

To estimate the maximum number of quantum states supported by the transverse potential in the undistorted part, we take the prescription given in the chapter 2 where we have $n_{\max} \approx 3$. The initial and final wave functions of the positron are given by

$$\begin{aligned} \psi_n(x, y, z) &= \frac{1}{L} \left(\frac{\alpha}{\sqrt{\pi} 2^n n!} \right)^{1/2} \exp(ik_z z) \exp(ik_y y) \exp(-\frac{1}{2} \alpha^2 x^2) H_n(\alpha x) \\ \psi_f(x, y, z) &= L^{-3/2} \exp(i\vec{k}_f \cdot \vec{r}) \end{aligned}$$

As discussed in previous chapters the coupling constant α is given by $\sqrt{(m_{\perp} \omega / \hbar)}$ with transverse mass $m_{\perp} (=7m)$ [8]. The distortions of planar channel shifts particle motion in transverse direction (x) whereas in ' z ' direction the propagation is nearly constant. The expression for dechanneling probability of a particle with initial bound state $|n\rangle$ (due to channel distortion) to a final scattering state is given by

$$\chi_n = \frac{1}{\hbar^2} \left| \int V_R^{fn} e^{i\omega_{fn} t} dt \right|^2 \quad \text{with } V_R^{fn} = \langle \psi_f | V_R(x, t) | \psi_n \rangle \quad (4.2)$$

Substituting the appropriate wavefunctions and incorporating the time-dependent distortion term in the above equation, we have

$$\chi_n = \frac{1}{\hbar^2} \left| \int \langle f | \frac{mb}{\pi} \frac{\gamma^3 v_z^3 r t}{(r^2 + \gamma^2 v_z^2 t^2)^2} x | n \rangle e^{i\omega_{fn} t} dt \right|^2$$

$$\begin{aligned}
&= \frac{1}{\hbar^2} \left| \frac{1}{L^{5/2}} \left(\frac{\alpha}{\sqrt{\pi} 2^n n!} \right)^{1/2} \frac{mb}{\pi} \left[\int \exp(-ik_f^{(x)} x) x \exp(-\alpha^2 x^2/2) H_n(\alpha x) dx \right] \right. \\
&\times \left. \left\{ \int \exp(-ik_f^{(y)} y) \exp(ik_y y) dy \right\} \left\{ \int \exp(-ik_f^{(z)} z) \exp(ik_z z) dz \right\} \int \frac{t_0 t e^{i\omega_{fn} t}}{(t_0^2 + t^2)^2} dt \right|^2 \\
&\text{where } t_0 = \frac{r}{\gamma v_z}
\end{aligned}$$

Thus one can easily notice that space and time co-ordinates can be separated out; after performing the contour integration w.r.t time we get

$$\begin{aligned}
\chi_n &\Rightarrow \frac{1}{\hbar^2} \left| \left(\frac{\alpha}{L^5 \sqrt{\pi} 2^n n!} \right)^{1/2} \frac{mb}{\pi} \frac{\omega_{fn}}{2} e^{-\omega_{fn} t_0} \left[\int \exp(-ik_f^{(x)} x) x \exp(-\alpha^2 x^2/2) H_n(\alpha x) dx \right] \right. \\
&\times \left. \left\{ \int \exp(-ik_f^{(y)} y) \exp(ik_y y) dy \right\} \left\{ \int \exp(-ik_f^{(z)} z) \exp(ik_z z) dz \right\} \right|^2 \\
&= \left(\frac{\alpha}{\sqrt{\pi} 2^n n!} \right) \left(\frac{mb\omega_{fn}}{2\hbar} \right)^2 \exp \left\{ -2 \frac{\omega_{fn} r}{\gamma v_z} \right\} \frac{1}{L} |I_x|^2 \left(\frac{2\pi}{L} \right)^2 \delta(k_y - k_y^{(f)}) \delta(k_z - k_z^{(f)}) \\
&\text{with } I_x = \int \exp(-ik_f^{(x)} x) x \exp(-\alpha^2 x^2/2) H_n(\alpha x) dx
\end{aligned} \tag{4.3}$$

Due to scattering, the particle makes transition from a given initial state $|n\rangle$ to continuum of states and the dechanneling probability can be obtained by considering the transitions to a group of closely spaced states. Hence total dechanneling probability to any one of final states is obtained by integration over density of final states [9], i.e.,

$$\bar{\chi}_n = \left(\frac{L}{2\pi} \right)^3 \int \chi_n dk^x dk_f^y dk_f^z \tag{4.4}$$

The straight forward integration in \mathbf{k} -space leads to the expression

$$\begin{aligned}
\bar{\chi}_n &= \left(\frac{\alpha}{2\pi \sqrt{\pi} 2^n n!} \right) \left(\frac{mb}{2\hbar} \right)^2 \\
&\times \left\{ \int \omega_{fn}^2 \exp \left\{ \frac{-2\omega_{fn} r}{\gamma v_z} \right\} \left| \int_{-\infty}^{\infty} \exp(-ik_f^{(x)} x) \exp \left(-\frac{\alpha^2 x^2}{2} \right) H_n(\alpha x) dx \right|^2 dk_x \right\} \\
&= \left(\frac{\alpha^2}{2\pi \sqrt{\pi} 2^n n!} \right) \left(\frac{mb}{2\hbar} \right)^2 \left\{ \int \omega_{fn}^2 \exp \left\{ \frac{-2\omega_{fn} r}{\gamma v_z} \right\} e^{-q^2} \left| \int x e^{-\frac{1}{2}\alpha^2 (x+x_0)^2} H_n(\alpha x) dx \right|^2 dq \right\}
\end{aligned} \tag{4.5}$$

where $\omega_{fn} = (E_f(q) - E_n/\hbar)$ and $x_0 = iq/\alpha$.

In the above expression E_f is final energy background in which the particle propagates after getting dechanneled. Because the remaining integrand has a **pronounced maximum** at $q = q_{\max}$, the term $\omega_{fn}^2 \exp(-2\omega_{fn}r/\gamma v_z)$ is assumed to be **constant with** $\omega_{fn}(q) \longrightarrow \tilde{\omega}$, where ω depends on n and is given by $\omega_{fn}(q_{\max})$. Since $E_f(q) \gg E_n$, we assume that ω is independent of n and the above equation can be written as

$$\bar{\chi}_n = \left(\frac{\alpha^2}{2\pi\sqrt{\pi}2^n n!} \right) \exp \left\{ \frac{-2\tilde{\omega}r}{\gamma v_z} \right\} \left(\frac{mb\tilde{\omega}}{2\hbar} \right)^2 \left\{ \int e^{-q^2} \left| \int x e^{-\frac{1}{2}\alpha^2(x+x_0)^2} H_n(\alpha x) dx \right|^2 dq \right\}$$

Using the Rodrigues formula for H_n and incorporating appropriate expressions, we obtain total dechanneling probability χ_n and it is given by [10]

$$\bar{\chi}_n = (2n+1) \bar{\chi}_0 \quad \text{with} \quad \bar{\chi}_0 = \left(\frac{m\tilde{\omega}b}{2\sqrt{2}\hbar\alpha} \right)^2 \exp \left(-\frac{2\tilde{\omega}r}{\gamma v_z} \right). \quad (4.6)$$

The above expression for χ_0 is obtained with specific reference to initially well channeled particles. Corresponding to a given initial state (say $|n\rangle$), the dechanneling probability is maximum for those channels that are situated at or below the dechanneling radius r_n (i.e., critical distance of the channel from the dislocation at or below which the particle completely gets dechanneled) and this happens for $\tilde{\omega} = \frac{\gamma v_z}{r}$.

Invoking $\bar{\chi}_n(r_n) = 1$ for $r \leq r_n$, we have

$$\bar{\chi}_n(r) = (2n+1) \left(\frac{mb\gamma v_z}{2\sqrt{2}\hbar\alpha e} \right)^2 \frac{1}{r^2} \quad \text{for } r \leq r_n$$

$$\text{with} \quad \bar{\chi}_n(r) = 1$$

$$\bar{\chi}(r_n) = 1 \Rightarrow (2n+1) \left(\frac{mb\gamma v_z}{2\sqrt{2}\hbar\alpha e} \right)^2 \frac{1}{r_n^2} = 1.$$

$$\Rightarrow (2n+1) \frac{m^2 b^2 \gamma^2 v_z^2}{8\hbar^2 \alpha^2 e^2} \frac{1}{r_n^2} = 1$$

$$\text{i.e. } r_n^2 = (2n+1) \left(\frac{\gamma 2Eb^2}{8\hbar\omega e^2} \right) = (2n+1) \left(n + \frac{1}{2} \right) \left[\frac{\gamma Eb^2}{4(n+1/2)\hbar\omega e^2} \right]$$

$$= \left(n + \frac{1}{2}\right)^2 \left\{ \frac{\gamma E b^2}{2(n + 1/2) \hbar \omega e^2} \right\}$$

In the above Eqns., $e \approx 2.718$. An estimate of upper bound for dechanneling radius with reference to a particle of initial state $|n\rangle$ is obtained as

$$r_n^{(u)} \approx \left(n + \frac{1}{2}\right) \frac{b}{2.718} \sqrt{\frac{\gamma E}{2E_n}} \quad (4.7)$$

with the quantized transverse energy $E_n = (n + 1/2) \hbar \omega$.

As per the above procedure, we get an estimate of upper bound for dechanneling radius ($r_n^{(u)}$). However, one will be interested to have an estimate for the minimum distance of the channel from the dislocation. It is well known that the dechanneling process means, the transverse energy of the particle approaches its critical value before getting dechanneled. Incorporation of the same in the present r_n expression, provides a lower bound for r_n as $r_n^{(l)}$. This is done by replacing E_n by total transverse energy $E_\perp = (n_{\max} + 1/2) \hbar \omega - E_{n_{\max}} = E_3$. Hence we get lower bound for r_n as $r_n^{(l)}$ given by

$$r_n^{(l)} \approx \left(n + \frac{1}{2}\right) \frac{b}{2.718} \sqrt{\frac{\gamma E}{2E_\perp}} \quad (4.8)$$

Thus present quantum calculation shows r_0, r_1, r_2 have lower bound and as well as an upper bound (a finite range) while r_3 has only one value ($r_n^{(u)} = r_n^{(l)}$). In the present calculation we have $n_{\max} = 3$ and also $E_3 = E_\perp$; hence r_3 provides quantum mechanical definition for dechanneling radius as it implies that the particle acquired transverse energy as much as E_\perp and obviously this corresponds to dechanneling radius for $|3\rangle$. Fig. 4.2 shows clearly these two limits for $|n\rangle = |0\rangle$ (i.e., initially well-channeled particles).

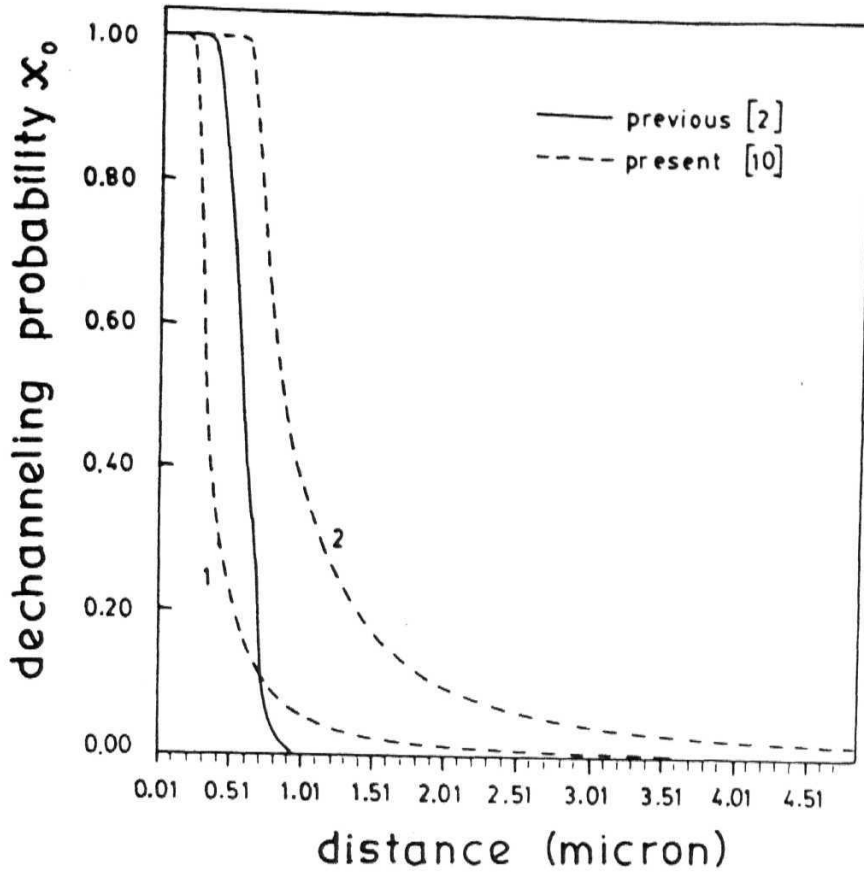


Fig. 4.2 : Variation of dechanneling probability for initially well channeled particles ($\bar{\chi}_0$) with channel distance from the dislocation. $\bar{\chi}_0$ corresponding to lower bound and upper bound are denoted as 1 and 2 respectively.

Obviously this is of practical interest and provides the definition to dechanneling radius and at the same time, to a certain extent, enables us to relax the approximations mentioned above. The dechanneling cross-section with reference to an initial state $|n\rangle$ is obtained by the expression

$$\bar{\lambda}_n = \int \chi_n(r) dr = (2n + 1) \int \left(\frac{mb\gamma v_z}{2\sqrt{2}\hbar\alpha e} \right)^2 \frac{1}{r^2} dr$$

Instead of $\lambda_n = (2n + 1) \int \bar{\chi}_0(r) dr$, we start with general expression $\lambda_n = \int \bar{\chi}_n(r) dr$. There is slight difference in these two approaches. When we integrate the expression in the general form (i.e., with index n), the integration limits involve corresponding r_n instead of r_0 . This is physically more appropriate since we are interested in the dechanneling width corresponding to a specific initial state, which in turn depends

on the corresponding r_n . Thus the usage of general expression for $\bar{\lambda}_n$ provides more accuracy and clarity.

$$\bar{\lambda}_n = (2n+1) \left(\frac{mb\gamma v_z}{2\sqrt{2}\hbar\alpha e} \right)^2 \frac{2}{r_n} \Rightarrow \bar{\lambda}_n = (2n+1) \bar{\lambda}_0$$

where $\bar{\lambda}_0 = 2 r_0$ (4.9)

Here λ_0 is the dechanneling width corresponding to initially well channeled particles ($|n\rangle = |0\rangle$). Assuming the curvature of the channel as constant, *Quere* [6] obtained this expression in classical framework. Thus we reproduced the well-known classical expression in our formulation and this result is obtained in a *natural* way. We have estimated the dechanneling widths ($\bar{\lambda}_n^{(u)}$ and $\bar{\lambda}_n^{(l)}$) using Eqns. (4.7 to 4.9) for positrons along Al(111) and results are given in table 1(a).

Classically, above E_\perp is equivalent to the critical transverse energy, given by $E_\perp^c \approx E\psi_p^2$, where ψ_p is planar critical angle [11]. So for the case of non-relativistic positive particles and other heavy ions ($\gamma = 1$), one may replace E_\pm by equivalent classical expression i.e., $E\psi_p^2 = 2\pi Z_1 Z_2 e^2 N_p a_{T,F}$, we have

$$\bar{\lambda} = 2 r_0 = \sqrt{\frac{E}{4\pi Z_1 Z_2 e^2 N_p a_{T,F}}} \left(\frac{b}{2.718} \right)$$

and

$$\bar{\lambda}_{Quere} = \sqrt{\frac{bE}{8.6 Z_1 Z_2 e^2 N_p}}$$

Thus an estimate of dechanneling width for initially well channeled particles ($\bar{\lambda}$) is obtained as

$$\boxed{\bar{\lambda} = 0.3 \bar{\lambda}_{Quere} \sqrt{\frac{b}{a_{T,F}}} = (0.44) \bar{\lambda}_{Quere} Z_2^{1/6} \sqrt{b}} \quad (4.10)$$

where b is in Å. Using above equation, the dechanneling width for *He* ions has also been estimated and compared with existing theory and experimental data [12]. These details are given in table 1(b), showing reasonable agreement

Table 1

a) Dechanneling widths for Positrons in Al for various initial states

<i>Particulars of the crystal</i>	<i>Dechanneling widths in μm</i>						
	$\bar{\lambda}_o$		$\bar{\lambda}_1$		$\bar{\lambda}_2$		$\bar{\lambda}_3$
	$\lambda_o^{(l)}$	$\lambda_o^{(u)}$	$\lambda_1^{(l)}$	$\lambda_1^{(u)}$	$\lambda_2^{(l)}$	$\lambda_2^{(u)}$	$\lambda_3^{(l)} = \lambda_3^{(u)}$
<i>Al(111), $b = 2.86\text{\AA}$</i>	0.47	1.24	1.41	2.16	2.35	2.82	3.3

b) Dechanneling width for He in Al

(Here E is expressed in Mev)

<i>Particulars of the crystal</i>	<i>Dechanneling width ($\bar{\lambda}$) in \AA</i>		
	Experimental [12]	Quere	Present
<i>Al(111), $b = 2.86\text{\AA}$</i>	$85\sqrt{E}$	$79\sqrt{E}$	$90\sqrt{E}$

4.3 Results and Discussion:

We have studied the dechanneling phenomena using time dependent formulation where we obtained the expressions for dechanneling radius hence for the dechanneling width. These expressions are qualitatively similar to the expression obtained by equating the deflecting force to the restoring force [13]. In the present calculation we obtain an expression for dechanneling width for the *first time* purely on the basis of quantum mechanical considerations. By incorporating appropriate limits in the present expression for dechanneling width, equivalent classical expression is also obtained. For example, in the case of heavy non-relativistic particle where $\gamma \sim 1$, the above expression is identical to the one obtained in classical analysis. The present procedure provides a simple and convenient way to estimate the order of magnitude of the effect and its scaling with particle energy and planar potential. This expression is very close to that obtained by Quere's classical analysis where continuum model and phase dependence of the approaching particle are considered. Quantitatively the present calculation may over-estimate the actual dechanneling width by a numerical factor and this may be because of the semiclassical approximation namely the maximization of dechanneling probability and fixing ω correspondingly. However one may put appropriate numerical constant to fit with experimental data as was done by Lindhard for his power law potential ($C = \sqrt{3}$).

The result also confirms the results of earlier chapter, where one can notice that $r_0 = \sqrt{\frac{4\gamma E}{\pi Z_1 Z_2 e^2 C N_p}} \Rightarrow r_0 \propto \sqrt{\gamma E}$, so that dechanneling cross-section varies linearly with E and for higher energies this will be slower than E as seen in Eqn.(4.8). It is $\propto \sqrt{E}$ as proposed in the case of heavy particles in classical framework [6, 14]. These results also conform the qualitative energy dependence i.e., dechanneling cross-section

varies linearly with E at relativistic energies as confirmed by the bent crystal channeling experiments done by R. A. Carrigan, Jr. [15], He also mentioned that increasing the bending is in "some sense" like raising the atomic number of the crystal. From the Eqn.(4.10) one can see that the dechanneling radius increases with Z_2 which means that the critical region increases with Z_2 and this in turn implies that the channels are distorted heavily. So the present theory shows that the bending increases with Z_2 and hence also applicable for the channeling studies with bent crystals . So one may infer that materials with higher values of Z_2 are appropriate for bending of beams. Fig. (4.2) shows comparison of present calculation with the work done as part of previous chapter. As expected, dechanneling probability falls off sharply(for large curvature i.e., large distortion as compared to that obtained with bound-bound transitions in sudden approximation. On the other hand for sufficiently smaller curvatures, the dechanneling probability decreases slowly as compared to that obtained with bound-bound transitions. We expect present theory to be valid for wider range of dislocation concentrations. The quantum mechanical results under suitable limits reproduce the known classical results qualitatively. The quantitative agreement is also satisfactory as seen from table I. This shows the basic concepts applied to this complicated problem for the first time lead to some interesting results especially, in the light of bent crystal channeling.

References

- [1] L. N. S. Prakash Goteti and Anand P. Pathak
J. Phys. Cond. matter 9, 1709 (1997).
- [2] L. N. S. Prakash Goteti and Anand P Pathak *Phys. Rev. B* 58, 5243 (1998)
- [3] Keniji Kimura, Takashi Oshiyama and Michi-hiko Mannami
Jpn. J. Appl. Phys. 21, 1222 (1982); Keniji Kimura, Shin-ichi Sawada
and Michi-hiko Mannami *Jpn. J. Appl. Phys.* 21, 1228 (1982)
- [4] L. Wielunski, D. Wielunska, G. Delia Mea, and A. Tuross
Nucl. Instrum. Meth. 168, 323 (1980); D. Wielunska, L. Wielunski
and A. Tuross *Phys. Stat. Sol (a)* 67, 413 (1981) and 68, 45 (1981).
- [5] Konard Gartner, Karl Hehl and Gerald Schlotzhauer
Nucl. Instrum. Meth. in Phys. Res. B 4, 63 (1984).
- [6] Y. Quere *Phys. stat. sol.* 30, 713 (1968)
- [7] H. G. Van Bueren, *Imperfections in crystals* (North Holland, Amsterdam, 1960).
- [8] M. A. Kumakhov, and R. Wedell *Phys. Stat. Sol. (b)* 84, 581 (1977).
- [9] L.D. Landau and E.M. Lifshitz *Quantum Mechanics* (Pergamon, Oxford, 1965)
- [10] L. N. S. Prakash Goteti and Anand P. Pathak *Phys. Rev. B* 59, 8516 (1999).
- [11] A. P. Pathak *Rad. effects* 61, 1 (1982).
- [12] S. T. Picraux, E. Rimini, G. Foti and S. Campisano *Phys. Rev B* 18, 2078 (1978).
- [13] Anand P. Pathak *Rad. effects* 30, 193 (1976).
- [14] J. Mory and Y. Quere *Rad. Effects.* 13, 57 (1972).
- [15] R. A. Carrigan Jr., in :- “*Relativistic channeling*” ed:- Richard A. Carrigan Jr.,
and J. A. Ellison NATO ASI series B (plenum, N.Y., 1986) Vol. 165 pp.339-368.

Chapter 5

Summary and Conclusions

The channeling phenomena and its several applications in defects and radiation damage **have** been studied extensively by several authors within the frame work of classical mechanics. In the introductory chapter, with a preview to the theory of channeling, the classical aspects of effects of defects have been discussed. As the particle velocity increases, the quantal corrections to the classical description are negligible. The kind of description (whether classical or quantum) is governed by the product of mass of the particle and the strength of the particle-crystal interaction potential.

Morover, in recent years the interaction of light particles (like positrons) with matter acquired a special significance because of their sensitiveness and importance in probing various kind of defects present in the solids. The realization of *hidden discreteness* present in these systems motivated us to work in this direction as it has taken over usual classical approach, especially for these light particles. This is so, particularly in the context of electron/positron channeling radiation spectroscopy where there were clear indications of discreteness in the transverse energy. These aspects (like sensitivity and discreteness) stimulated us for the development of these quantum mechanical formulations with specific reference to positrons.

It is well established that the motion of positively charged particles in the transverse direction can be described by the harmonic oscillator to a first approximation, whereas in the case of electron channeling the shape of the transverse potential is an

inverted parabola; transverse motion being confined within the cusp shaped potential centered around the axis or plane of atoms.

We have investigated the quantum aspects of the processes in the context, of the effects of extended defects (specially stacking faults and dislocations) on channeled **particles**, keeping in mind their specific applications to channeling radiation spectroscopy. Restricting to positron channeling, on the specific assumption that the crystal is otherwise perfect, channeling and dechanneling probabilities corresponding to stacking fault and dislocation situations, have been calculated using the sudden approximation. For the case of stacking fault, the dechanneling process is described through the effects of obstruction to the channeling particle and one can notice that resulting dechanneling probabilities obtained from these quantum mechanical treatments do not have explicit energy dependence as was the case in classical description. We also compare the present results with those obtained by classical approach; the comparison of classical dechanneling probability with present quantum mechanical results is fairly good as the classical results fall in between χ_0 and χ_1 calculated from the present quantum description. The effects of temperature on the dechanneling probability (χ_0) for initially well-channeled particles are considered through the thermal correction to the screening function $a_{T,F}$ where we show the variation of χ_0 with p_{\pm} is linear as that was noticed in the classical calculations.

In the case of dislocations the dechanneling is mainly due to the distortions of the planar channel. These distortions give rise to additional centrifugal energy in transverse direction which eventually increases the transverse energy of the particle beyond the potential barrier to cause dechanneling. Classically this corresponds to centrifugal force exceeding the restoring force and shifting of the equilibrium axis away from the geometrical axis of the planar /axial channel. Quantum Mechanically this is equivalent to the scattering of bound states from the corresponding perturbation

potential to the scattering states. In chapter 3, we studied the dechanneling processes by continuous distortions of the planar channels, mapping to three distinct regions, and invoking corresponding displaced and modified wavefunctions. This happens for channels far away from the dislocation which in turn implies applicability of present calculation to lower concentrations (i.e. no interaction between dislocations). On the other hand the channels close to the dislocation axis are distorted so heavily in that regime, that one can not talk of crystallographic channels since their long range order is reduced as discussed in classical analysis.

For the dislocation case, we found that dechanneling cross-section/width varies as $E^{1/2}$ in the same way that was noticed in the classical description. However, in relativistic regime, this dependence is almost linear, confirming the observations in the bent crystal channeling experiments.

In both the cases of stacking fault and dislocation, we notice interesting left-right symmetry inbuilt in these problems that are not clearly realized in classical descriptions. In the present simple model calculations, these effects are manifested in natural way. The usefulness and completeness of these descriptions lie in the fact that the general expression obtained by us is useful for arbitrary values of quantum numbers; apart from these calculations, this result can be used in various fields.

The present theory is valid as long as the number of bound states supported by the transverse potential (surrounded by the planar channel) is small. This happens for light particles like positrons in Mev range.

We improve the formulation developed in the chapter 3, by invoking the time dependence in the distortion term where the dechanneling is studied using time dependent perturbation theory. Here a complete formulation of the dislocation problem is deduced starting with a well defined initial state problem and detailed calculation is

presented in the frame work of quantum mechanics. The expressions for **dechanneling** probabilities are derived by incorporating the fact that dechanneling probability is maximum for channels that are situated at or below a critical distance $r = r_0$ from the dislocation and this happens for $\omega = \gamma v_z / r_0$. The expression for dechanneling radius and hence for the dechanneling width is derived for the *first time* in the literature, purely on the basis of quantum mechanical considerations. Here we find that $A = 2r_0$; akin to that given in classical analysis. By incorporating appropriate limits in the present expression for dechanneling width, equivalent classical expression is obtained and usefulness of this time dependent approach lies in the fact that the results obtained here are in good agreement with those from the existing classical theory and as well as experiment.

These results also confirm the qualitative energy dependence in the classical limit and confirm with those results given on the basis of sudden approximation used in the chapter 3. In this time dependent framework, we present for the first time that the bending of the channel increases with Z_2 and it varies as Z_2^1 . Thus we made an attempt to integrate normal dechanneling with bent crystal dechanneling. We expect this theory to be valid even for sufficiently higher dislocation concentrations. The quantum mechanical results under suitable limits reproduce the known classical results qualitatively and the quantitative agreement is also satisfactory.

Possible Future work in this direction

In our investigations we concentrated mainly on quantum aspects of dechanneling mechanism for planar case with reference to positrons. However, the extension of this formulation to axial case might be very interesting where one has to deal with two dimensional Schrodinger equation and corresponding wave functions are degenerate. Here one can expect this degeneracy might be lifted to some extent by the presence of these defects.

These calculations are very important in the context of channeling radiation, which is due to the spontaneous transition among various quantum states. Here the population of the quantum states is to be considered both at the entry surface (i.e., just before entering into the crystal) and at the defect site as this corresponds to final population. The product of these populations and the transition probability yields radiation intensity. Moreover the possible degeneracy in the wavefunctions will be reflected through the spread in radiation frequencies and line widths.

The general expression obtained in chapter 2 is applicable when the coupling constants of the wavefunctions in the overlap integral are same. However one can try for similar kind of expression when the coupling constants differ as in the dislocations, treated in chapter 3.

As reported in this thesis, the effect of periodicity in the transverse direction is not significant for our dechanneling probability calculations and the energies under consideration. However these effects are important for lower energies where the number of quantum states $n_{\max} \approx 1$. In that case we have to incorporate these periodic effects in the wavefunctions using Bloch functions where one has to match the wavefunctions to get quasi momenta. This kind of formulation will incorporate the detailed effects of

band structure.

The effects of temperature are to be incorporated in the dechanneling calculations because these probabilities are influenced by the thermal fluctuations of atomic **planes/rows**. These effects are incorporated in stacking fault case in terms of thermal correction term ρ_{\perp} . However at sufficiently higher temperatures this kind of fluctuation causes **further** dechanneling because, there the phonon excitation plays an important role at higher temperatures. Hence more rigorous treatment is needed to get more insight into the actual physical phenomena of these effects.

Present work contains important results and provides several interesting features in the dechanneling process of light particles. We hope that this will initiate further development of such theoretical models and yield many more useful results. More refined experiments are to be done to check the validity of such models so that one can have improvements and further developements of these models in near future.

L. N. S. **Prakash** Goteti
Research Scholar
School of Physics
University of Hyderabad
Central Univ. **P.O.**
Hyderabad 500 046
Email : **appsprs@uohyd.ernet.in**

CURRICULUM **VITAE**

Name : L. N. **S. PRAKASH GOTETI**
Nationality.....: Indian
Date of birth.....: 05 - 06 - 1971,
Postal Address : Research Scholar
School of Physics
University of Hyderabad
Hyderabad 500 046, India
Phone: +91 - 40 - 3010500 - 4400
Email: **appsprs@uohyd.ernet.in**

Educational Qualifications:

Ph. D (Condensed Matter Theory - Ion - Solid Interactions) (thesis submitted)
M.Phil (Phys.)- 1995 - University of Hyderabad, Hyderabad
M.Sc.(Phys.) 1994 - University of Hyderabad, Hyderabad

Under the supervision of Professor Anand P. Pathak,
School of Physics, University of Hyderabad
(see RESEARCH OUTLINE & PUBLICATIONS for details).

Publication with titles of **articles**, names of journals and dates (a) research, (b) others

(a) Journals :

1. *Scattering of pious and channeled muons by impurities in Single Crystals*
Azher. M. **Siddiqui**, V. Harikumar, **L. N. S.** Prakash Goteti and Anand **P.** Pathak
Modem Physics Lett. B **10**, 745 (1996)
2. *The effects of stacking faults on dechanneling*
• A quantum mechanical calculation
L. N. S. Prakash Goteti and Anand P. Pathak
J. Phys. Condens. matter **9**, 1709 (1997)
3. *Dechanneling by Dislocations*
- A Model Quantum Mechanical calculation
L. N. S. Prakash Goteti and Anand P. Pathak *Phys. Rev. B* **58**, 5243 (1998).
4. *Dechanneling by Dislocations - A time dependent approach*
L. N. S. Prakash Goteti and Anand P Pathak
Phys. Rev. B 59, 8516 (1999),
5. *An experimental study of stopping power for Mev heavy ions*
Annu Sharma, **Shyam** Kumar, **S. K.** Sharma, **N.** Nath, V. Harikumar,
A. P. Pathak, **L. N. S.** Prakash Goteti, **S. K.** Hui and **D. K.** Avasthi
J. Phys. G 25, 135 (1999).
6. *Quantum models for dechanneling by point defects and extended defects*
Anand P Pathak, **L. N. S.** Prakash Goteti and Azher **M.** Siddiqui
AIP Conference Series (*Denton accelerator Conference*) (in press).

(b) Others :

(I) Book

1. *Effects of Strains and Defects on Channeling*
A. P. Pathak, **V.** Harikumar, and **L. N. S.** Prakash Goteti, in *Advances in Theoretical Physics* edited by **A. P.** Pathak *Narosa Publishing House, New Delhi*
pp. 170 - 176 (1996).
2. *Channeling and channeling Radiation in Semiconductor Superlattices*
Anand P. Pathak, Azher M. Siddiqui, **L. N. S.** Prakash Goteti and V. Harikumar in
Semiconductor Materials and Devices edited by **O. P.** Agnihotri and V. K. Jain
Narosa Publishing House, New Delhi, pp. 241 - 258 (1998).

(II) Conference/Symposium proceedings :

1. **L. N. S. Prakash Goteti and A. P. Pathak**, *Proceedings of DAE solid state physics symposium 1995, Jadavpur* (vol 38C, page 66).
2. **L. N. S. Prakash Goteti and A. P. Pathak**, *Abstracts of Conference on Frontiers on material modelling and design 1996, Kalpakkam* (page 89).
3. **L. N. S. Prakash Goteti and A. P. Pathak**, *Proceedings of DAE solid state physics symposium 1996, Mumbai* (vol 39C, page 193).
4. **A. P. Pathak and L. N. S. Prakash Goteti** *Proceedings of International Conference on Physics of disordered materials 1997, Jaipur* (INV 7).

(III) Conference/Symposium /School participated :

1. **Participated in DAE solid state physics symposium ,December 27 - 31, 1995, Jadavpur** and presented 20 min. talk on “ Quantum description of dechanneling by stacking faults”.
2. **Participated in Conference on Frontiers on material modelling and design, August 21 - 23,1996, Kalpakkam** and presented a poster on “ Quantum description of dechanneling by dislocations in metals ”.
3. **Participated in DAE solid state physics symposium ,December 27 - 31, 1996, Mumbai** and presented a poster on “A Quantum model for effects of dislocations in axial channeling ”.
4. **Participated in International Conference on Physics of disordered materials January, 27 - 29 ,1997, Jaipur.**
5. Participated in *School on Physics of Beams* from 13 - 01 - 1997 to 25 - 01 - 1997 at **CAT, Indore.**
6. Participated in *Advanced Lecture Series* from 14 - 02 - 1997 to 04 - 03 - 1997 held at **Nuclear Science Centre, New Delhi.** Participated in three day seminar on *Physics of Semiconductor devices* from 05 - 03 - 1999 to 07 - 03 -1999 held at **University of Hyderabad, Hyderabad.**

Memberships of Scientific Societies

Indian Physics Association (IPA)
Life Membership No. **MAS/LM/10896**
Tata Institute of Fundamental Research
Colaba, MUMBAI - 400 005
INDIA

Institute of Electronics & Electrical Engrs.
(IEEE)
Membership No. **41233594, PIN #3944**
Piscataway NJ, 08855-1331,
USA